UNIVERSITY OF CALIFORNIA, SAN DIEGO

Acid-base Sensing and Regulation in Marine Animals

A dissertation submitted in partial satisfaction of the requirements for the degree of Doctor of Philosophy

in

Marine Biology

by

Jinae Nicole Bartlett Roa

Committee in charge:

Professor Martin Tresguerres, Chair
Professor Ronald S. Burton
Professor Lena G. Gerwick
Professor Susan S. Taylor
Professor Victor D. Vacquier

2017

The Dissertation of Jinae Nicole Bartlett Roa is approved, and it is acceptable in quality and form for publication on microfilm and electronically:

_____

_____

_____

_____

_____

Chair

University of California, San Diego

2017

EPIGRAPH

All men dream: but not equally. Those who dream by night in the dusty recesses of their minds wake in the day to find that it was vanity: but the dreamers of the day are dangerous men, for they may act on their dreams with open eyes, to make them possible. This I did.

-T.E. Lawrence

TABLE OF CONTENTS

LIST OF ABBREVIATIONS

AE	anion exchanger
A-IC	A-type intercalated cell
AKAP	A-kinase-anchoring proteins
ATP	adenosine triphosphate
B-IC	B-type intercalated cell
CA	carbonic anhydrase
cAMP	cyclic adenosine monophosphate
DDA	2,5-dideoxyadenosine
EPAC	exchange proteins activated by cAMP
GPCR	G-protein coupled receptor
MR	mitochondrion-rich
NHE	Na^+/H^+ exchanger
NKA	Na^+/K^+-ATPase
PDE	phosphodiesterase
pH_e	extracellular pH
pH_i	intracellular pH
PKA	protein kinase A
sAC	soluble adenylyl cyclase
tmACs	transmembrane adenylyl cyclases
VHA	vacuolar-type H^+-ATPase

LIST OF FIGURES

LIST OF TABLES

ACKNOWLEDGMENTS

First and foremost, I would like to acknowledge and thank my advisor Martin Tresguerres. Words cannot express my gratitude for the guidance you provided me through the years; in no uncertain terms, you have changed my life for the better. I am a better researcher, presenter, and writer because you took the time to train me. Your honest feedback challenged me and helped me grow, and your friendship helped me find a home at SIO. Thank you for the countless letters of recommendation and the numerous opportunities to engage with the international scientific community at conferences around the world. Most of all, thank you for your support during some of the most difficult times in my life. We bonded through science, basketball, BBQ and beer—for that I am truly lucky.

I would also like to thank the other members of my committee: Victor Vacquier, Susan Taylor, Lena Gerwick, and Ronald Burton. Vic, thank you for spending time with me every few months to discuss my projects, for your professional advice on how to achieve my goals, and for writing several invaluable letters of recommendation. Susan, thank you for prompting lively discussions at my committee meetings with your overall interest and enthusiasm, for inviting me to speak to your laboratory about my research, and for supporting my aspirations to work as a UC President's Postdoctoral Fellow. Lena, thank you for taking time to meet with me to discuss my research and for the kind words of support you often shared with me. Ron, thank you for

helping me expand my expectations of where my research could go and for your constant support throughout this process. You all were integral parts of my training and I excelled, in part, due to your mentorship.

To Megan Barron and Jason Ho, those early years in the laboratory with you are unforgettable. We were learning and struggling together, and you guys helped me push through many failed experiments and some difficult coursework. Over the years the laboratory has changed so much, but it has always been filled with wonderful people who took the time to listen and support me, including Lauren Linsmayer, Garfield Kwan, Daniel Yee, Katie Barott, Sidney Perez, Corey Jew, Radha Karra, Yuzo Yanagitsuru, Jenny Tu, Jörn Thomsen, and Cristina Salvador. And thank you to Christian Munévar, Lara Jansen, and Mikayla Ortega who, as undergraduates, helped with animal husbandry and let me serve as their mentor.

I would not have been able to conduct any of the research presented in this dissertation without the help of Andy Nosal and Phil Zerofski. Andy introduced me to the joys of working with leopard sharks, and spent many mornings collecting animals for my project. Phil was essential for all aquarium matters: he collected animals, maintained tanks, and assisted with general husbandry and animal care.

Several gracious programs and institutions have funded me during my PhD. The UCSD San Diego Fellowship funded my first two years, as well as partially funded my third year in conjunction with the NIH Training Grant in

Marine Biotechnology (GM067550). It was through the NIH training grant that I was able to work as an intern at a local San Diego biotechnology company with Dr. Scott Rapoport. Scott, thank you for facilitating the internship and for supporting me during my time there. And finally, the William Townsend Porter Predoctoral Fellowship from the American Physiological Society funded my final two years. The Porter committee and the APS as a whole have shown me an amazing amount of support over the years, not only through the Porter Fellowship but also through numerous travel grants. Through one of these travel grants I met Dr. Alice Villalobos. Alice, thank you for guiding me through my first national conference as an MS student, and then continuing to support me during my PhD by email, phone, and in person.

Last, but never least, my family has given me the strength to endure. Carolyn, my mother, showed me how to approach life with grit, determination, and a sense of personal responsibility. Marquis and Jordan, my older and younger brother, fed my desire to compete and strive for the best; and in my second year at SIO, when Carolyn passed, they helped me feel less alone. And Ramil, my 111, provided the compassion necessary to hold it all together.

Chapter II, in full, is a reprint of the material as it appears in the following citation: Roa JN, Munévar CL, Tresguerres M. 2014. Feeding induces translocation of vacuolar proton ATPase and pendrin to the membrane of leopard shark (*Triakis semifasciata*) mitochondrion-rich gill cells. Comparative Biochemistry and Physiology, Part A: Molecular and Integrative

Physiology 174: 29–37. doi: 10.1016/j.cbpa.2014.04.003. The dissertation author was the primary investigator and author of this paper.

Chapter III, in full, is a reprint of the material as it appears in the following citation: Roa JN, Tresguerres M. 2016. Soluble adenylyl cyclase is an acid-base sensor in epithelial base-secreting cells. American Journal of Physiology, Cell Physiology 311: C340–C349. doi: 10.1152/ ajpcell.00089.2016. The dissertation author was the primary investigator and author of this paper.

Chapter IV, in full, is a reprint of the material as it appears in the following citation: Roa JN, Tresguerres M. 2017. Bicarbonate-sensing soluble adenylyl cyclase is present in the cell cytoplasm and nucleus of multiple shark tissues. Physiological Reports 5: e13090. doi: 10.14814/phy2.13090. The dissertation author was the primary investigator and author of this paper.

Chapter V, in full, is a reprint of the material as it appears in the following citation: Wilson CM, Roa JN, Cox GK, Tresguerres M, Farrell AP. 2016. Introducing a novel mechanism to control heart rate in the ancestral pacific hagfish. Journal of Experimental Biology 219: 3227–3236. doi: 10.1242/jeb.138198. The dissertation author was the co-primary investigator and co-author of this paper.

VITA

2007 Bachelor of Science, University of California, Santa Barbara

2011 Master of Science, California State University, Long Beach

2017 Doctor of Philosophy, University of California, San Diego

FIRST-AUTHOR PUBLICATIONS

Roa JN, Tresguerres M. 2017. Bicarbonate-sensing soluble adenylyl cyclase is present in the cell cytoplasm and nucleus of multiple shark tissues. Physiological Reports 5: e13090.

Roa JN, Tresguerres M. 2016. Soluble adenylyl cyclase is an acid-base sensor in epithelial base-secreting cells. American Journal of Physiology, Cell Physiology 311: C340–C349.

Wilson CM[‡], Roa JN[‡], Cox GK, Tresguerres M, Farrell AP. 2016. Introducing a novel mechanism to control heart rate in the ancestral pacific hagfish. Journal of Experimental Biology 219: 3227–3236.
[‡]Equal author contributions

Roa JN, Munévar CL, Tresguerres M. 2014. Feeding induces translocation of vacuolar proton ATPase and pendrin to the membrane of leopard shark (*Triakis semifasciata*) mitochondrion-rich gill cells. Comparative Biochemistry and Physiology, Part A: Molecular & Integrative Physiology 174: 29–37.

ADDITIONAL PUBLICATIONS

Clifford AM, Goss GG, Roa JN, Tresguerres M. 2015. Acid/base and ionic regulation in hagfish. Hagfish Biology. Boca Raton: CRC Press. 277–297.

Tresguerres M, Barott KL, Barron ME, Roa JN. 2014. Established and potential physiological roles of bicarbonate-sensing soluble adenylyl cyclase (sAC) in aquatic animals. Journal of Experimental Biology 217: 663–672.

Bagulayan A, Bartlett-Roa JN, Carter AL, Inman BG, Keen EM, Orenstein EC, Patin NV, Sato KNS, Sibert EC, Simonis AE, Van Cise AM, Franks PJS. 2012. Journey to the center of the gyre: The fate of the Tohoku Tsunami debris field. Oceanography 25: 200–207.

ABSTRACT OF THE DISSERTATION

Acid-base Sensing and Regulation in Marine Animals

by

Jinae Nicole Bartlett Roa

Doctor of Philosophy in Marine Biology

University of California, San Diego, 2017

Professor Martin Tresguerres, Chair

Regulation of acid-base stress (i.e. carbon dioxide [CO_2], pH, and bicarbonate [HCO_3^-]) is essential for proper functioning of cells, organs, and whole-animals; however, the mechanisms for sensing acid-base stress are largely unknown in marine animals. Therefore, for my dissertation research I investigated the evolutionarily conserved acid-base sensor soluble adenylyl

cyclase (sAC, adcy10) in leopard sharks (*Triakis semifasciata*), round rays (*Urolophus halleri*), and hagfish (*Eptatretus stoutii*).

Leopard shark gills have two acid-base regulatory cell types: acid-secreting Na^+/K^+-ATPase (NKA)-rich and base-secreting V-H^+-ATPase (VHA)-rich cells. Base-secreting VHA-rich cells also contain the Cl^-/HCO_3^- exchanger pendrin. In starved sharks, VHA and pendrin are present in the cell cytoplasm; but, in fed sharks, each translocates to the basolateral and apical membrane, respectively. This translocation is likely mediated by HCO_3^--stimulated sAC, which is highly abundant in both acid- and base-secreting leopard shark gill cells. sAC is also present in other tissues, including rectal gland, cornea, intestine, muscle, and heart tissues; and it is present in the cell nucleus, where it likely mediates regulation of gene expression.

In round rays, sAC is also highly abundant in acid-secreting NKA-rich and base-secreting VHA-rich cells. Additionally, sAC is co-expressed along with hormone-regulated transmembrane adenylyl cyclases (tmACs, adcy1-9). However, sAC, and not tmACs, is essential for VHA translocation to the cell membrane of isolated base-secreting gill cells exposed to extracellular alkalosis, an indication that this process is locally regulated by sAC without the involvement of whole-animal hormone regulation.

In hagfish, sAC is present in both atrial and ventricle heart chambers; and sAC regulates heart beat rate in isolated hearts recovering from anoxia

exposure, a previously unknown role for HCO_3^--activated sAC-cAMP signal transduction pathway that has potential implications for the mammalian heart.

CHAPTER I

General introduction

Acid-base homeostasis and stress. An organism achieves acid-base homeostasis when the levels of carbon dioxide (CO_2), hydrogen (H^+) and bicarbonate (HCO_3^-) ions are relatively stable within a range that allows for the normal biochemical and physiological functions of cells and organisms. Acid-base homeostasis is continuously challenged by metabolic and environmental stressors that change the normal acid-base status of cells and whole-animals. Acid-base stress can be the result of essential functions; for example, H^+ is generated directly by various metabolic processes and also indirectly by the hydration of metabolic and environmental CO_2. Because increased H^+ concentration can alter protein structure and enzyme function, it can affect virtually every aspect of cell biology. As will be discussed in the following dissertation, vertebrate animals have developed mechanisms to sense acid-base stress (Δ $CO_2/H^+/HCO_3^-$) in order to effectively regulate intracellular and extracellular H^+ concentration (pH).

Acid-base sensors. The ability to sense acid-base stress is essential for proper pH regulation and maintenance of blood acid-base status. One such sensing mechanism involves the evolutionarily conserved acid-base sensor soluble adenylyl cyclase (sAC, ADCY10). sAC is a recently discovered Class III adenylyl cyclase (AC) that is directly stimulated by HCO_3^- to produce the second messenger cyclic adenosine monophosphate (cAMP) (Buck et al., 1999; Chen et al., 2000). sAC is distinct from other mammalian adenylyl

cyclases, which include nine transmembrane adenylyl cyclases (tmACs, ADCY1-9). Unlike membrane-bound tmACs, sAC lacks a membrane-spanning domain and is typically found soluble throughout the cytoplasm or closely associated with organelles like the cell nucleus, mitochondria, lysosomes, centrioles and microtubules (Buck et al., 1999; Rahman et al., 2016; Zippin et al., 2003). And while tmACs are activated by traditional AC activators like forskolin and respond to extracellular stimuli (e.g. hormone signaling) *via* G-protein coupled receptor (GPCR) activation, sAC is unaffected by forskolin and responds to intracellular stimuli (e.g. HCO_3^-) generated within the cell or, through the action carbonic anhydrases (CA), from the extracellular environment (Figure 1.1). Both tmACs and sAC rely on two catalytic domains (C1 and C2) to produce cAMP from substrate ATP; however, sAC's catalytic domains are more closely related to HCO_3^--responsive adenylyl cyclases from cyanobacteria (Chen et al., 2000), suggesting that not only is sAC an evolutionarily conserved acid-base sensor but that sAC and tmACs were adapted in response to different physiological conditions.

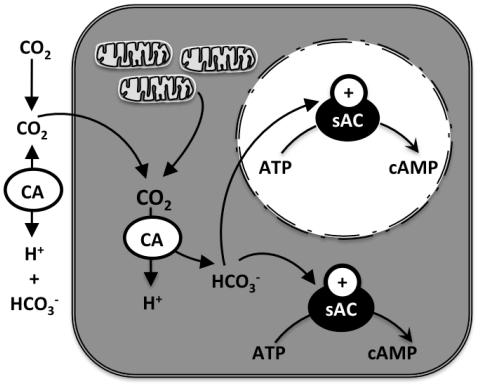

Figure 1.1: sAC is an intracellular $CO_2/H^+/HCO_3^-$ acid-base sensor.

In mammals, a single sAC gene undergoes alternative splicing to yield multiple sAC proteins. The two predominant isoforms include a 187 kDa full-length sAC (sAC_{fl}) and a 48 kDa truncated sAC (sAC_t) protein (Buck et al., 1999). sAC_{fl} contains the two N-terminal catalytic domains and several poorly characterized C-terminal domains, including an autoinhibitory, p-loop, leucine zipper, and heme binding domain (Buck et al., 1999; Chaloupka et al., 2006; Middelhaufe et al., 2012). However, sAC_t contains only the two catalytic domains. sAC_{fl} and sAC_t have a similar ATP substrate affinity and are both activated by physiologically relevant HCO_3^- concentrations (EC_{50}= ~20mM); but sAC_t is 10-fold more enzymatically active because it lacks an autoinhibitory region present in sAC_{fl} (Buck et al., 1999; Chaloupka et al., 2006; Chen et al., 2000; Geng et al., 2005; Litvin et al., 2003). Although sAC is directly stimulated by HCO_3^- (Chen et al., 2000), sAC can also act as the *de facto* sensor for intracellular pH (pH_i) and CO_2, and extracellular CO_2, as intracellular and extracellular carbonic anhydrases (CA) rapidly facilitate formation of a $CO_2/H^+/HCO_3^-$ equilibrium (reviewed in Tresguerres et al., 2011) (Figure 1.1).

Normally C1 and C2 combine as an intramolecular heterodimer to form an active site and a degenerated inactive pocket: the active site binds ATP and catalyzes cAMP formation; the inactive pocket binds a variety of activators, including forskolin (for tmACs) and HCO_3^- (for sAC) (Kleinboelting et al., 2014; reviewed in Sinha and Sprang, 2006). When ATP is bound to the active site,

the molecule is 'cyclicized' by removal of the β- and γ-phosphate to produce cAMP; and when HCO_3^- is bound to the inactive pocket it facilitates ATP binding by recruiting metal cofactors (eg. Mg^{2+}, Mn^{2+}, etc.). HCO_3^- also induces an allosteric change that increases V_{max} turnover rate for ATP without changing K_m substrate affinity for ATP, thereby releasing sAC from rate-limiting substrate oversaturation of ATP. Additionally, mammalian sAC activity is modulated by Ca^{2+} bound to the B-site in the active site; it reduces K_m for ATP and acts synergistically with HCO_3^- to increase cAMP production (Kleinboelting et al., 2014; Litvin et al., 2003; Steegborn et al., 2005). In addition to sAC_{fl} and sAC_t, a few recently discovered somatic sAC (sAC_{som}) proteins may be tissue- or organelle-specific isoforms, but these C2-only proteins are unable to produce cAMP (Chen et al., 2014; Farrell et al., 2008); simply, they are incapable of binding the ATP substrate because they lack the required C1.

Although sAC is currently the only identified intracellular acid-base sensor that acts through the cAMP signal transduction pathway, research suggests some GPCRs coupled with tmACs act as extracellular acid-base sensors (Ludwig et al., 2003). For example, GPCR 4 (GPR4) is activated by a decrease in extracellular pH (pH_e) to increase cAMP production (Ludwig et al., 2003), a mechanism that may take place in mammalian kidney acid-base regulatory cells (Sun et al., 2010). Cells with both sAC and pH_e-sensing GPCR/tmAC would have a greater ability to differentially respond to a range of

acid-base stresses, as well as more complex cAMP signaling networks. However, there is little information on potential interactions between sAC and tmACs signaling and how it may relate to $CO_2/H^+/HCO_3^-$ sensing in general. Future research can utilize sAC- and tmAC-specific inhibitors to investigate the complex mechanisms of acid-base sensing and regulation by intracellular cAMP signal transduction. Specifically, the small molecule KH7, which is a sAC-specific inhibitor (IC_{50} = 10 μM) (Hess et al., 2005); and 2,5-dideoxyadenosine (DDA), which is a tmAC-specific inhibitor (IC_{50} = 8 μM) (Bitterman et al., 2013; Dessauer and Gilman, 1997). These inhibitors provide the ability to identify the effects of cAMP produced by either sAC or tmAC on downstream effectors during acid-base stress.

cAMP signaling microdomains. cAMP acts as a second messenger in the cAMP signal transduction pathway where it affects multiple physiological processes through post-translational modification of target proteins. Some downstream effectors of cAMP signaling include protein kinase A (PKA), cyclic nucleotide gated channels, and exchange proteins activated by cAMP (EPAC). Prior to the discovery of sAC, cAMP signal transduction was thought to occur through cAMP diffusion away from plasma membrane-bound tmACs. However, this simple model of whole-cell cAMP diffusion would result in a generalized signal for all downstream effectors in the cytoplasm, thus preventing signal specificity. The current model includes cAMP signaling microdomains with

sAC as an intracellular source of cAMP (Buck et al., 1999; Chen et al., 2000). cAMP signaling microdomains rely on localized cAMP production from tmACs or sAC, with cAMP diffusion limited by phosphodiesterases (PDE) tethered to locations throughout the cell by A-kinase-anchoring proteins (AKAP) (Buck et al., 1999; Zippin et al., 2003; Zippin et al., 2004)(Figure 1.2). By enlisting microdomains, the whole cell and individual organelles receive distinct cAMP signals and are capable of differential responses, which become important when cells must distinguish between multiple stress-induced cAMP signals.

A sAC-dependent cAMP signaling microdomain was recently linked to regulation of gene expression in nuclei from mammalian cells (Zippin et al., 2004). Prior to the concept of cAMP signaling microdomains and identification of sAC in the nucleus, regulation of gene expression was attributed solely to extracellular signals such as hormones and subsequent tmAC activation by GPCR/G proteins. With the discovery of sAC in the nucleus, the model for gene regulation now includes sAC activity as a local source of cAMP that is stimulated by increased HCO_3^- to produce cAMP, PKA activation, PKA-

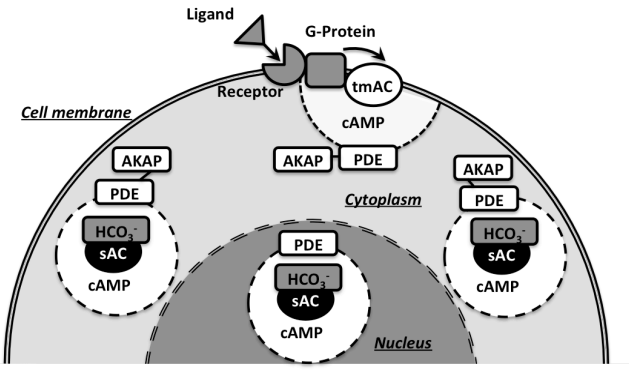

Figure 1.2: Intracellular cAMP signaling microdomains.

dependent phosphorylation of the transcription factor cAMP response binding protein (CREB), and up or down regulation of target genes (Zippin et al., 2004). Potential target genes of sAC-stimulated regulation of gene expression include those involved in acid-base stress response and those involved in metabolism. Since aerobic metabolism produces CO_2, sAC activity could reflect metabolic activity and serve as an intrinsic metabolic control of gene expression (Figure 1.1). So far, research in the area of cAMP signaling microdomains and sAC in the nucleus has been limited to established cultures of mammalian cells. Thus, one objective of my dissertation was to develop an alternative (non-mammalian) model to study general mechanisms of acid-base regulation and regulation of gene expression by sAC in the nucleus.

Intracellular and extracellular acid-base regulation. pH_i regulation is accomplished through a combination of passive buffering and active transport. Passive buffering involves ion sequestration as free H^+ or hydroxide (OH^-) ions combine with various protein amino acid residues, phosphates, and intracellular CO_2/HCO_3^-; the end result being a natural intracellular buffering capacity and smaller changes in pH. Active transport involves secretion or absorption of H^+ or HCO_3^- as necessary, processes that can be pushed forward by the action of intracellular CA and the reversible hydration/dehydration of metabolic CO_2. While all cells use active transport to regulate pH_i to some degree, vertebrate animals have developed specialized

organs that regulate blood pH_e. This active acid-base regulation occurs in specialized epithelial tissues, where polarized cells mediate transepithelial transport of H^+, HCO_3^-, and other acid-base relevant ions (e.g. Na^+, Cl^-) between the blood and the external environment to maintain systemic acid-base homeostasis (reviewed in Claiborne et al., 2002). In general, specific cell subtypes are specialized for H^+ secretion, HCO_3^- and Na^+ absorption (and compensate low blood pH -acidosis-), and other cell subtypes are specialized for HCO_3^- secretion, H^+ and Cl^- absorption (and compensate high blood pH -alkalosis-). The use of these epithelial tissues is evolutionarily important for vertebrates because it reduces the range of acid-base stress experienced by other tissues throughout the body.

Blood acid-base regulation in mammals. In the collecting duct of the mammalian kidney two epithelial cell types are responsible for blood acid-base regulation. A-type intercalated cells (A-ICs) are acid-secreting, and are identified by expression the vacuolar H^+-ATPase (VHA) and the Cl^-/HCO_3^- anion exchanger AE1 on the apical and basolateral membranes, respectively (Alper et al., 1989; Sabolić et al., 1997). B-type intercalated cells (B-ICs) are base-secreting, and are identified by expression of the Cl^-/HCO_3^- anion exchanger pendrin and VHA on the apical and basolateral membranes, respectively (Brown et al., 1988; Royaux et al., 2001). Thus, both cell types express VHA (although on opposite membrane domains) but AE1 is only

expressed in A-ICs and pendrin is only expressed in B-ICs (reviewed in Brown et al., 2012). In line with the opposing acid- and base-secretory functions of A-ICs and B-ICs, these cells also respond differentially to acid-base stress: during metabolic acidosis A-ICs are activated and B-ICs are inactivated; during metabolic alkalosis A-ICs are inactivated and B-ICs are activated. But for both cell types activation/inactivation involves VHA translocation to or away from the cell membrane (Sabolić et al., 1997). However, because the collecting duct of the mammalian kidney is notoriously difficult to work with, most of the primary research on mechanisms of VHA translocation during acid-base stress was conducted using clear cells of the epididymis, which are functionally and embryologically similar to kidney A-ICs (Hinton and Turner, 1988). In clear cells, sAC is essential for cell activation, with intracellular cAMP production responsible for VHA translocation to the apical membrane and subsequent acid secretion (Pastor-Soler et al., 2003). It remains unclear how A-ICs and B-ICs differentiate between metabolic acidosis/alkalosis and coordinate the appropriate response, but similar to clear cells, research implicates the cAMP signal transduction pathway (Paunescu et al., 2010). This hypothesis is further supported by the presence of sAC in both A-ICs and B-ICs (Paunescu et al., 2008), as well as high mRNA expression of the pH_e-sensing GPR4 in the kidney collecting duct (Sun et al., 2010). However, more research is necessary to determine GPR4 protein localization, the physiological role of GPR4 acid-base sensing during stress, and the interplay

of sAC/tmAC cAMP signal transduction pathways during blood acid-base regulation.

Blood acid-base regulation in sharks and rays. Similar to mammals, shark and ray gills have two epithelial cell types that are responsible for blood acid-base regulation. Acid-secreting cells abundantly express the Na^+/K^+-ATPase (NKA) in the basolateral membrane and are thus known as "NKA-rich cells"; and they also express apical Na^+/H^+ exchanger 3 (NHE3) (Choe et al., 2007; Choe et al., 2005). Base-secreting cells abundantly express VHA and are thus called "VHA-rich cells"; and they also express the anion exchanger pendrin (Piermarini et al., 2002; Reilly et al., 2011; Tresguerres et al., 2010b). Thus far research on acid-base sensing and regulation in sharks and rays has solely focused on the VHA-rich base-secreting cells. Under normal conditions, VHA is found diffuse throughout the cytoplasm; however during experimentally induced blood alkalosis, VHA translocates to the basolateral membrane (Tresguerres et al., 2005). VHA at the basolateral membrane mediates blood acid-base regulation directly by 'pumping' H^+ into the blood and indirectly by energizing intracellular HCO_3^- accumulation and eventual secretion *via* apical pendrin. Subsequent research showed VHA translocation is reliant on microtubules (Tresguerres et al., 2006) and CA (Tresguerres et al., 2007). VHA translocation occurs under natural conditions as well, most notably during a post-feeding 'alkaline tide' where blood pH remains significantly elevated for

an extended period (~12-17hrs depending on meal size) (Tresguerres et al., 2007; Tresguerres et al., 2010b; Wood et al., 2005). Recent research has implicated that sAC is essential for sensing this acid-base stress in the gills of dogfish shark (*Squalus acanthias*) (Tresguerres et al., 2010b). Dogfish shark sAC (dfsAC) is a ~110 kDa protein and, similar to mammalian sAC, contains the C1 and C2 catalytic domains and is stimulated by physiologically relevant HCO_3^- concentration (EC_{50}= ~5mM) to produce cAMP. Furthermore, sAC was found essential for VHA translocation and blood acid-base regulation during the 'alkaline tide' (Tresguerres et al., 2010b), an indication that sAC is a physiologically relevant acid-base sensor in sharks. Similar to clear cells serving as a model for acid-base sensing and regulation by A-ICs, VHA-rich cells could serve as a model for acid-base sensing and regulation by B-ICs.

In dogfish gills, sAC was generally present throughout the gill epithelium (Tresguerres et al., 2010b); however, specific expression of sAC in NKA- or VHA-rich cells was not explored. And while NKA-rich cells have previously been described as mitochondrion-rich (MR) cells (Wilson et al., 2002), direct evidence for VHA-rich cells as MR cells is lacking. Therefore, it is currently unclear if NKA- and VHA-rich cells both express sAC and if both are MR cells; and it is unknown if there are other sAC-expressing MR cells present in shark gills. Lastly, the metabolic fuel used by MR cells to create the ATP necessary for proper function is also unknown. In teleost fish gills, MR cells share a common apical opening and seem to be coupled with glycogen-rich

cells; and glycogen content declined during freshwater and seawater transitions when the MR cells are most active, suggesting that glycogen utilization provided the required energy (Tseng et al., 2007). Thus far, no study has looked at the role of glycogen, glycogen-rich cells, and sAC-induced glycogen depletion during acid-base regulation by NKA- and VHA-rich cells.

Sharks and ray gill cells as a model to study mechanisms for acid-base sensing and regulation. The functional specificity of shark and ray gill makes it an excellent model for the study of acid-base regulation at the cellular and systemic levels. First, shark and ray NKA- and VHA-rich gill cells are functionally analogous to mammalian kidney acid- and base-secreting cells, but gill acid-base regulatory cells are larger, more abundant, and easier to culture than mammalian kidney cells. Second, shark and rays rely solely on gill epithelial cells for acid-base regulation because, unlike mammals, aquatic animals are unable to modify ventilation rate to control blood CO_2 concentration (Claiborne et al., 2002). Shark and ray gills also transport ions exclusively for acid-base regulatory purposes (Heisler, 1988); unlike teleost fishes that also use their gills for osmoregulation. Third, sharks and rays experience large changes in acid-base homeostasis as a part of their normal physiology. Feeding (Wood et al., 2005), exhaustive exercise (Richards et al., 2003), changes in water temperature (Heisler, 1988), and environmental hypercapnia (Heisler, 1988) are all accompanied by pronounced acid-base

stress ranging from pH_e 7.4 and no HCO_3^- after exercise (Richards et al., 2003) to pH_e 8.2 and 6 mM HCO_3^- in the post-feeding period (Wood et al., 2005). Consistent with these diverse sources of acid-base stress, shark sAC is active at a wide range of HCO_3^- concentrations, with the HCO_3^- dose-response for sAC activation in dogfish sharks greatest between 2-15 mM with an EC_{50} = ~5 mM (Tresguerres et al., 2010b) which matches the normal blood HCO_3^- concentration present in sharks (Wood et al., 2005). Therefore, not only is it possible to investigate acid-base regulation by experimentally inducing extremely alkaline or acidic conditions *in vivo*, but it is also possible to reproduce those extreme, yet physiologically relevant conditions, in the laboratory. Taking advantage of isolated shark and ray gill cells, my dissertation addressed the question of whether acid-base sensing and regulation is influenced by hormone, nerve, or paracrine regulation; any responses observed in isolated cells would be under local intra- and extracellular control and not whole-animal physiological processes. Those experiments are not possible with mammalian kidney cells.

Acid-base sensing and regulation in other tissues. Although vertebrates maintain blood acid-base homeostasis as described above, tissues and cells can still experience local changes in acid-base status that can affect proper function and/or serve as regulatory signals. Therefore, tissues must be able to sense and regulate acid-base stress independently

from systemic blood acid-base regulatory processes in kidneys and gills. Indeed, sAC has been identified in nearly every mammalian tissue studied to date (reviewed in Levin and Buck, 2015). For example, in the epididymis, the sAC-cAMP-PKA signaling pathway helps maintain sperm quiescence by promoting VHA translocation to the apical membrane and subsequent luminal acid secretion (Pastor-Soler et al., 2003; Pastor-Soler et al., 2008). In sperm, sAC facilitates the motility and maturation required for fertilization (Esposito et al., 2004; Hess et al., 2005). In the pancreas, sAC induces β cell insulin secretion following glucose-induced ATP production and Ca^{2+} influx (Ramos et al., 2008). In the eye, sAC in the ciliary body mediates aqueous humor removal, an important process used to decrease intraocular pressure and treat diseases of the eye like glaucoma (Lee et al., 2011). And in the lungs, sAC regulates ciliary beat frequency, which is used to remove mucus and debris from the lungs (Schmid et al., 2007).

At the beginning of my dissertation, sAC had only been identified in a few non-mammalian animals. In the gills of dogfish sharks, sAC was known to facilitate VHA translocation to the basolateral membrane of base-secreting gill cells and blood acid-base homeostasis (Tresguerres et al., 2010b). In sea urchin (*Strongylocentrotus purpuratus*) sperm, sAC had been reported to mediate motility and maturation (Nomura and Vacquier, 2006; Nomura et al., 2005). In the intestine of teleost fishes, sAC was known to facilitate NaCl and water absorption (Carvalho et al., 2012; Tresguerres et al., 2010a). And in

corals, sAC activity was reported to be extraordinarily high (Barott et al., 2013); however, sAC's physiological roles in coral was unknown. In my dissertation I use molecular, cellular, and whole-animal experiments to expand on this knowledge of sAC as an evolutionarily conserved acid-base sensor and its role in blood and tissue acid-base regulation in elasmobranchs (sharks, rays, etc.).

Evolutionarily adapted use for acid-base sensing and regulation in hagfish. Hagfish, along with lampreys, are found at the base of the vertebrate phylogenetic tree as a part of the Agnatha superclass of jawless fish (Kuratani et al., 2002). Thus, the acid-base sensing mechanisms in hagfish could provide insight about the degree of evolutionarily conservation of sAC as an acid-base sensor. For the purposes of this dissertation I focused on the role of acid-base sensors during regulation of cardiac function. Unlike the mammalian heart, hagfish hearts lack cardiac innervation (Axelsson et al., 1990); and yet they tightly regulate heart beat rate, presumably though cardiac pacemaker cells and stimulation of the cAMP signal transduction pathway (reviewed in Farrell, 2007). However, it was unclear whether hormone-stimulation of tmAC or HCO_3^--stimulation of sAC is responsible for this cAMP-regulated heart beat rate control.

Objectives. The broader goal of this dissertation was to characterize mechanisms for acid-base sensing and regulation in marine animals at the molecular, cellular, and whole-animal level, focusing on leopard sharks (*Triakis semifasciata*), Pacific round rays (*Urolophus halleri*), and Pacific hagfish (*Eptatretus stoutii*). This research has addressed the fundamental question of how organisms sense and regulate acid-base homeostasis. The knowledge contained in this dissertation adds to the foundation of information on whole-animal acid-base regulation; and it provides insights on acid-base sensing *via* sAC in different tissues and cell types as well as in the nuclear sAC-cAMP signaling microdomain. This broader goal was accomplished through the following objectives:

1. Characterization of gill acid- and base-secreting cells: are they also MR cells? Does the localization of ion-transporting proteins in base-secreting VHA-rich gill cells change during post-feeding alkalosis?
2. Investigation of acid-base sensing and regulation by sAC in isolated base-secreting VHA-rich gill cells exposed to extracellular alkalosis.
3. Exploration of acid-base sensing by sAC in the cell cytoplasm and nucleus of multiple shark tissues.
4. Investigation of intracellular glycogen content as a metabolic fuel source used by gill MR cells during acid-base regulation.
5. Exploration of evolutionarily adapted uses for cAMP signal transduction and acid-base sensing by sAC in normal and anoxic hagfish hearts.

References

Alper, S. L., Natale, J., Gluck, S., Lodish, H. F. and Brown, D. (1989). Subtypes of intercalated cells in rat-kidney collecting duct defined by antibodies against erythroid band-3 and renal vacuolar H^+-ATPase. *Proc. Natl. Acad. Sci. USA* **86**, 5429–5433.

Axelsson, M., Farrell, A. P. and Nilsson, S. (1990). Effects of hypoxia and drugs on the cardiovascular dynamics of the Atlantic hagfish *Myxine glutinosa*. *J. Exp. Biol.* **151**, 297–316.

Barott, K. L., Helman, Y., Haramaty, L., Barron, M. E., Hess, K. C., Buck, J., Levin, L. R. and Tresguerres, M. (2013). High adenylyl cyclase activity and in vivo cAMP fluctuations in corals suggest central physiological role. *Sci. Rep.* **3**, 1379.

Bitterman, J. L., Ramos-Espiritu, L., Diaz, A., Levin, L. R. and Buck, J. (2013). Pharmacological distinction between soluble and transmembrane adenylyl cyclases. *J. Pharmacol. Exp. Ther.* **347**, 589–598.

Brown, D., Bouley, R., Paunescu, T. G., Breton, S. and Lu, H. A. J. (2012). New insights into the dynamic regulation of water and acid-base balance by renal epithelial cells. *Am. J. Physiol. Cell Physiol.* **302**, C1421–33.

Brown, D., Hirsch, S. and Gluck, S. (1988). An H^+-ATPase in opposite plasma membrane domains in kidney epithelial cell subpopulations. *Nature* **331**, 622–624.

Buck, J., Sinclair, M. L., Schapal, L., Cann, M. J. and Levin, L. R. (1999). Cytosolic adenylyl cyclase defines a unique signaling molecule in mammals. *Proc. Natl. Acad. Sci. USA* **96**, 79–84.

Carvalho, E. S. M., Gregório, S. F., Power, D. M., Canário, A. V. M. and Fuentes, J. (2012). Water absorption and bicarbonate secretion in the intestine of the sea bream are regulated by transmembrane and soluble adenylyl cyclase stimulation. *J. Comp. Physiol. B, Biochem. Syst. Environ. Physiol.* **182**, 1069–1080.

Chaloupka, J. A., Bullock, S. A., Iourgenko, V., Levin, L. R. and Buck, J. (2006). Autoinhibitory regulation of soluble adenylyl cyclase. *Mol. Reprod. Dev.* **73**, 361–368.

Chen, X., Baumlin, N., Buck, J., Levin, L. R., Fregien, N. and Salathe, M. (2014). A soluble adenylyl cyclase form targets to axonemes and rescues beat regulation in soluble adenylyl cyclase knockout mice. *Am. J. Respir.*

Cell Mol. Biol. **51**, 750–760.

Chen, Y., Cann, M. J., Litvin, T. N., Iourgenko, V., Sinclair, M. L., Levin, L. R. and Buck, J. (2000). Soluble adenylyl cyclase as an evolutionarily conserved bicarbonate sensor. *Science* **289**, 625–628.

Choe, K. P., Edwards, S. L., Claiborne, J. B. and Evans, D. H. (2007). The putative mechanism of Na^+ absorption in euryhaline elasmobranchs exists in the gills of a stenohaline marine elasmobranch, *Squalus acanthias*. *Comp. Biochem. Physiol., Part A Mol. Integr. Physiol.* **146**, 155–162.

Choe, K. P., Kato, A., Hirose, S., Plata, C., Sindic, A., Romero, M. F., Claiborne, J. B. and Evans, D. H. (2005). NHE3 in an ancestral vertebrate: primary sequence, distribution, localization, and function in gills. *Am. J. Physiol. Regul. Integr. Comp. Physiol.* **289**, R1520–34.

Claiborne, J. B., Edwards, S. L. and Morrison-Shetlar, A. I. (2002). Acid-base regulation in fishes: cellular and molecular mechanisms. *J. Exp. Zool.* **293**, 302–319.

Dessauer, C. W. and Gilman, A. G. (1997). The catalytic mechanism of mammalian adenylyl cyclase. Equilibrium binding and kinetic analysis of P-site inhibition. *J. Biol. Chem.* **272**, 27787–27795.

Esposito, G., Jaiswal, B. S., Xie, F., Krajnc-Franken, M. A. M., Robben, T. J. A. A., Strik, A. M., Kuil, C., Philipsen, R. L. A., van Duin, M., Conti, M. and Gossen, J. A. (2004). Mice deficient for soluble adenylyl cyclase are infertile because of a severe sperm-motility defect. *Proc. Natl. Acad. Sci. USA* **101**, 2993–2998.

Farrell, A. P. (2007). Cardiovascular systems in primitive fishes. *Fish Physiol.* **26**, 53-120.

Farrell, J., Ramos, L., Tresguerres, M., Kamenetsky, M., Levin, L. R. and Buck, J. (2008). Somatic 'soluble' adenylyl cyclase isoforms are unaffected in Sacy tm1Lex/Sacy tm1Lex “knockout” mice. *PLoS ONE* **3**, e3251.

Geng, W., Wang, Z., Zhang, J., Reed, B. Y., Pak, C. Y. C. and Moe, O. W. (2005). Cloning and characterization of the human soluble adenylyl cyclase. *Am. J. Physiol. Cell Physiol.* **288**, C1305–16.

Heisler, N. (1988). Acid-base regulation. In: *Physiology of Elasmobranch Fishes*. Berlin: Springer, 215–252.

Hess, K. C., Jones, B. H., Marquez, B., Chen, Y., Ord, T. S., Kamenetsky,

M., Miyamoto, C., Zippin, J. H., Kopf, G. S., Suarez, S. S., Levin, L. R., Williams, C. J., Buck, J. and Moss, S. B. (2005). The “soluble” adenylyl cyclase in sperm mediates multiple signaling events required for fertilization. *Dev. Cell* **9**, 249–259.

Hinton, B. T. and Turner, T. T. (1988). Is the epididymis a kidney analogue? *Physiol.* **3**, 28–31.

Kleinboelting, S., Diaz, A., Moniot, S., van den Heuvel, J., Weyand, M., Levin, L. R., Buck, J. and Steegborn, C. (2014). Crystal structures of human soluble adenylyl cyclase reveal mechanisms of catalysis and of its activation through bicarbonate. *Proc. Natl. Acad. Sci. USA* **111**, 3727–3732.

Kuratani, S., Kuraku, S. and Murakami, Y. (2002). Lamprey as an evo-devo model: lessons from comparative embryology and molecular phylogenetics. *Genesis* **34**, 175–183.

Lee, Y. S., Tresguerres, M., Hess, K., Marmorstein, L. Y., Levin, L. R., Buck, J. and Marmorstein, A. D. (2011). Regulation of anterior chamber drainage by bicarbonate-sensitive soluble adenylyl cyclase in the ciliary body. *J. Biological Chem.* **286**, 41353–41358.

Levin, L. R. and Buck, J. (2015). Physiological roles of acid-base sensors. *Ann. Rev. Physiol.* **77**, 347–362.

Litvin, T. N., Kamenetsky, M., Zarifyan, A., Buck, J. and Levin, L. R. (2003). Kinetic properties of “soluble” adenylyl cyclase. Synergism between calcium and bicarbonate. *J. Biol. Chem.* **278**, 15922–15926.

Ludwig, M.-G., Vanek, M., Guerini, D., Gasser, J. A., Jones, C. E., Junker, U., Hofstetter, H., Wolf, R. M. and Seuwen, K. (2003). Proton-sensing G-protein-coupled receptors. *Nature* **425**, 93–98.

Middelhaufe, S., Leipelt, M., Levin, L. R., Buck, J. and Steegborn, C. (2012). Identification of a haem domain in human soluble adenylate cyclase. *Biosci. Rep.* **32**, 491–499.

Nomura, M. and Vacquier, V. D. (2006). Proteins associated with soluble adenylyl cyclase in sea urchin sperm flagella. *Cell Motil. Cytoskeleton* **63**, 582–590.

Nomura, M., Beltrán, C., Darszon, A. and Vacquier, V. D. (2005). A soluble adenylyl cyclase from sea urchin spermatozoa. *Gene* **353**, 231–238.

Pastor-Soler, N. M., Hallows, K. R., Smolak, C., Gong, F., Brown, D. and

Breton, S. (2008). Alkaline pH- and cAMP-induced V-ATPase membrane accumulation is mediated by protein kinase A in epididymal clear cells. *Am. J. Physiol. Cell Physiol.* **294**, C488–94.

Pastor-Soler, N., Beaulieu, V., Litvin, T. N., Da Silva, N., Chen, Y., Brown, D., Buck, J., Levin, L. R. and Breton, S. (2003). Bicarbonate-regulated adenylyl cyclase (sAC) is a sensor that regulates pH-dependent V-ATPase recycling. *J. Biol. Chem.* **278**, 49523–49529.

Paunescu, T. G., Da Silva, N., Russo, L. M., McKee, M., Lu, H. A. J., Breton, S. and Brown, D. (2008). Association of soluble adenylyl cyclase with the V-ATPase in renal epithelial cells. *Am. J. Physiol. Renal Physiol.* **294**, F130–8.

Paunescu, T. G., Ljubojevic, M., Russo, L. M., Winter, C., McLaughlin, M. M., Wagner, C. A., Breton, S. and Brown, D. (2010). cAMP stimulates apical V-ATPase accumulation, microvillar elongation, and proton extrusion in kidney collecting duct A-intercalated cells. *Am. J. Physiol. Renal Physiol.* **298**, F643–54.

Piermarini, P. M., Verlander, J. W., Royaux, I. E. and Evans, D. H. (2002). Pendrin immunoreactivity in the gill epithelium of a euryhaline elasmobranch. *Am. J. Physiol. Regul. Integr. Comp. Physiol.* **283**, R983–92.

Rahman, N., Ramos-Espiritu, L., Milner, T. A., Buck, J. and Levin, L. R. (2016). Soluble adenylyl cyclase is essential for proper lysosomal acidification. *J. Gen. Physiol.* **148**, 325–339.

Ramos, L. S., Zippin, J. H., Kamenetsky, M., Buck, J. and Levin, L. R. (2008). Glucose and GLP-1 stimulate cAMP production via distinct adenylyl cyclases in INS-1E insulinoma cells. *J. Gen. Physiol.* **132**, 329–338.

Reilly, B. D., Cramp, R. L., Wilson, J. M., Campbell, H. A. and Franklin, C. E. (2011). Branchial osmoregulation in the euryhaline bull shark, Carcharhinus leucas: a molecular analysis of ion transporters. *J. Exp. Biol.* **214**, 2883–2895.

Richards, J. G., Heigenhauser, G. J. F. and Wood, C. M. (2003). Exercise and recovery metabolism in the Pacific spiny dogfish (*Squalus acanthias*). *J. Comp. Physiol. B, Biochem. Syst. Environ. Physiol.* **173**, 463–474.

Royaux, I. E., Wall, S. M., Karniski, L. P., Everett, L. A., Suzuki, K., Knepper, M. A. and Green, E. D. (2001). Pendrin, encoded by the

Pendred syndrome gene, resides in the apical region of renal intercalated cells and mediates bicarbonate secretion. *Proc. Natl. Acad. Sci. USA* **98**, 4221–4226.

Sabolić, I., Brown, D., Gluck, S. L. and Alper, S. L. (1997). Regulation of AE1 anion exchanger and H^+-ATPase in rat cortex by acute metabolic acidosis and alkalosis. *Kidney International* **51**, 125–137.

Schmid, A., Sutto, Z., Nlend, M.-C., Horvath, G., Schmid, N., Buck, J., Levin, L. R., Conner, G. E., Fregien, N. and Salathe, M. (2007). Soluble adenylyl cyclase is localized to cilia and contributes to ciliary beat frequency regulation via production of cAMP. *J. Gen. Physiol.* **130**, 99–109.

Sinha, S. C. and Sprang, S. R. (2006). Structures, mechanism, regulation and evolution of class III nucleotidyl cyclases. *Rev. Physiol. Biochem. Pharmacol.* **157**, 105–140.

Steegborn, C., Litvin, T. N., Levin, L. R., Buck, J. and Wu, H. (2005). Bicarbonate activation of adenylyl cyclase via promotion of catalytic active site closure and metal recruitment. *Nat. Struct. Mol. Biol.* **12**, 32–37.

Sun, X., Yang, L. V., Tiegs, B. C., Arend, L. J., McGraw, D. W., Penn, R. B. and Petrovic, S. (2010). Deletion of the pH sensor GPR4 decreases renal acid excretion. *J. Am. Soc. Nephrol.* **21**, 1745–1755.

Tresguerres, M., Katoh, F., Fenton, H., Jasinska, E. and Goss, G. G. (2005). Regulation of branchial V-H^+-ATPase, Na^+/K^+-ATPase and NHE2 in response to acid and base infusions in the Pacific spiny dogfish (Squalus acanthias). *J. Exp. Biol.* **208**, 345–354.

Tresguerres, M., Levin, L. R. and Buck, J. (2011). Intracellular cAMP signaling by soluble adenylyl cyclase. *Kidney International* **79**, 1277–1288.

Tresguerres, M., Levin, L. R., Buck, J. and Grosell, M. (2010a). Modulation of NaCl absorption by HCO_3^- in the marine teleost intestine is mediated by soluble adenylyl cyclase. *Am. J. Physiol. Regul. Integr. Comp. Physiol.* **299**, R62–71.

Tresguerres, M., Parks, S. K., Katoh, F. and Goss, G. G. (2006). Microtubule-dependent relocation of branchial V-H^+-ATPase to the basolateral membrane in the Pacific spiny dogfish (*Squalus acanthias*): a role in base secretion. *J. Exp. Biol.* **209**, 599–609.

Tresguerres, M., Parks, S. K., Salazar, E., Levin, L. R., Goss, G. G. and Buck, J. (2010b). Bicarbonate-sensing soluble adenylyl cyclase is an

essential sensor for acid/base homeostasis. *Proc. Natl. Acad. Sci. USA* **107**, 442–447.

Tresguerres, M., Parks, S. K., Wood, C. M. and Goss, G. G. (2007). V-H^+-ATPase translocation during blood alkalosis in dogfish gills: interaction with carbonic anhydrase and involvement in the postfeeding alkaline tide. *Am. J. Physiol. Regul. Integr. Comp. Physiol.* **292**, R2012–R2019.

Tseng, Y.-C., Huang, C.-J., Chang, J. C.-H., Teng, W.-Y., Baba, O., Fann, M.-J. and Hwang, P.-P. (2007). Glycogen phosphorylase in glycogen-rich cells is involved in the energy supply for ion regulation in fish gill epithelia. *Am. J. Physiol. Regul. Integr. Comp. Physiol.* **293**, R482–91.

Wilson, J. M., Morgan, J. D., Vogl, A. W. and Randall, D. J. (2002). Branchial mitochondria-rich cells in the dogfish *Squalus acanthias*. *Comp. Biochem. Physiol., Part A Mol. Integr. Physiol.* **132**, 365–374.

Wood, C. M., Kajimura, M., Mommsen, T. P. and Walsh, P. J. (2005). Alkaline tide and nitrogen conservation after feeding in an elasmobranch (*Squalus acanthias*). *J. Exp. Biol.* **208**, 2693–2705.

Zippin, J. H., Chen, Y., Nahirney, P., Kamenetsky, M., Wuttke, M. S., Fischman, D. A., Levin, L. R. and Buck, J. (2003). Compartmentalization of bicarbonate-sensitive adenylyl cyclase in distinct signaling microdomains. *FASEB J.* **17**, 82–84.

Zippin, J. H., Farrell, J., Huron, D., Kamenetsky, M., Hess, K. C., Fischman, D. A., Levin, L. R. and Buck, J. (2004). Bicarbonate-responsive “soluble” adenylyl cyclase defines a nuclear cAMP microdomain. *J. Cell Biol.* **164**, 527–534.

CHAPTER II

Feeding induces translocation of vacuolar proton ATPase and pendrin to the membrane of leopard shark (*Triakis semifasciata*) mitochondrion-rich gill cells

Comparative Biochemistry and Physiology, Part A 174 (2014) 29–37

Contents lists available at ScienceDirect

Comparative Biochemistry and Physiology, Part A

journal homepage: www.elsevier.com/locate/cbpa

Feeding induces translocation of vacuolar proton ATPase and pendrin to the membrane of leopard shark (*Triakis semifasciata*) mitochondrion-rich gill cells

Jinae N. Roa, Christian L. Munévar, Martin Tresguerres *

Marine Biology Research Division, Scripps Institution of Oceanography, University of California San Diego, 9500 Gilman Drive, La Jolla, CA 93092-0202, USA

ARTICLE INFO

Article history:
Received 6 March 2014
Received in revised form 9 April 2014
Accepted 10 April 2014
Available online 16 April 2014

Keywords:
Alkaline tide
Elasmobranch
Na^+/K^+-ATPase
Pendrin
Proton pump
slc26a4
Sodium pump
V-H^+-ATPase

ABSTRACT

In this study we characterized mitochondrion-rich (MR) cells and regulation of acid/base (A/B) relevant ion-transporting proteins in leopard shark (*Triakis semifasciata*) gills. Immunohistochemistry revealed that leopard shark gills posses two separate cell populations that abundantly express either Na^+/K^+-ATPase (NKA) or V-H^+-ATPase (VHA), but not both ATPases together. Co-immunolocalization with mitochondrial Complex IV demonstrated, for the first time in shark gills, that both NKA- and VHA-rich cells are also MR cells, and that all MR cells are either NKA- or VHA-rich cells. Additionally we localized the anion exchanger pendrin to VHA-rich cells, but not NKA-rich cells. In starved sharks, VHA was localized throughout the cell cytoplasm and pendrin was present at the apical pole (but not in the membrane). However, in a significant number of gill cells from fed leopard sharks, VHA translocated to the basolateral membrane (as previously described in dogfish), and pendrin translocated to the apical membrane. Our results highlight the importance of translocation of ion-transporting proteins to the cell membrane as a regulatory mechanism for A/B regulation.

1. Introduction

The fish gill epithelium has specialized cells that transport H^+ and HCO_3^- between the blood and the surrounding water thus maintaining blood acid/base (A/B) homeostasis. Unlike the gills of teleost fishes, which transport ions for both A/B balance and osmoregulation, the gills of marine elasmobranchs transport ions exclusively for A/B regulatory purposes. Moreover, elasmobranch gills are responsible for ~97% of A/B regulation, with the rectal gland and kidneys facilitating iono- and osmoregulation, respectively (Heisler, 1988). The functional specificity of the elasmobranch gill makes it an excellent model for the study of A/B regulation at the cellular and systemic levels without interference from other ion-transporting processes.

In Atlantic stingray (*Dasyatis sabina*) (Piermarini and Evans, 2001), dogfish shark (*Squalus acanthias*) (Tresguerres et al., 2005), and bull shark (*Carcharhinus leucas*) (Reilly et al., 2011), Na^+/K^+-ATPase (NKA) and V-H^+-ATPase (VHA) are abundantly expressed in distinct gill cell subpopulations: NKA- and VHA-rich cells, respectively. NKA-rich cells express apical Na^+/H^+ exchangers 3 (NHE3) and are considered "acid-secreting, base absorbing and sodium absorbing" cells (Choe et al., 2005, 2007; Reilly et al., 2011), while VHA-rich cells co-express an anion exchanger homologous to human pendrin (SLC26A4) and are considered "base-secreting, acid and chloride absorbing" cells (Piermarini et al., 2002; Reilly et al., 2011). Because NKA- and VHA-rich cells are specialized for active ion transport, both are thought to also be mitochondrion-rich (MR) cells (reviewed in Evans et al., 2005). However, only NKA-rich cells have been confirmed to also be MR cells, based on dual staining with anti-NKA antibodies and toluidine blue to highlight cell morphology (Wilson et al., 2002). While VHA-rich cells are typically assumed to also be MR cells based on their shape and location within the gill filament, there is no direct evidence supporting this assumption. It is also unknown whether all MR cells are either NKA- or VHA-rich cells or if other MR cell subtypes exist.

Normally, NKA is present in the cell basolateral membrane and VHA is located in cytoplasmic vesicles of elasmobranch gill cells. However, during experimentally induced blood alkalosis, VHA translocates into the basolateral membrane of dogfish gill cells (Tresguerres et al., 2005). The mechanism involves extra- and intracellular carbonic anhydrases that transfer increased plasma [HCO_3^-] inside gill cells (Gilmour et al., 2007; Tresguerres et al., 2007), where it is sensed by HCO_3^--sensitive soluble adenylyl cylcase to produce cAMP, which

Abbreviations: VHA, V-H^+-ATPase, vacuolar proton ATPase; NKA, Na^+/K^+-ATPase, sodium potassium ATPase; MR, mitochondrion-rich.

* Corresponding author.
E-mail address: mtresguerres@ucsd.edu (M. Tresguerres).

http://dx.doi.org/10.1016/j.cbpa.2014.04.003
1095-6433/

triggers VHA translocation (Tresguerres et al., 2010, 2014). Basolateral VHA absorbs H^+ into the blood and energizes HCO_3^- secretion to seawater, thus counteracting blood alkalosis. In dogfish, the VHA translocation is essential for compensating naturally occurring alkalosis such as during the post-feeding blood alkalosis (Tresguerres et al., 2007). As H^+ is secreted into the stomach to aid in food digestion, an equimolar amount of HCO_3^- is absorbed into the blood, thus causing metabolic alkalosis (Wood et al., 2005, 2009). Similar to dogfish infused with $NaHCO_3$, VHA in gills from fed dogfish translocates to the basolateral membrane in a timeframe that is consistent with absorption of H^+ into the blood and secretion of excess HCO_3^- into seawater (Tresguerres et al., 2007). Presumably, the VHA translocation helps shape the typical 'alkaline tide'. While the alkaline tide has only been studied in detail in dogfish, it likely also takes place in most other marine elasmobranchs. In particular, leopard sharks (*Triakis semifasciata*) increase H^+ secretion into the stomach after a meal (Papastamatiou and Lowe, 2004, 2005) and thus should also experience postprandial blood alkalosis.

Intracellular HCO_3^- in VHA-rich cells is presumably exchanged for seawater Cl^- *via* apical pendrin (slc26a4). However, while several studies have suggested an involvement of pendrin in chloride uptake in freshwater fish (Perry et al., 2009; Piermarini et al., 2002), pendrin function has not been studied in relation to A/B regulation in fish gills. Intriguingly, pendrin seems predominantly located on the apical pole, but not directly in the apical membrane of gill cells from Atlantic stingray (Piermarini et al., 2002) and bull sharks (Reilly et al., 2011) acclimated to seawater. This raises the possibility that pendrin, like VHA, is translocated to the cell membrane during alkalosis.

In this study, we used immunofluorescence to investigate MR cells in leopard shark gills. We immunolabeled leopard shark gills to determine: (1) if NKA- and VHA-rich cells are distinct subpopulations, (2) if both NKA- and VHA-rich cells are also MR cells, (3) if all MR cells are either NKA- or NKA-rich cells, (4) localization of the anion exchanger pendrin, and (5) if feeding results in translocation of ion-transporting proteins to the cell membrane.

2. Materials and methods

2.1. Experimental animals

All experiments were approved by the SIO-UCSD animal care committee under protocol number #S10320 in compliance with the IACUC guidelines for the care and use of experimental animals. Juvenile leopard sharks were born in the experimental aquarium at Scripps Institution of Oceanography (SIO) from pregnant females caught from La Jolla Shores, CA, USA. Sharks were housed in tanks with flowing seawater and were fed chopped squid or mackerel 3 times a week. Samples were collected 2–3 days after feeding.

2.2. Feeding experiments

A total of 8 juvenile leopard sharks were used (mean body mass 145.5 ± 8.4 g; mean length 34.3 ± 0.83 cm; 3 male, 5 female), with 4 sharks in each treatment (starved *vs.* fed). Sharks were starved for five days, after which 4 randomly selected sharks were sacrificed and gill tissue collected ("starved" treatment). The remaining sharks were force-fed with blended squid worth ~5% of their body weight. After 24 h, sharks were sacrificed and gill tissue collected ("fed" treatment). The 24 h-post feeding sampling time was selected based on leopard shark gastric pH dynamics after feeding (Papastamatiou and Lowe, 2004), as well as systemic pH dynamics after feeding in dogfish sharks (Wood et al., 2005). Together with another study in dogfish (Tresguerres et al., 2007), the literature indicates that branchial base secretion in sharks is maximal or near maximal around 24 h after feeding.

2.3. Tissue preparation

Specimens were euthanized by an overdose of tricaine methanesulfonate (0.5 $g \cdot L^{-1}$). Gill samples were fixed in 0.2 M cacodylate buffer, 3.2% paraformaldehyde, 0.3% glutaraldehyde for 6 h, transferred to 50% ethanol for 6 h, and stored in 70% ethanol until further processing for immunohistochemistry as described in Tresguerres et al. (2005).

2.4. Antibodies

Two commercially available anti-NKA antibodies were used for this study: monoclonal mouse anti-NKA antibodies raised against the chicken α-subunit (Developmental Studies Hybridoma Bank, Iowa City, IA, USA) and polyclonal rabbit anti-NKA antibodies raised against the mammalian α-subunit (Santa Cruz Biotechnology, Dallas, TX, USA). The mouse monoclonal anti-OxPhos antibody (Invitrogen, Grand Island, NY, USA) is against a highly conserved epitope in mitochondrial Complex IV, subunit 1. Antibodies against pendrin were raised against amino acids 630–643 from mammalian SLC26A4; these antibodies are known to specifically recognize pendrin from diverse elasmobranchs (Piermarini et al., 2002; Reilly et al., 2011). Custom-made polyclonal rabbit antibodies were against a conserved peptide in the VHA B-subunit (AREEVPGRRGFPGY). Fluorescent secondary antibodies goat anti-mouse Alexa Fluor 568 and goat anti-rabbit Alexa Fluor 488 were obtained from Invitrogen (Grand Island, NY, USA).

2.5. Western blot analysis

Frozen gill samples were weighed, immersed in liquid nitrogen, pulverized in a porcelain grinder, combined 1:10 w/v with ice-cold buffer (280 mM NaCl, 6 mM KCl, 5 mM $NaHCO_3$, 3 mM $MgCl_2$, 0.5 mM $NaSO_4$, 1 mM Na_2HPO_4, 350 mM urea, 70 mM trimethylamine N-oxide, 5 mM glucose, 1:100 protease inhibitor cocktail, Sigma), and homogenized using a glass homogenizer for 30 s. The sample was centrifuged at 3000 *g* for 10 min (4 °C) and the supernatant removed as the "crude homogenate fraction". Protein concentration was determined in triplicate using the Bradford method (Bio-Rad, Hercules, CA, USA). 5–20 μg of total protein was separated on 7.5% polyacrylamide mini gel (60 V 15 min, 200 V 45 min) and transferred to a polyvinylidene difluoride (PVDF) membrane (Bio-Rad). After transfer, PVDF membranes were incubated in blocking buffer (tris buffered saline, 1% tween, 5% milk) at room temperature for 1 h and incubated in the primary antibody at 4 °C overnight (anti-VHA = 1:1000). PVDF membranes were washed 3× and incubated in secondary antibody (1:10,000) at room temperature for 1 h. Bands were made visible through addition of ECL Prime Western Blotting Detection Reagent (GE Healthcare, Waukesha, WI, USA) and imaged and analyzed in a BioRad Universal III Hood using ImageQuant software (BioRad). PVDF membranes incubated in blocking buffer with anti-VHA antibodies and 10-fold excess blocking peptide served as control and did not show any bands.

2.6. Immunohistochemistry

Gills fixed and stored in 70% ethanol as described above were serially dehydrated in 95% ethanol (10 min), 100% ethanol (10 min), and xylene (3 × 10 min). Tissues were transferred from xylene to paraffin (55 °C) (3 × 30 min), after which paraffin blocks were left to solidify overnight. Sections were cut at 7 μm using a rotary microtome; three consecutive sections of each sample were placed on slides and left on a slide warmer (37 °C) overnight. Paraffin was removed in xylene (10 min × 3) and sections rehydrated in 100% ethanol (10 min), 95% ethanol (10 min), 70% ethanol (10 min), and PBS. Non-specific binding was reduced by incubating the sections in blocking buffer (PBS, 2% normal goat serum, 0.02% keyhole limpet hemocyanin, pH 7.8) for 1 h.

Sections were then incubated in the primary antibody overnight at 4 °C (dilutions: anti-NKA = 1:500; anti-VHA = 1:500; anti-OxPhos = 1:500; anti-pendrin = 1:20). Slides were washed 3× in PBS and sections incubated in the appropriate secondary antibody (1:500) at room temperature for 1 h; followed by incubation with the nuclear stain Hoechst 33342 (Invitrogen, Grand Island, NY, USA) (5 μg/mL) for 5 min. Slides were then washed 3× in PBS and sections were permanently mounted in Fluorogel with tris buffer (Electron Microscopy Sciences, Hatfield, PA, USA). Immunofluorescence was detected using an epifluorescence microscope (Zeiss AxioObserver Z1) connected to a metal halide lamp and appropriate filters. Some images were captured using structured illumination (Zeiss Apotome2). Digital images were adjusted, for brightness and contrast only, using Zeiss Axiovision software and Adobe Photoshop. Antigen retrieval was required for anti-pendrin, which involved incubating slides in heated (95 °C) citrate unmasking buffer (10 mM citric acid, 0.05% Tween20, pH 6.0) for 20 min following rehydration. For anti-VHA, control sections were incubated in blocking buffer with anti-VHA antibodies and 10-fold excess blocking peptide.

2.7. Dual immunolocalization of NKA and VHA

Mouse anti-NKA and rabbit (1:500) anti-VHA (1:500) antibodies were diluted together in blocking buffer and applied onto slides as described above. Goat anti-mouse Alexa-Fluor 568 (1:500) and goat anti-rabbit Alexa-Fluor 488 (1:500) were diluted together and used for the secondary antibody incubation. Controls used to eliminate the possibility of cross-reactivity between antibodies included incubation with both primary antibodies together with only one secondary antibody, incubation with one primary antibody and both secondary antibodies, and incubation with only secondary antibodies. Control sections only stained positive when the corresponding primary and secondary antibodies were combined and no cross-reactivity was observed.

2.8. Colocalization of mitochondria, NKA, and VHA

For double immunolabeling of NKA and OxPhos, or VHA and OxPhos, sections were incubated in a solution of rabbit anti-NKA or rabbit anti-VHA antibodies (1:500) combined with mouse anti-OxPhos antibody (1:500); secondary antibodies and controls were as described in the previous section.

Co-localization with all three antibodies was achieved over two days. Initially, NKA- and VHA-rich cells were labeled with respective primary rabbit antibodies. Following incubation overnight, sections were washed as described above, incubated in the secondary Alexa-Fluor 488 anti-rabbit antibodies (1 h, room temperature), and washed. Sections were then incubated with mouse anti-OxPhos antibodies overnight, and ultimately with Alexa-Fluor 568 anti-mouse antibodies. This procedure resulted in both NKA and VHA immunolabeled in green, and mitochondria immunolabeled in red.

2.9. Immunolocalization of pendrin to NKA- and VHA-rich cells

For immunolocalization of pendrin to NKA- or VHA-rich cells sections were first incubated in rabbit anti-pendrin. Following incubation overnight, sections were washed as described above, incubated in the appropriate secondary antibodies (1 h, room temperature), washed again and blocked. Sections were then incubated with either mouse anti-NKA or rabbit anti-VHA antibodies overnight, and completed as described above.

2.10. Quantification of VHA and pendrin translocation

For VHA and pendrin translocation analyses, the number of cells displaying cytoplasmic or distinct membrane immunostaining was counted (Tresguerres et al., 2006, 2010) (basolateral membrane for VHA, apical membrane for pendrin). For each of the 4 specimens from each treatment (starved, fed), 3 immunostained gill sections were analyzed and all cells with positive VHA (total number of cells analyzed = 1310; 614 starved group; 696 fed group) or pendrin (total number of cells analyzed = 1839; 771 starved group; 1068 fed group) staining were counted at 300× and 600× magnification. Cells with distinct signal in the basolateral (VHA) or apical (pendrin) membrane were considered as having "Membrane staining" for each protein. Cells without distinct membrane staining (cytoplasmic and intermediate staining, see Tresguerres et al., 2006, 2010) were grouped together as "Cytoplasmic staining" for each protein. Percentages of total cells with either membrane or cytoplasmic staining were transformed to the arcsine of the square root of the value before statistical analysis. To test for differences in localization between starved (n = 4) and fed (n = 4) groups, separate t-tests were conducted for VHA- and pendrin-positive cells. Data are given as mean ± SEM and statistical significance was set at $P < 0.05$.

3. Results

3.1. Dual immunolocalization of NKA and VHA

The custom rabbit polyclonal anti-VHA antibodies recognized a 55 kDa band on western blots and labeled cells along the interlamellar region of the gill filament, but did not in control blots and sections when the antibody was combined with the blocking peptide (Fig. 1). Immunoreactivity of NKA and VHA was present in separate cell populations in the gills of leopard sharks. The anti-NKA antibody resulted in distinct basolateral staining, and the anti-VHA antibody resulted in primarily cytoplasmic staining, with only a few cells (less than 1%) showing basolateral staining. Based on double labeling with anti-NKA and anti-VHA antibodies on the same gill sections, NKA- and VHA-rich cells are distinct cell types (Fig. 2).

3.2. Colocalization of NKA and VHA with mitochondria

Anti-OxPhos antibodies strongly labeled cells in interlamellar regions of leopard shark gills. MR cells were visible at short exposure time but at longer exposure times all cells displayed positive signal as expected since all cells contain mitochondria (Fig. 3A). Cells with strong Oxphos signal also had strong NKA or VHA signal, indicating both NKA- and VHA-rich cells are also MR cells (Fig. 3B, C). To determine if NKA- and VHA-rich cells are the only MR cell subtypes present in leopard shark gills, NKA, VHA (both in green), and OxPhos (in red) were immunolabeled on the same section. The results showed that all MR cells are either NKA- or VHA-rich cells (Fig. 4).

3.3. Immunolocalization of pendrin in VHA-rich cells

In starved sharks, pendrin immunoreactivity was present in the apical pole (but not in the apical membrane) of cells along the interlamellar region. Pendrin immunoreactivity was specific to VHA-rich cells (Fig. 5A), with colocalization of pendrin and VHA found near the apical pole of VHA-rich cells (Fig. 5B). Pendrin was not present in NKA-rich cells (Fig. 5C).

3.4. Translocation of VHA and pendrin in gills from fed sharks

In starved leopard sharks, VHA and pendrin immunoreactivity was almost exclusively present in the cytoplasm (Fig. 6A, B; Table 1). However, feeding induced translocation of VHA to the basolateral membrane and pendrin to the apical membrane in a fraction of MR cells (Fig. 6C, D; Table 1). Optical sectioning and z-stack reconstruction confirmed membrane localization of both VHA and pendrin after feeding (Fig. 7).

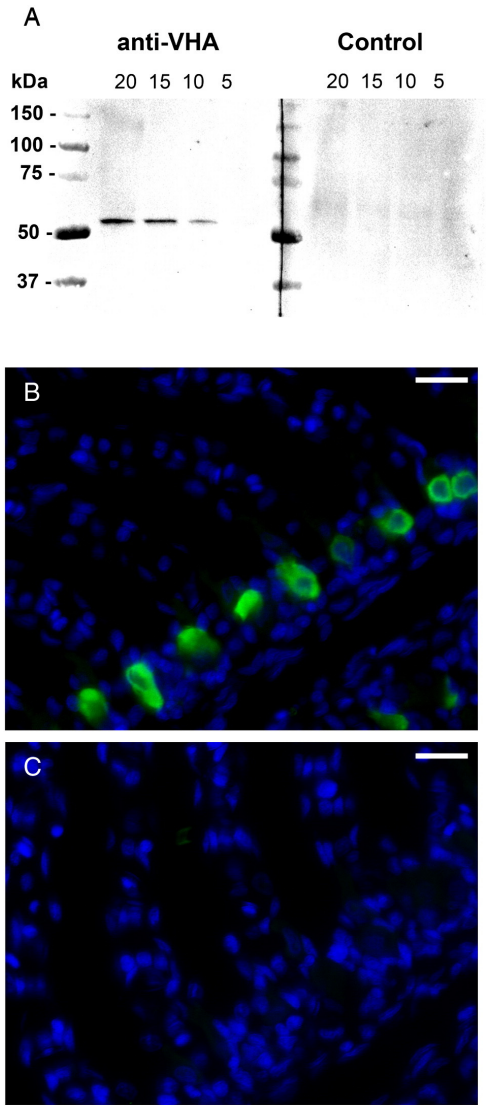

Fig. 1. Specificity of the anti-VHA antibodies in leopard shark gills. A) Western blot with gill crude homogenate showing a single and specific 55 kDa band when 20, 15, and 10 μg of total protein were loaded, but, at this exposure time, not in 5 μg (anti-VHA). The band was not evident when the antibodies were preincubated with excess blocking peptide (Control). B) VHA immunoreactivity in cells along the interlamellar region of a gill section. C) No signal was evident in the consecutive section treated anti-VHA antibodies preincubated with excess blocking peptide. VHA in green, nuclei in blue. Scale bar = 20 μm. (For interpretation of the references to color in this figure legend, the reader is referred to the web version of this article.)

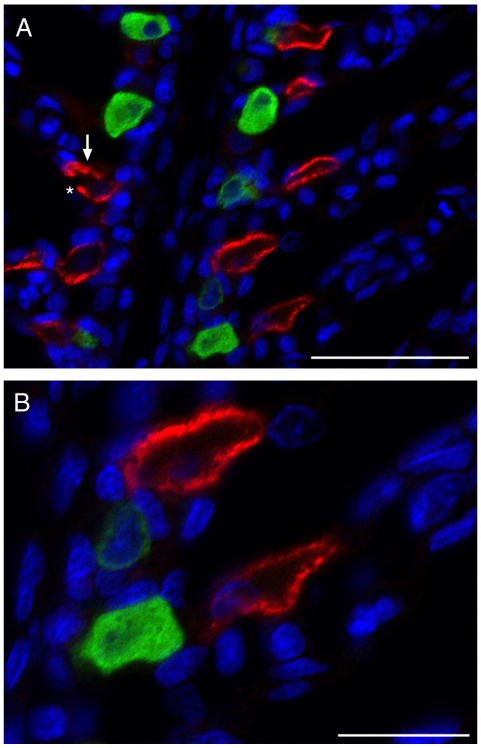

Fig. 2. NKA- and VHA-rich cells in leopard shark gills. Dual immunolocalization of NKA (red) and VHA (green), with NKA immunoreactivity along the basolateral membrane and VHA immunoreactivity diffuse throughout the cytoplasm. NKA- and VHA-rich cells were always observed as separate populations. An arrow and asterisk indicate basolateral and apical membranes on a representative cell, respectively. Nuclei in blue. Scale bar = 50 μm (A) or 20 μm (B). (For interpretation of the references to color in this figure legend, the reader is referred to the web version of this article.)

4. Discussion

Our results show that leopard shark gills have two distinct populations of NKA- and VHA-rich cells (likely acid- and base-secreting, respectively) (Evans et al., 2005; Tresguerres et al., 2005). We also established that both NKA- and VHA-rich cells are MR cells; to our knowledge this is the first time that this has been shown conclusively for elasmobranch VHA-rich cells. Additionally, we showed that all MR cells in leopard shark gills are either NKA- or VHA-rich, suggesting all MR cells are either acid- or base-secreting. Further exploration revealed that pendrin is exclusively localized in VHA-rich cells. Lastly, feeding induced VHA translocation from cytoplasmic vesicles to the basolateral membrane and pendrin translocation to the apical membrane of a fraction of leopard shark gill cells.

4.1. NKA- and VHA-rich cells are MR cells

NKA immunoreactivity was always along the basolateral membrane and VHA immunoreactivity was generally distributed throughout the cytoplasm. NKA and VHA were expressed in separate cells, similar to Atlantic stingray (Piermarini et al., 2002; Piermarini and Evans, 2001), dogfish shark (Tresguerres et al., 2005), and bull shark (Reilly et al., 2011). The presence of NKA and VHA in two distinct cell populations separates elasmobranchs from teleost fishes. In freshwater teleosts, simultaneous expression of NKA and VHA is thought to drive Na^+ uptake and NH_3 excretion during osmoregulation and nitrogen balance (Evans, 2011), and has been shown in gills from rainbow trout (Galvez et al., 2002; Lin et al., 1994; Wilson et al., 2000a), killifish (Katoh et al., 2003), mudskipper (Wilson et al., 2000b), zebrafish (Liao et al., 2009), and several species of intertidal blennies (Uchiyama et al., 2012). Marine teleost gills also have several types of NKA-rich cells and although

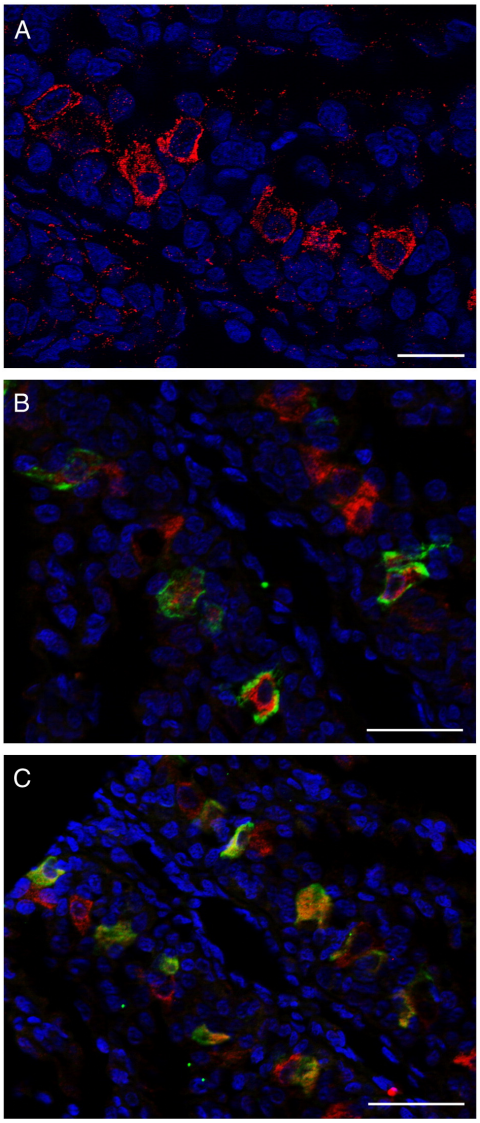

Fig. 3. NKA-, VHA-, and mitochondrion-rich (MR) cells in leopard shark gills. (A) MR cells, evident by strong anti-OxPhos immunoreactivity, were present along the interlamellar gill region. At longer exposure times all cells displayed a positive signal. Colocalization of NKA (B, green) or VHA (C, green) and MR cells (red) indicated that NKA- and VHA-rich cells are also MR cells. Nuclei in blue. Scale bar = 50 μm. (For interpretation of the references to color in this figure legend, the reader is referred to the web version of this article.)

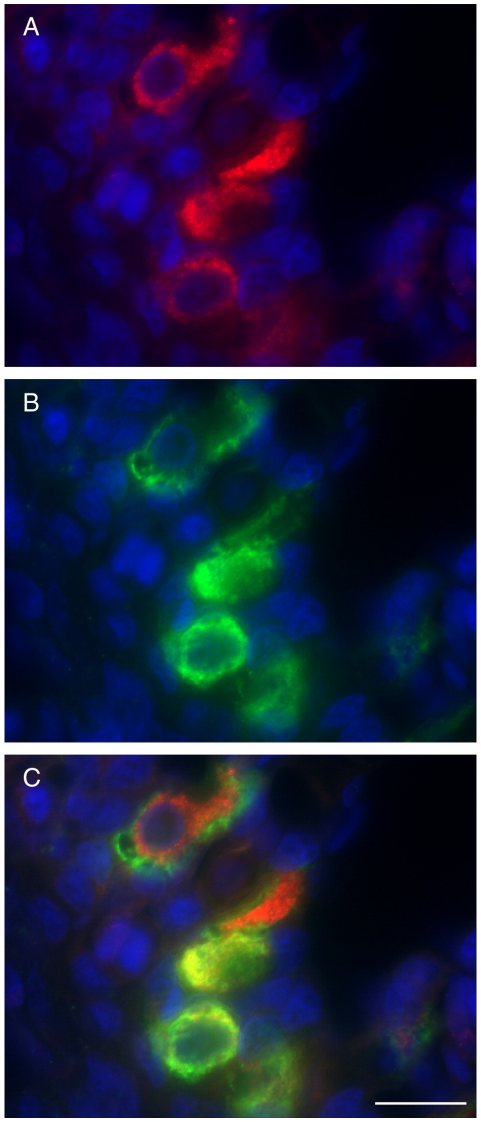

Fig. 4. Mitochondrion-rich (MR) cell types in leopard shark gills are enriched for NKA or VHA. Mitochondrial complex IV, indicative of MR cells (A, red) and NKA- and VHA-rich cells (B, both in green) were present throughout the interlamellar region. (C) MR cells were enriched in either NKA (distinct green signal along the basolateral membrane) or VHA (diffuse green signal throughout the cytoplasm, seen as yellow due to colocalization with mitochondrial complex IV (red). Nuclei in blue. Scale bar = 20 μm. (For interpretation of the references to color in this figure legend, the reader is referred to the web version of this article.)

not widely reported, NKA and VHA may co-localize in the same cell as observed in a small population of branchial MR cells from longhorn sculpin (Catches et al., 2006). Thus, unlike teleost gill cells that carry out multiple ion-transporting functions and may express both pumps simultaneously, elasmobranch NKA- and VHA-rich cells are separate cell types specialized for A/B regulation.

To explore if NKA- and VHA-rich cells were also MR cells, we immunolabeled mitochondrial Complex IV (OxPhos) in leopard shark gills. Previously, MR cells were typically identified using qualitative structural analysis (Wilson et al., 1997, 2000b), vital dyes such as mitotracker (Galvez et al., 2002), or based on high NKA abundance (Edwards et al., 2002). Our results show it is possible to visualize MR cells by immunolabeling. Since Complex IV ("cytochrome c oxidase") is a highly conserved enzyme, these antibodies are useful in labeling MR cells from diverse species. In fact, our laboratory has successfully

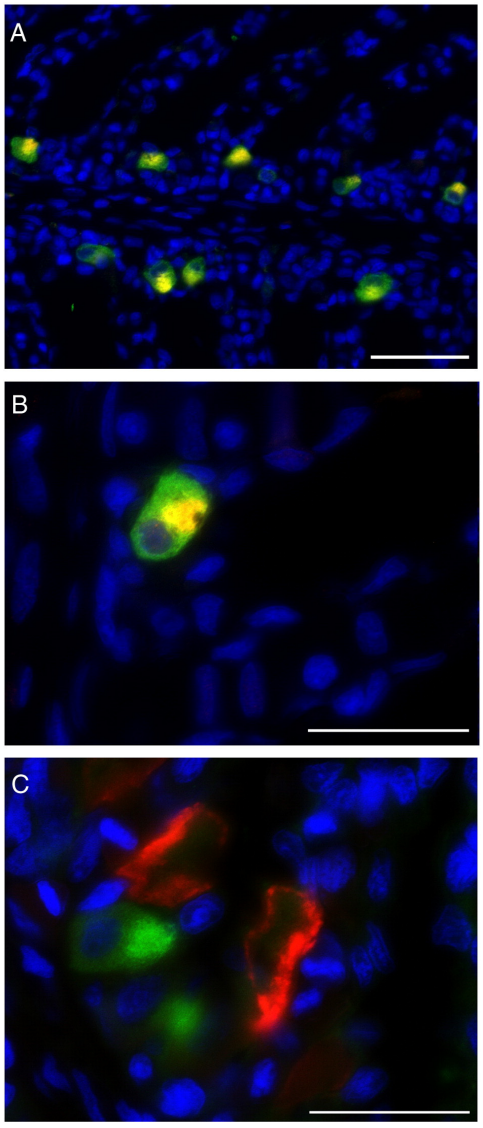

Fig. 5. Pendrin and VHA- or NKA-rich cells. A) Pendrin (red) and VHA (green) colocalization (yellow) was observed in gill cells along the interlamellar region. B) Pendrin immunoreactivity observed in the apical pole (but not in the membrane) of gill cells. C) Pendrin (green) and NKA (red) did not colocalize to the same cell. Nuclei in blue. Scale bar = 50 μm (A) or 20 μm (B, C). (For interpretation of the references to color in this figure legend, the reader is referred to the web version of this article.)

used these antibodies in shark (this study), worm and coral tissues (unpublished observations). Although all cells have mitochondria, MR cells can be identified by intense OxPhos immunoreactivity at short exposure times. Numerous MR cells were observed along the interlamellar region of the gill; colocalization of OxPhos with NKA or VHA revealed that NKA- and VHA-rich cells were also MR cells. Additionally, prior to this study, the number of MR cell subtypes in elasmobranch gills was unknown; but we show here that there are two MR cell subtypes: NKA- and VHA-rich cells. However, we cannot rule out the existence of MR, NKA- or VHA-rich, cell subtypes (*i.e.* cells that express either ATPase and differentially express other proteins).

Next, we investigated the relationship between NKA- and VHA-rich MR cells and another other ion-transporting protein, the anion exchanger pendrin. Pendrin immunoreactivity was present near the apical pole of a subset of gill cells and colocalized with VHA-rich cells (but not NKA-rich cells). These results support the hypothesis (Piermarini et al., 2002) that shark gill VHA-rich cells are functionally analogous to the mammalian base-secreting β-intercalated renal cells, which also express VHA and pendrin (Royaux et al., 2001). Since VHA-rich cells in shark gills are by far more abundant than in mammalian kidneys, they represent an excellent model for the study of cellular mechanisms for base secretion and further efforts should be pursued for developing cell cultures of these cells.

4.2. The effect of feeding on VHA and pendrin sub-cellular localization

Feeding induced translocation of VHA to the basolateral membrane, and of pendrin to the apical membrane in a fraction of gill cells from leopard sharks. Based on other established models for ion transport and A/B regulation such as dogfish (Tresguerres et al., 2005, 2006, 2007, 2010), bull shark (Reilly et al., 2011), and Atlantic stingray (Piermarini et al., 2002) gills, as well as mammalian kidney (Paunescu et al., 2008; Royaux et al., 2001), we expect that translocation of VHA and pendrin leads to upregulation of HCO_3^- secretion and H^+ absorption. In dogfish, feeding induces a pronounced blood alkalosis that is fully compensated ~24 h later ('alkaline tide') (Wood et al., 2005, 2009). Previous reports suggest that leopard sharks also undergo a post-feeding alkalosis (Papastamatiou and Lowe, 2004, 2005). Therefore, it is reasonable to assume that the translocation of VHA to the basolateral membrane and of pendrin to the apical membrane is a compensatory response to blood alkalosis.

The actual fraction of cells demonstrating VHA and pendrin translocation is likely proportional to the blood A/B stress. For example, distinct VHA translocation to the basolateral membrane occurred in 85% of VHA-positive gill cells from 12 h base-infused dogfish sharks, while it only occurred in 56% of VHA-positive cells in 6 h base-infused sharks (Tresguerres et al., 2006). Comparatively, sharks in our study demonstrated distinct VHA and pendrin translocation in ~10% of cells. This is likely explained by feeding inducing a much milder alkalosis compared to experimental base-infusion. We only quantified cells that had most VHA and pendrin in the cell membrane (distinct membrane staining) to conservatively consider cells that had became activated for HCO_3^- secretion. However, protein translocation is a dynamic and graded mechanism, and some of the cells that we categorized as "Cytoplasmic staining" likely had higher amounts of VHA and pendrin in their membranes compared to starved fish. Thus, our quantification method most likely underestimated the number of cells involved in base secretion.

To our knowledge, this is the first report of pendrin insertion into the apical membrane in response to alkalosis in an intact organism. However, cAMP-dependent translocation of pendrin to the apical membrane has previously been reported in rat cortical collecting duct (CCD) cells (Azroyan et al., 2012). Reports of VHA translocation to the cell membrane are more common, and they include translocation to the apical membrane in kidney (Gong et al., 2010; Paunescu et al., 2008), epididymis (Pastor-Soler et al., 2003), intestinal lumen (Collaco et al., 2013), blowfly salivary glands (Dames et al., 2006), and gills of the green shore crab (Weihrauch et al., 2002). In those organs, apical VHA secretes acid for diverse purposes such as blood A/B regulation, sperm inactivation, and ammonia excretion. In addition, VHA in sternal cells from the isopod *Pocellio scaber* is basolateral during $CaCO_3$ secretion and apical during $CaCO_3$ resorption (Ziegler et al., 2004). Translocation of VHA from the cytoplasm to the basolateral membrane has only been previously described in detail in dogfish gill cells (see Introduction); the

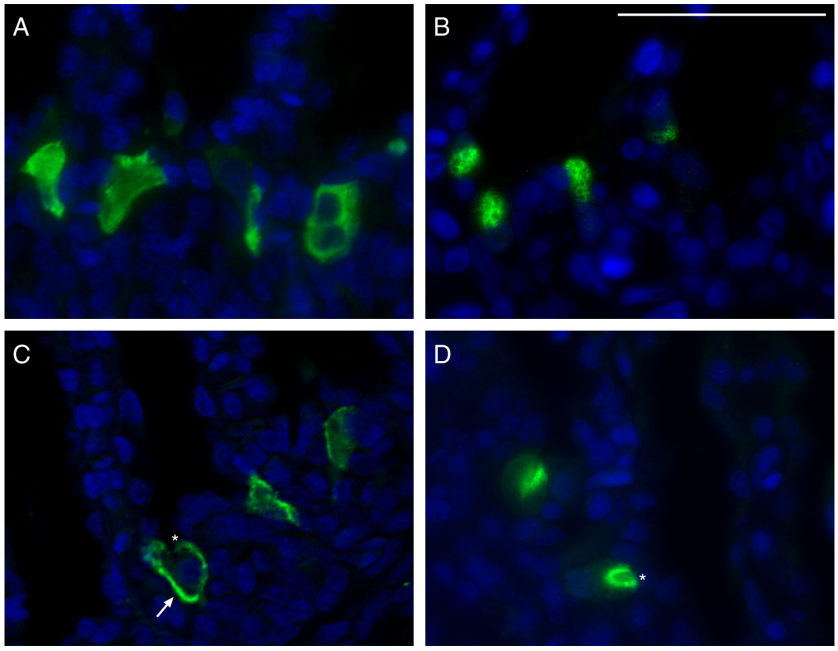

Fig. 6. VHA and pendrin immunoreactivity in the gills of starved and fed sharks. Representative images of cytoplasmic VHA (A) and pendrin (B) immunoreactivity in the gills of starved sharks. In fed sharks, VHA translocated to the basolateral membrane (C) and pendrin translocated to the apical membrane (D). An arrow and asterisks indicate basolateral and apical membranes on representative cells, respectively. VHA and pendrin in green, nuclei in blue. Scale bar = 20 μm. (For interpretation of the references to color in this figure legend, the reader is referred to the web version of this article.)

current report suggests that it is a generalized mechanism to upregulate base secretion in elasmobranchs.

Importantly, translocation of pre-existing VHA protein, without the need for increased protein abundance, is enough to compensate for experimentally-induced, 6 h acute alkalosis (Tresguerres et al., 2006), as well as for dealing with post-feeding alkalosis (Tresguerres et al., 2007). For example, total VHA protein abundance did not change in gills from post-fed and 6 h base-infused dogfish sharks; but VHA protein abundance in the membrane increased significantly. Therefore, in the case of VHA and probably also pendrin, it is likely that protein translocation (not changes in gene expression) is more important during short term and physiological relevant changes in A/B status. Mechanisms such as protein translocation would not be evident using increasingly popular transcriptomic techniques such as qPCR or RNAseq, highlighting the importance of immunolocalization studies.

Table 1
Sub-cellular localization of VHA and pendrin in gills from starved and fed leopard sharks.

	Cytoplasmic (%)		Membrane (%)	
	Starved	Fed	Starved	Fed
VHA	99.49 ± 0.33	87.43 ± 0.73*	0.51 ± 0.33	12.57 ± 0.73*
Pendrin	99.83 ± 0.17	91.96 ± 2.51*	0.17 ± 0.17	8.04 ± 2.51*

Values for starved (n = 4) and fed (n = 4) sharks show percentage of cells demonstrating cytoplasmic, apical membrane (pendrin) or basolateral membrane (VHA) localization. Total number of cells analyzed, VHA = 1310 and pendrin = 1839.
* Indicate a statistically significant difference compared to the respective starved group (t-test, see Materials and methods for details on data transformation).

5. Conclusions

In summary, our results showed that leopard shark gills, like all other elasmobranchs studied so far, have separate acid-secreting NKA-rich cells, and base-secreting VHA- and pendrin-rich cells. Our results also showed that these two cell types constitute all MR cells in the gill epithelium. However, we cannot discard the existence of further subtypes that differentially express other ion-transporting proteins or regulatory properties. The observed translocation of pendrin to the apical membrane in fed fish, together with the previously described VHA translocation to the basolateral membrane, indicates that translocation of multiple ion-transporting proteins to different regions within a cell is an important mechanism for the regulation of blood A/B status. This would be a dynamic and energetically efficient mechanism, and in some cases it may be more physiologically relevant compared to regulation of gene expression.

Acknowledgments

We thank Mr. Phil Zerofski (SIO) for his excellent assistance with aquarium matters, and Ms. Lara Jansen and Mr. Jason Ho for helping with shark husbandry and experiments. Special thanks to Dr. Jonathan Wilson (CIIMAR, Portugal) for supplying the anti-pendrin antibodies. This work was supported by SIO funds and an Alfred P. Sloan Foundation Research Fellowship (grant #BR2013-103) to MT, an American Physiological Society Undergraduate Summer Research Fellowship to CM, and a California State University Sally Casanova Pre-Doctoral scholarship, San Diego Fellowship, and NIH Training Grant in Marine Biotechnology (GM067550) to JNR.

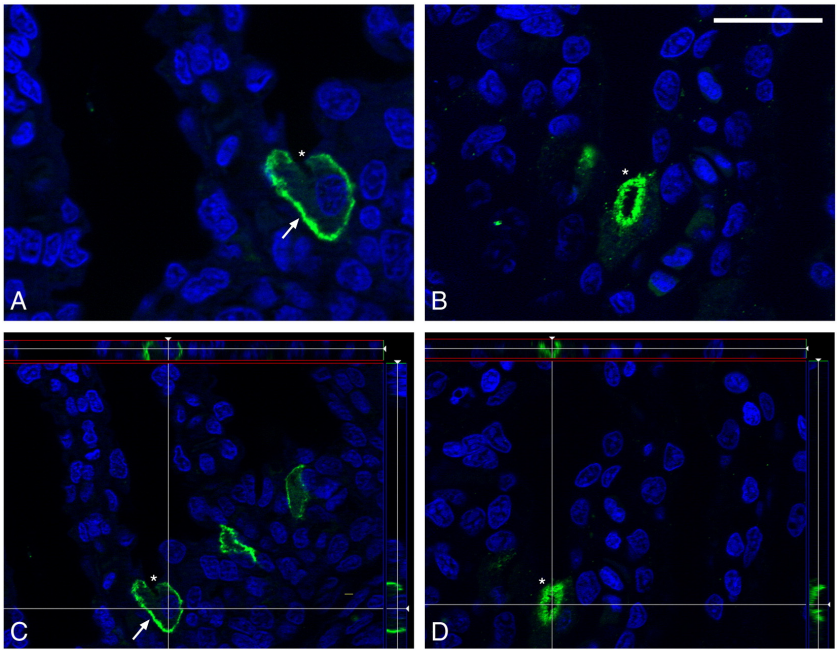

Fig. 7. Membrane localization of VHA and pendrin after feeding. Representative images of VHA in the basolateral membrane (A) and pendrin in the apical membrane (B) of branchial cells of fed leopard sharks. Images captured using optical sectioning and a Z-stack reconstruction of multiple images confined VHA (C) and pendrin (D) immunoreactivity to the membrane of its respective cell. Arrows and asterisks indicate basolateral and apical membranes on representative cells, respectively. VHA and pendrin in green, nuclei in blue. Scale bar = 20 μm. (For interpretation of the references to color in this figure legend, the reader is referred to the web version of this article.)

References

Azroyan, A., Morla, L., Crambert, G., Laghmani, K., Ramakrishnan, S., Edwards, A., Doucet, A., 2012. Regulation of pendrin by cAMP: possible involvement in β-adrenergic-dependent NaCl retention. Am. J. Physiol. Ren. Physiol. 302, F1180–F1187.

Catches, J.S., Burns, J.M., Edwards, S.L., Claiborne, J.B., 2006. Na^+/H^+ antiporter, V-H^+-ATPase and Na^+/K^+-ATPase immunolocalization in a marine teleost (*Myoxocephalus octodecemspinosus*). J. Exp. Biol. 209, 3440–3447.

Choe, K.P., Kato, A., Hirose, S., Plata, C., Sindic, A., Romero, M.F., Claiborne, J.B., Evans, D.H., 2005. NHE3 in an ancestral vertebrate: primary sequence, distribution, localization, and function in gills. Am. J. Physiol. Regul. Integr. Comp. Physiol. 289, R1520–R1534.

Choe, K.P., Edwards, S.L., Claiborne, J.B., Evans, D.H., 2007. The putative mechanism of Na(+) absorption in euryhaline elasmobranchs exists in the gills of a stenohaline marine elasmobranch, *Squalus acanthias*. Comp. Biochem. Physiol. A Mol. Integr. Physiol. 146, 155–162.

Collaco, A.M., Geibel, P., Lee, B.S., Geibel, J.P., Ameen, N.A., 2013. Functional vacuolar ATPase (V-ATPase) proton pumps traffic to the enterocyte brush border membrane and require CFTR. Am. J. Physiol. Cell Physiol. 305, C981–C996.

Dames, P., Zimmermann, B., Schmidt, R., Rein, J., Voss, M., Schewe, B., Walz, B., Baumann, O., 2006. cAMP regulates plasma membrane vacuolar-type H^+-ATPase assembly and activity in blowfly salivary glands. Proc. Natl. Acad. Sci. U. S. A. 103, 3926–3931.

Edwards, S.L., Donald, J.A., Toop, T., Donowitz, M., Tse, C.-M., 2002. Immunolocalisation of sodium/proton exchanger-like proteins in the gills of elasmobranchs. Comp. Biochem. Physiol. A Mol. Integr. Physiol. 131, 257–265.

Evans, D.H., 2011. Freshwater fish gill ion transport: August Krogh to morpholinos and microprobes. Acta Physiol. (Oxf.) 202, 349–359.

Evans, D.H., Piermarini, P.M., Choe, K.P., 2005. The multifunctional fish gill: dominant site of gas exchange, osmoregulation, acid-base regulation, and excretion of nitrogenous waste. Physiol. Rev. 85, 97–177.

Galvez, F., Reid, S.D., Hawkings, G., Goss, G.G., 2002. Isolation and characterization of mitochondria-rich cell types from the gill of freshwater rainbow trout. Am. J. Physiol. Regul. Integr. Comp. Physiol. 282, R658–R668.

Gilmour, K.M., Bayaa, M., Kenney, L., McNeill, B., Perry, S.F., 2007. Type IV carbonic anhydrase is present in the gills of spiny dogfish (*Squalus acanthias*). Am. J. Physiol. Regul. Integr. Comp. Physiol. 292, R556–R567.

Gong, F., Alzamora, R., Smolak, C., Li, H., Naveed, S., Neumann, D., Hallows, K.R., Pastor-Soler, N.M., 2010. Vacuolar H^+-ATPase apical accumulation in kidney intercalated cells is regulated by PKA and AMP-activated protein kinase. Am. J. Physiol. Ren. Physiol. 298, F1162–F1169.

Heisler, N., 1988. Acid-base regulation. In: Shuttleworth, T.J. (Ed.), Physiology of Elasmobranch Fishes. Springer:Verlag, Berlin, pp. 215–252.

Katoh, F., Hyodo, S., Kaneko, T., 2003. Vacuolar-type proton pump in the basolateral plasma membrane energizes ion uptake in branchial mitochondria-rich cells of killifish *Fundulus heteroclitus*, adapted to a low ion environment. J. Exp. Biol. 206, 793–803.

Liao, B.-K., Chen, R.-D., Hwang, P.-P., 2009. Expression regulation of Na^+–K^+-ATPase alpha1-subunit subtypes in zebrafish gill ionocytes. Am. J. Physiol. Regul. Integr. Comp. Physiol. 296, R1897–R1906.

Lin, H., Pfeiffer, D., Vogl, A.W., Pan, J., Randall, D.J., 1994. Immunolocalization of H^+-ATPase in the gill epithelia of rainbow trout. J. Exp. Biol. 195, 169–183.

Papastamatiou, Y.P., Lowe, C.G., 2004. Postprandial response of gastric pH in leopard sharks (*Triakis semifasciata*) and its use to study foraging ecology. J. Exp. Biol. 207, 225–232.

Papastamatiou, Y.P., Lowe, C.G., 2005. Variations in gastric acid secretion during periods of fasting between two species of shark. Comp. Biochem. Physiol. A Mol. Integr. Physiol. 141, 210–214.

Pastor-Soler, N., Beaulieu, V., Litvin, T.N., Da Silva, N., Chen, Y., Brown, D., Buck, J., Levin, L. R., Breton, S., 2003. Bicarbonate-regulated adenylyl cyclase (sAC) is a sensor that regulates pH-dependent V-ATPase recycling. J. Biol. Chem. 278, 49523–49529.

Paunescu, T.G., Da Silva, N., Russo, L.M., McKee, M., Lu, H.A.J., Breton, S., Brown, D., 2008. Association of soluble adenylyl cyclase with the V-ATPase in renal epithelial cells. Am. J. Physiol. Ren. Physiol. 294, F130–F138.

Perry, S.F., Vulesevic, B., Grosell, M., Bayaa, M., 2009. Evidence that SLC26 anion transporters mediate branchial chloride uptake in adult zebrafish (*Danio rerio*). Am. J. Physiol. Regul. Integr. Comp. Physiol. 297, R988–R997.

Piermarini, P.M., Evans, D.H., 2001. Immunochemical analysis of the vacuolar proton-ATPase B-subunit in the gills of a euryhaline stingray (*Dasyatis sabina*): effects of salinity and relation to Na(+)/K(+)-ATPase. J. Exp. Biol. 204, 3251–3259.

Piermarini, P.M., Verlander, J.W., Royaux, I.E., Evans, D.H., 2002. Pendrin immunoreactivity in the gill epithelium of a euryhaline elasmobranch. Am. J. Physiol. Regul. Integr. Comp. Physiol. 283, R983–R992.

Reilly, B.D., Cramp, R.L., Wilson, J.M., Campbell, H.A., Franklin, C.E., 2011. Branchial osmoregulation in the euryhaline bull shark, *Carcharhinus leucas*: a molecular analysis of ion transporters. J. Exp. Biol. 214, 2883–2895.

Royaux, I.E., Wall, S.M., Karniski, L.P., Everett, L.A., Suzuki, K., Knepper, M.A., Green, E.D., 2001. Pendrin, encoded by the Pendred syndrome gene, resides in the apical region of renal intercalated cells and mediates bicarbonate secretion. Proc. Natl. Acad. Sci. U. S. A. 98, 4221–4226.

Tresguerres, M., Katoh, F., Fenton, H., Jasinska, E., Goss, G.G., 2005. Regulation of branchial V-H^+-ATPase, Na^+/K^+-ATPase and NHE2 in response to acid and base infusions in the Pacific spiny dogfish (*Squalus acanthias*). J. Exp. Biol. 208, 345–354.

Tresguerres, M., Parks, S.K., Katoh, F., Goss, G.G., 2006. Microtubule-dependent relocation of branchial V-H^+-ATPase to the basolateral membrane in the Pacific spiny dogfish (*Squalus acanthias*): a role in base secretion. J. Exp. Biol. 209, 599–609.

Tresguerres, M., Parks, S.K., Wood, C.M., Goss, G.G., 2007. V-H^+-ATPase translocation during blood alkalosis in dogfish gills: interaction with carbonic anhydrase and involvement in the postfeeding alkaline tide. Am. J. Physiol. Regul. Integr. Comp. Physiol. 292, R2012–R2019.

Tresguerres, M., Parks, S.K., Salazar, E., Levin, L.R., Goss, G.G., Buck, J., 2010. Bicarbonate-sensing soluble adenylyl cyclase is an essential sensor for acid/base homeostasis. Proc. Natl. Acad. Sci. U. S. A. 107, 442–447.

Tresguerres, M., Barott, K.L., Barron, M.E., Roa, J.N., 2014. Established and potential physiological roles of bicarbonate-sensing soluble adenylyl cyclase (sAC) in aquatic animals. J. Exp. Biol. 217, 663–672.

Uchiyama, M., Komiyama, M., Yoshizawa, H., 2012. Structures and immunolocalization of Na^+, K^+-ATPase, Na^+/H^+ exchanger 3 and vacuolar-type H^+-ATPase in the gills of blennies (Teleostei: Blenniidae) inhabiting rocky intertidal areas. J. Fish Biol. 80, 2236–2252.

Weihrauch, D., Ziegler, A., Siebers, D., Towle, D.W., 2002. Active ammonia excretion across the gills of the green shore crab *Carcinus maenas*: participation of Na^+/K^+-ATPase, V-type H^+-ATPase and functional microtubules. J. Exp. Biol. 205, 2765–2775.

Wilson, J.M., Randall, D.J., Vogl, A.W., Iwama, G.K., 1997. Immunolocalization of proton-ATPase in the gills of the elasmobranch, *Squalus acanthias*. J. Exp. Zool. 278, 78–86.

Wilson, J.M., Laurent, P., Tufts, B.L., Benos, D.J., Donowitz, M., Vogl, A.W., Randall, D.J., 2000a. NaCl uptake by the branchial epithelium in freshwater teleost fish: an immunological approach to ion-transport protein localization. J. Exp. Biol. 203, 2279–2296.

Wilson, J.M., Randall, D.J., Donowitz, M., Vogl, A.W., Ip, A.K., 2000b. Immunolocalization of ion-transport proteins to branchial epithelium mitochondria-rich cells in the mudskipper (*Periophthalmodon schlosseri*). J. Exp. Biol. 203, 2297–2310.

Wilson, J.M., Morgan, J.D., Vogl, A.W., Randall, D.J., 2002. Branchial mitochondria-rich cells in the dogfish *Squalus acanthias*. Comp. Biochem. Physiol. A Mol. Integr. Physiol. 132, 365–374.

Wood, C.M., Kajimura, M., Mommsen, T.P., Walsh, P.J., 2005. Alkaline tide and nitrogen conservation after feeding in an elasmobranch (*Squalus acanthias*). J. Exp. Biol. 208, 2693–2705.

Wood, C.M., Schultz, A.G., Munger, R.S., Walsh, P.J., 2009. Using omeprazole to link the components of the post-prandial alkaline tide in the spiny dogfish, *Squalus acanthias*. J. Exp. Biol. 212, 684–692.

Ziegler, A., Weihrauch, D., Hagedorn, M., Towle, D.W., Bleher, R., 2004. Expression and polarity reversal of V-type H^+-ATPase during the mineralization-demineralization cycle in *Porcellio scaber* sternal epithelial cells. J. Exp. Biol. 207, 1749–1756.

Chapter II, in full, is a reprint of the material as it appears in the following citation: Roa JN, Munévar CL, Tresguerres M. 2014. Feeding induces translocation of vacuolar proton ATPase and pendrin to the membrane of leopard shark (*Triakis semifasciata*) mitochondrion-rich gill cells. Comparative Biochemistry and Physiology, Part A: Molecular and Integrative Physiology 174: 29–37. doi: 10.1016/j.cbpa.2014.04.003. The dissertation author was the primary investigator and author of this paper.

CHAPTER III

Soluble adenylyl cyclase is an acid-base sensor in epithelial base-secreting cells

Am J Physiol Cell Physiol 311: C340–C349, 2016.
First published June 22, 2016; doi:10.1152/ajpcell.00089.2016.

Soluble adenylyl cyclase is an acid-base sensor in epithelial base-secreting cells

Jinae N. Roa and Martin Tresguerres

Marine Biology Research Division, Scripps Institution of Oceanography, University of California San Diego, La Jolla, California

Submitted 31 March 2016; accepted in final form 16 June 2016

Roa JN, Tresguerres M. Soluble adenylyl cyclase is an acid-base sensor in epithelial base-secreting cells. *Am J Physiol Cell Physiol* 311: C340–C349, 2016. First published June 22, 2016; doi:10.1152/ajpcell.00089.2016.—Blood acid-base regulation by specialized epithelia, such as gills and kidney, requires the ability to sense blood acid-base status. Here, we developed primary cultures of ray (*Urolophus halleri*) gill cells to study mechanisms for acid-base sensing without the interference of whole animal hormonal regulation. Ray gills have abundant base-secreting cells, identified by their noticeable expression of vacuolar-type H^+-ATPase (VHA), and also express the evolutionarily conserved acid-base sensor soluble adenylyl cyclase (sAC). Exposure of cultured cells to extracellular alkalosis (pH 8.0, 40 mM HCO_3^-) triggered VHA translocation to the cell membrane, similar to previous reports in live animals experiencing blood alkalosis. VHA translocation was dependent on sAC, as it was blocked by the sAC-specific inhibitor KH7. Ray gill base-secreting cells also express transmembrane adenylyl cyclases (tmACs); however, tmAC inhibition by 2′,5′-dideoxyadenosine did not prevent alkalosis-dependent VHA translocation, and tmAC activation by forskolin reduced the abundance of VHA at the cell membrane. This study demonstrates that sAC is a necessary and sufficient sensor of extracellular alkalosis in ray gill base-secreting cells. In addition, this study indicates that different sources of cAMP differentially modulate cell biology.

soluble adenylyl cyclase; pH sensing; proton pump; cAMP; gill

REGULATION OF SYSTEMIC acid-base status is essential for animal homeostasis. Vertebrates developed specialized epithelia that transport H^+, HCO_3^-, and other acid-base-relevant ions between the blood and the external environment, thus maintaining a stable internal milieu (14, 20, 35). For example, specialized cells in kidney and gill epithelia either secrete H^+ and absorb HCO_3^- to correct blood acidosis or secrete HCO_3^- and absorb H^+ to correct blood alkalosis (13, 47). Regulation and coordination of H^+ and HCO_3^- secretion and absorption rely on the ability of these cells to sense blood acid-base status; however, the molecular and cellular sensing mechanisms are largely unknown. Soluble adenylyl cyclase (sAC, adcy10) is one of the few evolutionarily conserved acid-base sensors identified to date (7, 10). Like the traditional transmembrane adenylyl cyclases (tmACs, adcy1-9), sAC produces cAMP and, therefore, can potentially modulate multiple aspects of cell biology via PKA-dependent phosphorylation, exchange protein regulated by cAMP, and cyclic nucleotide-gated channels (42). However, unlike tmACs, which are modulated by hormonal/G protein-coupled receptor (GPCR) pathways, sAC activity is, instead, directly responsive to CO_2, pH, and HCO_3^- levels (38). The fact that sAC and tmACs can coexist in the same cell raises the following question: How can the same messenger molecule, in this case cAMP, modulate multiple aspects of cell biology in a coordinated fashion? A potential explanation involves "cAMP microdomains," each with a distinct source of cAMP and phosphodiesterases that restrict cross-communication of cAMP from the different sources (reviewed in Refs. 11 and 42).

In α-intercalated cells (α-ICs) of the mammalian kidney distal tubule, sAC colocalizes with vacuolar-type H^+-ATPase (VHA) at the apical pole (14, 20, 26, 35). In isolated α-ICs, cell-permeable cAMP induced insertion of VHA into the apical membrane, as well as elongation of microvilli and upregulation of H^+ secretion (13, 27, 47), and in α-ICs from kidney slices, addition of the sAC-specific inhibitor KH7 reduced VHA insertion into the apical membrane (7, 10, 15). However, a direct relationship between acid-base sensing by sAC and apical VHA accumulation has yet to be established in α-ICs, in part because α-ICs are relatively scarce and difficult to identify in culture and because isolated α-ICs, as well as kidney slices, cannot withstand experimental acid-base conditions that deviate from ideal (pH 7.4, ~25 mM HCO_3^-, 5% CO_2) (5, 15, 42). However, research on clear cells of the mammalian epididymis has advanced our mechanistic understanding about acid-base sensing and H^+ secretion in renal α-ICs, because they are functionally and embryologically similar (19, 38), and, unlike renal tubules, they can be isolated and perfused with saline solutions with a wide pH and HCO_3^- concentration range (11, 25, 42). In clear cells, sensing of luminal alkalization by sAC and subsequent cAMP production trigger the insertion of VHA into the apical membrane and H^+ secretion into the lumen, a process used to maintain the acidic luminal pH required to maintain sperm in the quiescent state (25).

The mammalian distal tubule also regulates systemic acid-base status with β-intercalated cells (β-ICs), which secrete HCO_3^- in exchange for luminal Cl^- via apical pendrin anion exchangers (31) and absorb H^+ via basolateral VHA (6). sAC colocalizes with pendrin at the apical pole of β-ICs and with VHA near the basolateral membrane (26), suggesting that sAC senses the acid-base status and regulates the activity of pendrin and VHA accordingly; however, functional studies on acid-base sensing and regulation in β-ICs are scarce. The base-secreting cells in the gill of elasmobranch fishes (e.g., sharks, skates, and rays) provide a great surrogate model to β-ICs, as they also express VHA (28, 39), pendrin (28, 30), and sAC (44). These cells can simply be referred to as "VHA-rich cells," because, unlike mammalian kidney cells, they are the only gill cells that express noticeable amounts of VHA (39). Furthermore, elasmobranchs experience pronounced postprandial

Address for reprint requests and other correspondence: M. Tresguerres, 9500 Gilman Dr., Mail Code 0202, La Jolla, CA 92093 (e-mail: mtresguerres@ucsd.edu).

blood alkalosis after feeding, whereby pH can increase by ~0.3 pH units and HCO_3^- concentration can more than double (from ~4 to >10 mM, depending on meal size) over 24 h (48–50). These characteristics are major advantages for inducing experimental alkalosis without compromising cell viability. Elasmobranchs provide two additional advantages for studies on acid-base sensing and regulation: *1*) unlike mammals, which use both lungs and kidneys for blood acid-base regulation, elasmobranchs exclusively rely on their gills to maintain blood acid-base homeostasis (17), and *2*) unlike the mammalian kidney and bony fish gills, elasmobranch gills transport ions only for acid-base purposes and are not involved in NaCl transport for salt and osmoregulation (for which elasmobranches use their unique rectal gland) (17). These two characteristics allow study of acid-base regulatory mechanisms without the interference of osmoregulation, thus facilitating interpretation of results.

Experiments with live sharks have provided abundant mechanistic information about acid-base sensing and regulation: sAC triggered the translocation of VHA from cytoplasmic vesicles into the basolateral membrane of VHA-rich cells in response to blood alkalosis (44) through a mechanism that also depends on carbonic anhydrases (CAs) (45) and functional microtubules (43). Blocking VHA translocation with pharmacological inhibitors of sAC, CA, and microtubule assembly prevented sharks from effectively regulating blood acid-base homeostasis, indicating that basolateral VHA absorbs H^+ into the blood and powers apical HCO_3^- into seawater to correct blood alkalosis (43–45). However, since those experiments were performed on live, whole animals, it is unclear if direct sensing by sAC is sufficient or if hormonal control also contributes to the acid-base-sensing mechanism of VHA-rich cells. However, this and other mechanistic aspects of acid-base sensing, signal transduction, and acid-base regulation can be studied only in cell cultures.

In this study we developed primary gill cell cultures from the Pacific round ray (*Urolophus halleri*) to study acid-base sensing by sAC in base-secreting VHA-rich cells. Similar to native elasmobranch gill epithelium (30), isolated VHA-rich cells had a large number of mitochondria and expressed both sAC and tmACs. Exposure of isolated gill cells to extracellular alkalosis led to VHA translocation from the cytoplasm to the cell membrane in a sAC-dependent manner, confirming sAC as a necessary acid-base sensor in base-secreting cells. Furthermore, the tmAC agonist forskolin induced removal of VHA from the cell membrane, supporting the presence of cAMP microdomains in ray gill base-secreting cells.

METHODS

Experimental animals. All experiments were approved by the Scripps Institute of Oceanography-University of California San Diego Animal Care Committee under protocol number S10320 in compliance with the Institutional Animal Care and Use Committee guidelines for the care and use of experimental animals. Round rays were caught from La Jolla Shores, CA, housed in tanks with flowing seawater, and fed chopped squid or mackerel three times a week. Gill samples for cell isolation experiments were collected 2–3 days after the animals were fed.

Gill tissue sampling. Specimens were euthanized by an overdose of tricaine methanesulfonate (0.5 g/l), and gill samples were taken for the different experimental procedures. For immunohistochemistry, gill samples were fixed in 0.2 M cacodylate buffer, 3.2% paraformaldehyde, and 0.3% glutaraldehyde for 6 h, transferred to 50% ethanol for 6 h, and stored in 70% ethanol until further processing, as described by Tresguerres et al. (39). For Western blot analysis, gill samples were flash-frozen in liquid nitrogen and stored at −80°C.

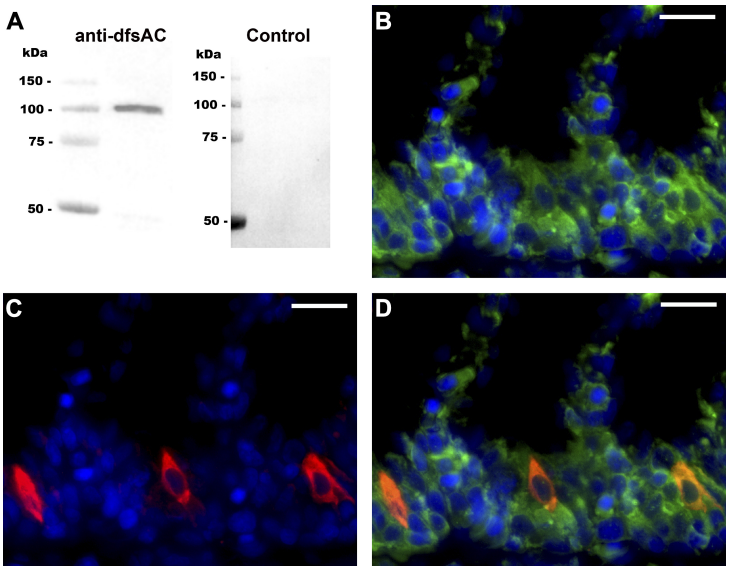

Fig. 1. Soluble adenylyl cyclase (sAC) in ray gills. *A*: anti-dogfish sAC (dfsAC) antibodies specifically recognized a 110-kDa shark sAC band in Western blots from gill crude homogenate, but not in peptide preabsorption control blots. *B–D*: sAC immunoreactivity was highly abundant in gill cells, with sAC (*B*, green) and vacuolar-type H^+-ATPase (VHA; *C*, red) immunoreactivity colocalized in VHA-rich base-secreting cells along the interlamellar gill region (*D*). Nuclei stained blue. Scale bars = 20 μm.

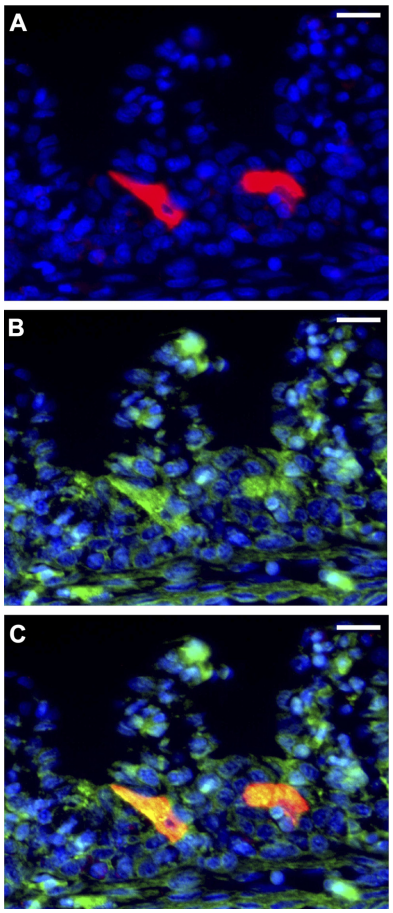

Fig. 2. Transmembrane adenylyl cyclases (tmACs) in vacuolar-type H^+-ATPase (VHA)-rich cells. *A–C*: VHA immunoreactivity (*A*, red) and BODIPY FL forskolin-labeled tmACs (*B*, green) are present together in cells along the interlamellar gill region (*C*). Nuclei stained blue. Scale bars = 20 μm.

Antibodies and reagents. Two custom-made polyclonal rabbit antibodies were used, one against a conserved peptide in the VHA B-subunit (30) (AREEVPGRRGFPGY) and the other against an epitope in the second catalytic domain of dogfish sAC (dfsAC) (44) (INNEFRNYQGRINKC). The anti-VHA antibodies specifically recognize the conserved VHA B-subunit in sharks (30, 44), corals (1), and marine worms (40). Another custom-made anti-VHA monoclonal mouse antibody against the same peptide was used to colocalize VHA and sAC on the same histological sections. BODIPY FL forskolin dye (Thermo Fisher Scientific, Waltham, MA) was used to determine tmAC localization [recently used to localize tmACs in mammalian cell cultures (8, 22) and zebrafish (21)], and MitoTracker Red (Thermo Fisher Scientific) was used to stain mitochondria in live cells. KH7 was a kind gift of Dr. Lonny Levin and Dr. Jochen Buck (Weill Cornell Medical College); forskolin and adenosine 3′,5′-cyclic monophosphorothioate (Sp-cAMP) were purchased from Enzo Life Sciences (Farmingdale, NY), and 2′,5′-dideoxyadenosine (DDA) was obtained from CalBiotech (Spring Valley, CA).

Western blotting. A procedure similar to that described by Roa et al. (30) was used to process frozen gill samples for Western blotting. Total protein (20 μg) was separated on a 7.5% polyacrylamide mini gel (60 V for 15 min, 200 V for 45 min) and transferred to a polyvinylidene difluoride (PVDF) membrane (Bio-Rad, Hercules, CA). After transfer, PVDF membranes were incubated in blocking buffer (Tris-buffered saline, 1% Tween, and 5% milk) at room temperature for 1 h and incubated in the primary antibody at 4°C overnight (3 μg/ml anti-dfsAC). PVDF membranes were washed three times and incubated in secondary antibody (1:10,000 dilution) at room temperature for 1 h. Bands were made visible through addition of ECL Prime Western blotting detection reagent (GE Healthcare, Waukesha, WI) and imaged and analyzed in a Bio-Rad Universal III hood using ImageQuant software (Bio-Rad). PVDF membranes incu-

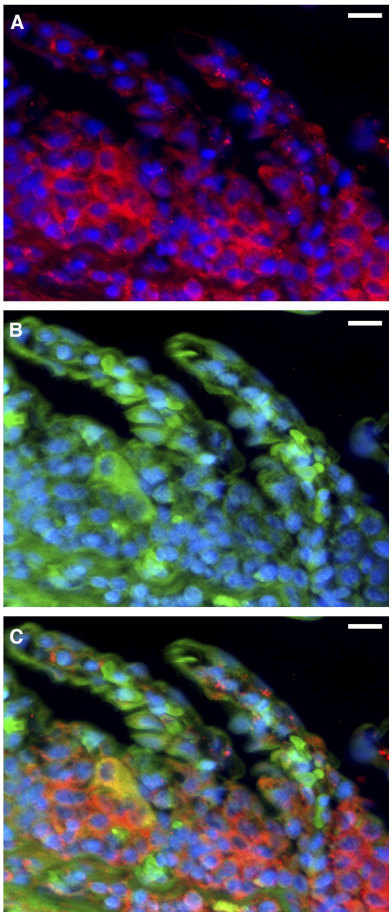

Fig. 3. Soluble adenylyl cyclase (sAC) and transmembrane adenylyl cyclases (tmACs) in ray gills. *A–C*: sAC immunoreactivity (*A*, red) and BODIPY FL forskolin-labeled tmACs (*B*, green) are present together in cells along the interlamellar gill region (*C*). Nuclei stained blue. Scale bars = 20 μm.

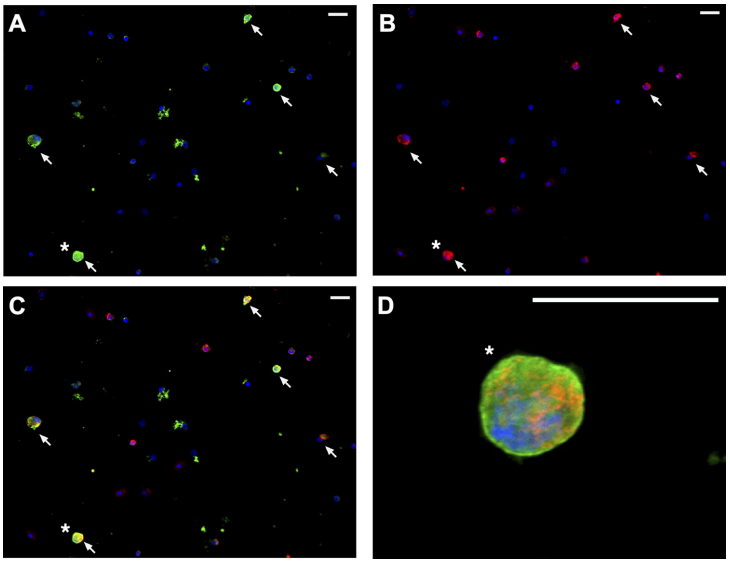

Fig. 4. Soluble adenylyl cyclase (sAC) in isolated gill cells. *A–C*: arrows indicate isolated mitochondrion-rich acid-base regulatory cells. sAC immunoreactivity was cytoplasmic (*A*, green), with viable mitochondrion-rich cells identified with MitoTracker Red (*B*, red), and merged image (*C*). *D*: higher magnification of the cell marked with an asterisk. Nuclei stained blue. Scale bars = 20 μm.

bated in blocking buffer with anti-dfsAC antibodies and threefold excess blocking peptide served as control and did not show any bands.

Immunohistochemistry. Gills fixed and stored in 70% ethanol as described above were processed using a procedure similar to that described by Roa et al. (30). Sections were blocked for 1 h (PBS, 2% normal goat serum, and 0.02% keyhole limpet hemocyanin, pH 7.7) and then incubated in the primary antibody overnight at 4°C (6 μg/ml anti-VHA, 12 μg/ml anti-dfsAC, and 10 μM BODIPY FL forskolin). Slides were washed three times in PBS, incubated in the appropriate secondary antibody (1:500 dilution) at room temperature for 1 h, incubated with the nuclear stain Hoechst 33342 (Invitrogen, Grand Island, NY; 5 μg/ml) for 5 min, washed three times in PBS, and permanently mounted in FluoroGel with Tris buffer (Electron Microscopy Sciences, Hatfield, PA). Immunofluorescence was detected using an epifluorescence microscope (Zeiss AxioObserver Z1) connected to a metal halide lamp and appropriate filters. Zeiss Axiovision software and Adobe Photoshop were used to adjust digital images for brightness and contrast only. Antigen retrieval was required for anti-dfsAC, which involved incubating slides in heated (95°C) citrate unmasking buffer (10 mM citric acid and 0.05% Tween 20, pH 6.0) for 30 min following rehydration. For anti-dfsAC, control sections incubated in blocking buffer with anti-dfsAC antibodies and 300-fold excess blocking peptide showed no visible sAC immunoreactivity.

Colocalization of sAC, VHA, and tmACs. For immunolocalization of sAC to VHA-rich cells, sections were processed as described above but incubated in a mixture of anti-dfsAC (rabbit) and anti-VHA (mouse) antibodies overnight and then in a mixture of goat anti-rabbit and anti-mouse secondary antibodies. Similarly, mixtures of BODIPY FL forskolin dye with anti-dfsAC or anti-VHA antibodies were used to colocalize tmACs with sAC or VHA, with sections incubated in BODIPY FL forskolin (30 min) and treated as described above.

Isolated gill cells. A collagenase digestion protocol used for isolating cells from trout gills (24) was optimized for ray gills. Gills were perfused through the heart with 50 ml of ice-cold heparinized shark saline (280 mM NaCl, 6 mM KCl, 5 mM $NaHCO_3$, 3 mM $MgCl_2$, 0.5 mM $NaSO_4$, 1 mM Na_2HPO_4, 350 mM urea, 70 mM trimethylamine *N*-oxide, 5 mM glucose, and 1:100 dilution of protease inhibitor

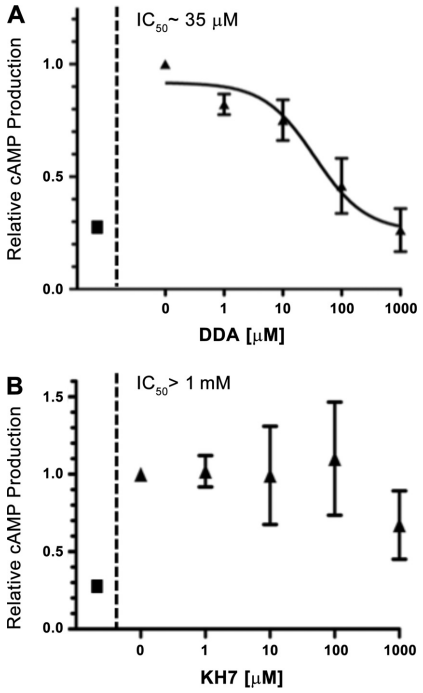

Fig. 5. Transmembrane adenylyl cyclase (tmAC) activity in ray gills. *A* and *B*: forskolin (10 μM) stimulated a 4-fold increase in cAMP over control cAMP concentrations (■), which was inhibited by low concentrations of 2′,5′-dideoxyadenosine (DDA, IC_{50} = 35 μM), but not KH7 (IC_{50} >1 mM).

cocktail, pH 7.7), and 5-mm-wide sections were dissected and incubated for 20 min (3 times) in a collagenase-saline solution (0.2 mg/ml). Cell suspensions were filtered onto a 50:50 FBS-saline solution to inactivate collagenase activity. Final cell suspensions were washed (3 times) with 10 ml of saline solution, centrifuged at 1,500 *g* (4°C), resuspended in 5 ml of saline solution, plated onto poly-L-lysine-coated coverslips, and allowed to settle for 2 h. After cells recovered, they were exposed to control saline (+DMSO), saline

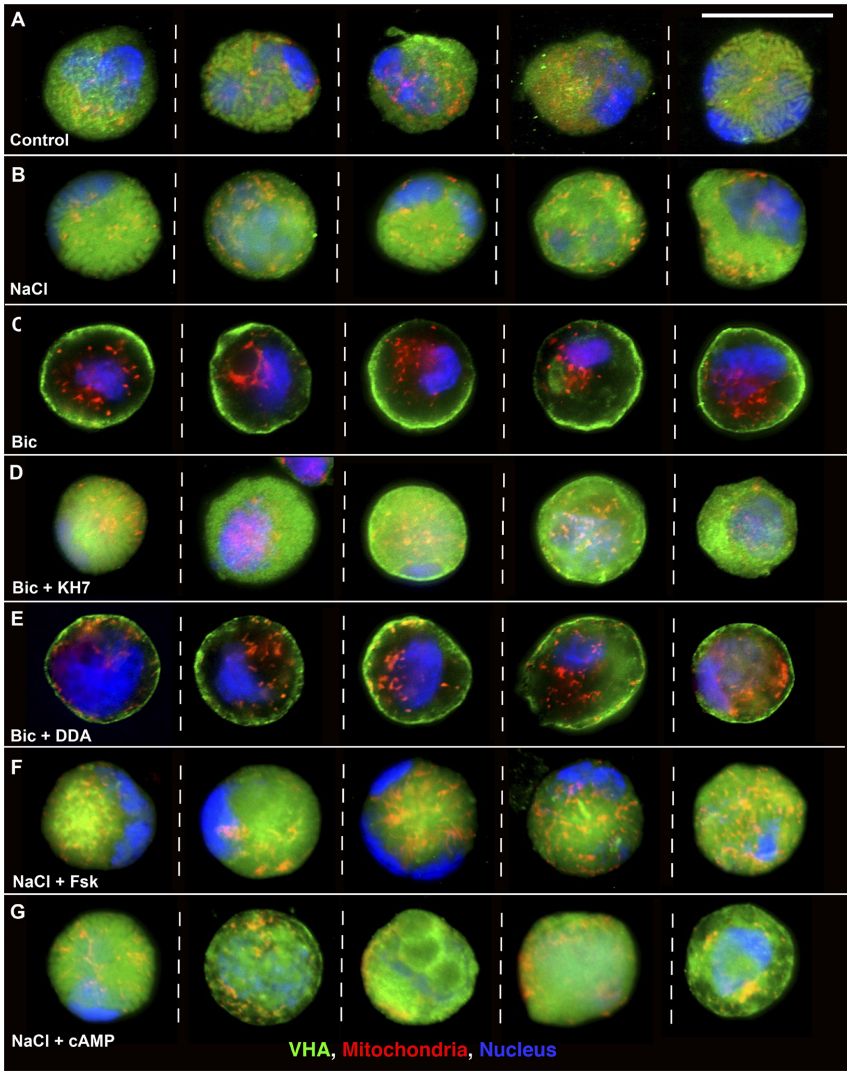

Fig. 6. Vacuolar-type H^+-ATPase (VHA) translocates to the cell membrane of isolated base-secreting cells exposed to extracellular alkalosis. Representative images of 5 separate cells (all cells from the same ray) show VHA (green) localization in isolated cells exposed to control (5 mM HCO_3^-, pH 7.75, $n = 59$), NaCl (5 mM HCO_3^- + 40 mM NaCl, pH 7.75, $n = 60$), Bic (40 mM HCO_3^-, pH 8.0, $n = 56$), Bic + KH7 (50 μM KH7 + 40 mM HCO_3^-, pH 8.0, $n = 60$), Bic + DDA (100 μM DDA + 40 mM HCO_3^-, pH 8.0, $n = 60$), NaCl + Fsk (10 μM forskolin + 5 mM HCO_3^- + 40 mM NaCl, pH 7.75, $n = 60$), and NaCl + cAMP (1 mM Sp-cAMP + 5 mM HCO_3^- + 40 mM NaCl, pH 7.75, $n = 40$). VHA was cytoplasmic in cells exposed to control (*A*) and NaCl (*B*); VHA translocated to the cell membrane in cells exposed to alkalosis (*C*, Bic). Alkalosis-induced VHA translocation was blocked by KH7 (*D*, Bic + KH7), but not by DDA (*E*, Bic + DDA). Additionally, VHA was cytoplasmic in cells exposed to forskolin (*F*, NaCl + Fsk) and Sp-cAMP (*G*, NaCl + cAMP). Nuclei stained blue; mitochondria stained red. Scale bars = 20 μm.

with additional 40 mM NaCl (320 mM NaCl + DMSO), NaCl saline + forskolin (10 μM forskolin in DMSO), NaCl saline + Sp-cAMP (1 mM Sp-cAMP in DMSO), saline with additional 40 mM $NaHCO_3$ (pH 8.0), and the latter saline with KH7 (50 μM KH7 in DMSO) or DDA (100 μM DDA in DMSO) for 30 min. Cells were then incubated in the active mitochondrial dye MitoTracker Red (200 nM, 30 min), fixed (shark saline, 3.2% paraformaldehyde, and 0.3% glutaraldehyde for 20 min), incubated in anti-VHA antibodies overnight, and processed for immunocytochemistry as described above. HCO_3^- and pH values of the incubation medium were confirmed using a CO_2 analyzer (Corning, Corning, NY) and UltraBASIC pH meter (Denver Instrument, Bohemia, NY).

cAMP assays. Tissue homogenates were incubated for 30 min at room temperature in an orbital shaker (300 rpm) in 100 mM Tris (pH 7.5), 5 mM ATP, 10 mM $MgCl_2$, 0.1 mM $MnCl_2$, 0.5 mM IBMX, 1 mM dithiothreitol, 20 mM creatine phosphate, and 100 U/ml creatine phosphokinase. For inhibition of tmAC activity, tissue homogenates were incubated in 10 μM forskolin and the indicated concentrations of KH7 and DDA. cAMP concentrations were determined using DetectX Direct Cyclic AMP Enzyme Immunoassay (Arbor Assays, Ann Arbor, MI).

Quantification of VHA translocation. VHA localization in response to each experimental treatment was determined in ~40–60 cells from two or three different rays. Starting from the upper-right corner of the field of view, the first ~20 VHA-positive cells with strong mitochondrial staining (30) were selected and individually imaged at ×600 magnification. The individual performing the imaging was not aware of the treatment that was being analyzed ("blind examiner"). Cells with distinct "ring" VHA immunostaining (strong signal in the cell membrane and lack of signal in the cytoplasm) were counted as cells with "membrane VHA localization," while cells without distinct membrane staining [cytoplasmic and intermediate staining (43, 44)] were grouped together as non-membrane-staining. Additionally, fluorescence intensity was quantified across the length of the cell using ImageJ analysis software. Fluorescence intensity histograms were created by drawing transects across individual cells while avoiding the nuclei. To avoid bias, two transects per cell were used, and the data were averaged. Data were normalized for cell size and background fluorescence, and then (above-average) fluorescence at the edge of the cell (first and last 10%) was quantified and divided by (above-average) total cell fluorescence to give "relative VHA membrane abundance" or VHA abundance from the edge to the center of each cell. This analysis was performed using a custom-made script written in Python programming language, into which images were input randomly to eliminate bias.

Statistical analysis. Individual cells were counted as experimental replicates (n = 40–60 cells from 2–3 rays), similar to previous studies from mammalian kidney intercalated cells and epididymal clear cells (25, 27). All quantitative data were arcsine-transformed, and experimental groups were analyzed for significant differences using a one- or two-way ANOVA and Bonferroni's multiple-comparison test ($P < 0.001$).

RESULTS

sAC is present in ray VHA-rich cells, alongside tmACs. Antibodies against dfsAC (anti-dfsAC) detected the predicted 110-kDa band for shark sAC in Western blots from ray gill extracts, but not in control blots (Fig. 1*A*). sAC immunofluorescence was present throughout the cytoplasm of gill cells in histological sections (Fig. 1*B*), and double immunolabeling with antibodies against VHA (Fig. 1*C*) also revealed high sAC abundance in base-secreting VHA-rich cells (Fig. 1*D*). Similar to results from previous studies of starved sharks (30, 39, 43–45), VHA was localized in the cytoplasm of starved ray gill cells. In addition, VHA-rich cells were labeled with BODIPY FL forskolin (Fig. 2), demonstrating that these cells express two distinct sources of cAMP: tmACs and sAC. In fact, sAC and tmACs colocalized in most cells throughout the ray gill epithelium (Fig. 3). As seen in histological gill sections, sAC was also present throughout the cytoplasm of gill isolated cells, including acid-base regulatory cells [identified by their abundant mitochondria (30), which were stained using the mitochondrial dye MitoTracker Red] (Fig. 4).

sAC inhibitor does not inhibit tmACs. In mammals, two types of adenylyl cyclases produce cAMP: tmACs, which are activated by hormones and GPCRs, and sAC. The only known pharmacological adenylyl cyclase activators are derivatives of forskolin, a natural plant dipentene that selectively binds tmACs, but not sAC (7, 34). DDA and KH7 are pharmacological inhibitors: DDA is tmAC-selective (IC_{50} = 8 μM) (3, 12), and the small molecule KH7 is sAC-selective (IC_{50} = 10 μM) (18). Tresguerres et al. (44) reported HCO_3^--stimulated, KH7-sensitive cAMP production in elasmobranch gill homogenates, as well as in purified elasmobranch sAC (EC_{50} HCO_3^- = 5 mM, IC_{50} KH7 = 10 μM). However, they did not test the effects of KH7 on elasmobranch tmACs. Therefore, we used forskolin-stimulated cAMP production to determine the inhibitory effects of DDA and KH7 on tmAC activity. Forskolin initiated a fourfold increase in cAMP activity (Fig. 5), an indication that tmACs are present and responsive to traditional forskolin-stimulated activation. DDA inhibited forskolin-stimulated tmAC activity (IC_{50} = 35 μM; Fig. 5*A*), and KH7 did not (IC_{50} >1 mM; Fig. 5*B*), thereby validating the use of DDA and KH7 in subsequent tmAC- and sAC-inhibitory experiments.

sAC-dependent VHA translocation to the cell membrane. In VHA-rich cells exposed to control saline (control: 5 mM HCO_3^-, pH 7.75) and high-NaCl saline (NaCl: 5 mM HCO_3^- +

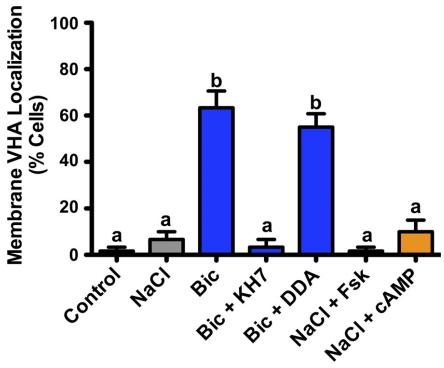

Fig. 7. sAC-dependent membrane vacuolar-type H^+-ATPase (VHA) localization in isolated base-secreting cells. Cells were exposed to control (5 mM HCO_3^-, pH 7.75, n = 59), NaCl (5 mM HCO_3^- + 40 mM NaCl, pH 7.75, n = 60), Bic (40 mM HCO_3^-, pH 8.0, n = 56), Bic + KH7 (50 μM KH7 + 40 mM HCO_3^-, pH 8.0, n = 60), Bic + DDA (100 μM DDA + 40 mM HCO_3^-, pH 8.0, n = 60), NaCl + Fsk (10 μM forskolin + 5 mM HCO_3^- + 40 mM NaCl, pH 7.75, n = 60), and NaCl + cAMP (1 mM Sp-cAMP + 5 mM HCO_3^- + 40 mM NaCl, pH 7.75, n = 40). 40 mM HCO_3^- ("Bic") significantly increased the percentage of cells with membrane VHA localization, which was inhibited by KH7, but not DDA ($P < 0.001$). Compared with control and NaCl cells, forskolin and Sp-cAMP had no effect on the percentage of cells with membrane VHA localization.

40 mM NaCl, pH 7.75), VHA was predominantly localized in the cytoplasm (Fig. 6, *A* and *B*). In cells exposed to alkaline, high-bicarbonate saline (Bic: 40 mM HCO_3^-, pH 8.0), VHA translocated to the cell membrane (Fig. 6*C*), which was similar to previous reports from live animals experiencing blood alkalosis (30, 39, 44). This alkalosis-induced VHA translocation was dependent on sAC, and not tmACs; VHA remained in the cytoplasm of cells exposed to the sAC-selective inhibitor KH7 (Bic + KH7; Fig. 6*D*) but translocated to the cell membrane of cells exposed to the tmAC-selective inhibitor DDA (Bic + DDA; Fig. 6*E*). Additionally, VHA was localized in the cytoplasm of cells exposed to the tmAC activator forskolin (NaCl + Fsk; Fig. 6*F*) and Sp-cAMP (NaCl + cAMP; Fig. 6*G*). Overall, the percentage of all cells with membrane VHA was significantly higher in cells exposed to alkaline saline, with or without DDA (Fig. 7). Furthermore, since VHA was cytoplasmic in cells exposed to high-NaCl saline, alkalosis, rather than increased ionic strength and osmolarity, is the trigger of VHA translocation.

An additional analysis of VHA translocation based on the histogram of fluorescence intensity across the length of each cell yielded identical results (see METHODS for details). VHA fluorescence intensity in control cells and cells exposed to NaCl, Bic + KH7, NaCl + Fsk, and NaCl + cAMP was higher in the cytoplasmic center; in cells exposed to Bic and Bic + DDA, it peaked at the membrane edge (Fig. 8), with significantly higher relative VHA abundance at the membrane (0–10% from the cell edge) and lower relative VHA abundance in the cytoplasm (40–50% from the cell edge; Fig. 9). Since KH7, but not DDA, prevented alkalosis-induced VHA translocation, we conclude that sAC in each isolated VHA-rich cell is the molecular sensor of alkalosis that initiates an acid-base regulatory response, as previously suggested by experiments in live sharks (44).

tmAC-dependent VHA movement away from the cell membrane. Since ray gill VHA-rich cells also express tmACs, we examined the effect of forskolin on VHA translocation. Our hypothesis was that if cAMP produced by tmAC had the same

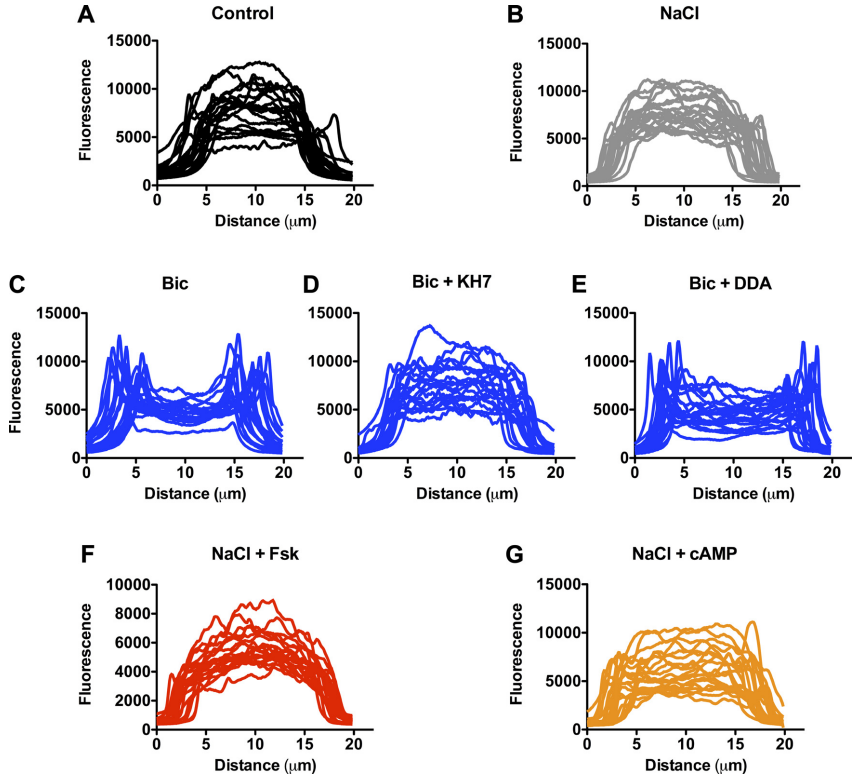

Fig. 8. Vacuolar-type H^+-ATPase (VHA) fluorescence intensity in isolated base-secreting cells. *A–G*: representative transects displaying VHA fluorescence intensity (created with ImageJ analysis software) of cells exposed to control (5 mM HCO_3^-, pH 7.75, n = 59), NaCl (5 mM HCO_3^- + 40 mM NaCl, pH 7.75, n = 60), Bic (40 mM HCO_3^-, pH 8.0, n = 56), Bic + KH7 (50 μM KH7 + 40 mM HCO_3^-, pH 8.0, n = 60), Bic + DDA (100 μM DDA + 40 mM HCO_3^-, pH 8.0, n = 60), NaCl + Fsk (10 μM forskolin + 5 mM HCO_3^- + 40 mM NaCl, pH 7.75, n = 60), and NaCl + cAMP (1 mM Sp-cAMP + 5 mM HCO_3^- + 40 mM NaCl, pH 7.75, n = 40).

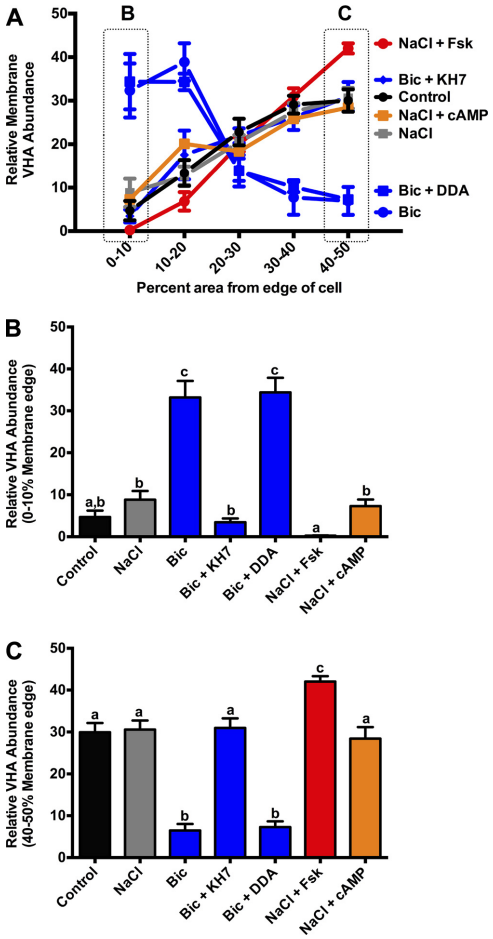

Fig. 9. Relative membrane vacuolar-type H^+-ATPase (VHA) abundance increased during extracellular alkalosis in isolated base-secreting cells. *A*: relative VHA abundance across cells exposed to control (5 mM HCO_3^-, pH 7.75, $n = 59$), NaCl (5 mM HCO_3^- + 40 mM NaCl, pH 7.75, $n = 60$), Bic (40 mM HCO_3^-, pH 8.0, $n = 56$), Bic + KH7 (50 μM KH7 + 40 mM HCO_3^-, pH 8.0, $n = 60$), Bic + DDA (100 μM DDA + 40 mM HCO_3^-, pH 8.0, $n = 60$), NaCl + Fsk (10 μM forskolin + 5 mM HCO_3^- + 40 mM NaCl, pH 7.75, $n = 60$), and NaCl + cAMP (1 mM Sp-cAMP + 5 mM HCO_3^- + 40 mM NaCl, pH 7.75, $n = 40$). *B*: 40 mM HCO_3^- ("Bic") significantly increased relative VHA abundance at the cell membrane (0–10% of the area from the edge of the cell), which was inhibited by KH7, but not DDA ($P < 0.001$). Compared with control and NaCl cells, forskolin and Sp-cAMP had no effect on relative membrane VHA abundance. *C*: 40 mM HCO_3^- ("Bic") significantly decreased relative VHA abundance in the cell cytoplasmic center (40–50% of the area from the edge of the cell), which was inhibited by KH7, but not DDA ($P < 0.001$). Compared with control and NaCl cells, forskolin significantly increased relative VHA abundance in the cell cytoplasmic center ($P < 0.001$), and Sp-cAMP had no effect.

effect as cAMP produced by sAC, VHA should translocate to the cell membrane, as observed during sAC stimulation by elevated bicarbonate. However, the effect of tmAC stimulation by forskolin is the opposite of the effect of stimulation by bicarbonate (Fig. 9*A*), as evidenced by less VHA at the cell membrane (Fig. 9*B*) and more VHA toward the center of the cell (Fig. 9*C*) than in the NaCl control cell. Addition of cell-permeable cAMP under control conditions had no effect on VHA translocation (Fig. 9), which is consistent with different pools of cAMP having opposing effects on VHA translocation, with no net effect.

DISCUSSION

Similar to previous studies on live sharks, exposure of isolated ray gill cells to alkaline conditions induced the translocation of VHA from the cytoplasm to the cell membrane, a process that was prevented by the sAC inhibitor KH7, but not by the tmAC inhibitor DDA. Thus, sAC in each VHA-rich cell is necessary and sufficient to sense alkalosis and trigger a compensatory response, as our experiments with isolated cultured cells rule out whole animal endocrine and paracrine signaling.

The results from this study, along with those from live elasmobranchs experiencing natural postfeeding (30, 45) and experimentally induced (39, 43, 44) blood alkalosis, yield the following model for sensing and counteracting blood alkalosis: elevated plasma HCO_3^- is dehydrated into CO_2 catalyzed by extracellular CA, which then diffuses inside gill VHA-rich cells and is hydrated back into H^+ and HCO_3^- by intracellular CA. The subsequent elevation of intracellular HCO_3^- stimulates sAC, which mediates, possibly via PKA-dependent phosphorylation of motor proteins, the microtubule-dependent translocation of VHA-containing vesicles from the cytoplasm to the basolateral membrane. The anion exchanger pendrin also translocates to the apical membrane in response to blood alkalosis (30); however, it is unknown whether this process is sAC-dependent. Basolateral VHA absorbs H^+ into the blood, and pendrin excretes HCO_3^- into seawater in exchange for Cl^-. H^+ absorbed by VHA combines with plasma HCO_3^-, generating more CO_2, and the process continues until plasma HCO_3^- returns to basal levels. The fact that VHA translocation still takes place in isolated and cultured gill VHA-rich cells demonstrates that this process is self-regulatory and self-sufficient. In addition to VHA-rich cells, sAC was present throughout the cytoplasm of other gill cells, suggesting that sAC regulates multiple other physiological processes. For example, sAC might regulate H^+ secretion and HCO_3^- absorption in acid-secreting Na^+-K^+-ATPase-rich cells, as well as the reversible hydration of CO_2 in pillar cells, as previously suggested (44). The ray gill cell cultures optimized in this study will be a valuable tool for the study of these and other elements of acid-base sensing and regulation.

Previous research has suggested a link between acid-base sensing by sAC and pH regulation by VHA in mammalian kidney β-ICs: metabolic alkalosis increased VHA abundance in basolateral membranes (32), and sAC colocalized with VHA at the basolateral region (26). However, functional studies on renal β-ICs are not available, probably because of their low abundance in the mammalian nephron, limited cell cultures, and their inability to tolerate exposure to highly alkaline

conditions in vivo without compromise to their viability. The cultured ray gill cells developed here circumvent these limitations, making them a promising surrogate model system for renal β-ICs. Furthermore, this acid-base-sensing and regulation model may apply to other epithelia known to have basolateral VHA-, sAC-, and cAMP-stimulated base secretion, but in which their potential link has not been studied. Some examples include mammalian pancreatic (29, 36, 46) and salivary (33) ducts, marine bony fish intestine (9, 16, 41), and insect midgut (4).

Staining with BODIPY FL forskolin suggested that, in addition to sAC, most ray gill cells express tmACs. This was confirmed by the robust forskolin-stimulated cAMP production in ray gill extracts that was sensitive to the tmAC inhibitor DDA. Furthermore, colocalization of VHA with sAC (using dual immunostaining) and with tmACs (using BODIPY FL forskolin staining) demonstrated the presence of both sAC and tmACs in VHA-rich cells. This situation also resembles the mammalian renal collecting duct, where α- and β-ICs are located, because it also expresses sAC (adcy10) (25, 26) and the tmACs (adcys2, adcys4, adcys5, adcys6, and adcys9) (2). However, DDA did not affect alkalosis-induced VHA translocation in cultured gill VHA-rich cells, and forskolin induced a redistribution of VHA away from the cell membrane. These results rule out a role of tmACs in triggering the VHA translocation and raise questions about the physiological roles of tmACs in these cells. Since tmAC stimulation induced an effect on VHA translocation that was the opposite of the effect of sAC, it is possible that tmACs are involved in the sensing of acidosis. For example, in mammalian renal collecting duct cells, tmACs are stimulated in response to extracellular metabolic acidosis through a mechanism that depends on the GPCR GPR4 (23, 37). We hypothesize that acid-base sensing and regulation in gill cells occur as a result of the coordinated action of sAC (which stimulates base secretion and inhibits acid secretion under alkalosis) and GPCR/tmAC (which stimulates acid secretion and inhibits base secretion under acidosis). Confirmation of this model will require, first, establishing whether any acid-sensing GPCRs are present in gill acid- and base-secreting cells. However, the subsequent experimental testing will not be trivial, because both sensing mechanisms depend on the same messenger molecule, cAMP, which complicates interpretation of results from experiments using cAMP agonists and antagonists.

In summary, this study established sAC as a sensor of alkalosis in ray gill base-secreting cells. Because sAC, the cAMP pathway, and VHA are widespread in eukaryotic cells, this could be an evolutionarily conserved mechanism for sensing and counteracting alkalosis.

ACKNOWLEDGMENTS

The authors are grateful to Phil Zerofski (Scripps Institute of Oceanography) for excellent assistance with experimental animal capture and husbandry and general aquarium matters.

GRANTS

J. N. Roa is supported by the William Townsend Porter Predoctoral Fellowship from the American Physiological Society. M. Tresguerres is supported by National Science Foundation Grant IOS 1354181 and Alfred P. Sloan Research Fellowship BR2013-103.

DISCLOSURES

No conflicts of interest, financial or otherwise, are declared by the authors.

AUTHOR CONTRIBUTIONS

J.N.R. and M.T. developed the concept and designed the research; J.N.R. performed the experiments; J.N.R. and M.T. analyzed the data; J.N.R. and M.T. interpreted the results of the experiments; J.N.R. prepared the figures; J.N.R. and M.T. drafted the manuscript; J.N.R. and M.T. edited and revised the manuscript; J.N.R. and M.T. approved the final version of the manuscript.

REFERENCES

1. **Barott KL, Venn AA, Perez SO, Tambutté S, Tresguerres M.** Coral host cells acidify symbiotic algal microenvironment to promote photosynthesis. *Proc Natl Acad Sci USA* 112: 607–612, 2015.
2. **Bek MJ, Zheng S, Xu J, Yamaguchi I, Asico LD, Sun XG, Jose PA.** Differential expression of adenylyl cyclases in the rat nephron. *Kidney Int* 60: 890–899, 2001.
3. **Bitterman JL, Ramos-Espiritu L, Diaz A, Levin LR, Buck J.** Pharmacological distinction between soluble and transmembrane adenylyl cyclases. *J Pharmacol Exp Ther* 347: 589–598, 2013.
4. **Boudko DY, Moroz LL, Harvey WR, Linser PJ.** Alkalinization by chloride/bicarbonate pathway in larval mosquito midgut. *Proc Natl Acad Sci USA* 98: 15354–15359, 2001.
5. **Breton S, Brown D.** Cold-induced microtubule disruption and relocalization of membrane proteins in kidney epithelial cells. *J Am Soc Nephrol* 9: 155–166, 1998.
6. **Brown D, Hirsch S, Gluck S.** An H^+-ATPase in opposite plasma membrane domains in kidney epithelial cell subpopulations. *Nature* 331: 622–624, 1988.
7. **Buck J, Sinclair ML, Schapal L, Cann MJ, Levin LR.** Cytosolic adenylyl cyclase defines a unique signaling molecule in mammals. *Proc Natl Acad Sci USA* 96: 79–84, 1999.
8. **Calebiro D, Nikolaev VO, Gagliani MC, de Filippis T, Dees C, Tacchetti C, Persani L, Lohse MJ.** Persistent cAMP-signals triggered by internalized G-protein-coupled receptors. *PLoS Biol* 7: e1000172, 2009.
9. **Carvalho ES, Gregório SF, Power DM, Canário AV, Fuentes J.** Water absorption and bicarbonate secretion in the intestine of the sea bream are regulated by transmembrane and soluble adenylyl cyclase stimulation. *J Comp Physiol B* 182: 1069–1080, 2012.
10. **Chen Y, Cann MJ, Litvin TN, Iourgenko V, Sinclair ML, Levin LR, Buck J.** Soluble adenylyl cyclase as an evolutionarily conserved bicarbonate sensor. *Science* 289: 625–628, 2000.
11. **Cooper DM.** Regulation and organization of adenylyl cyclases and cAMP. *Biochem J* 375: 517–529, 2003.
12. **Dessauer CW, Gilman AG.** The catalytic mechanism of mammalian adenylyl cyclase. Equilibrium binding and kinetic analysis of P-site inhibition. *J Biol Chem* 272: 27787–27795, 1997.
13. **Evans DH, Piermarini PM, Choe KP.** The multifunctional fish gill: dominant site of gas exchange, osmoregulation, acid-base regulation, and excretion of nitrogenous waste. *Physiol Rev* 85: 97–177, 2005.
14. **Frizzell RA, Field M, Schultz SG.** Sodium-coupled chloride transport by epithelial tissues. *Am J Physiol Renal Fluid Electrolyte Physiol* 236: F1–F8, 1979.
15. **Gong F, Alzamora R, Smolak C, Li H, Naveed S, Neumann D, Hallows KR, Pastor-Soler NM.** Vacuolar H^+-ATPase apical accumulation in kidney intercalated cells is regulated by PKA and AMP-activated protein kinase. *Am J Physiol Renal Physiol* 298: F1162–F1169, 2010.
16. **Guffey S, Esbaugh A, Grosell M.** Regulation of apical H^+-ATPase activity and intestinal HCO_3^- secretion in marine fish osmoregulation. *Am J Physiol Regul Integr Comp Physiol* 301: R1682–R1691, 2011.
17. **Heisler N.** Acid-base regulation. In: *Physiology of Elasmobranch Fishes*. Berlin: Springer, 1988, p. 215–252.
18. **Hess KC, Jones BH, Marquez B, Chen Y, Ord TS, Kamenetsky M, Miyamoto C, Zippin JH, Kopf GS, Suarez SS, Levin LR, Williams CJ, Buck J, Moss SB.** The "soluble" adenylyl cyclase in sperm mediates multiple signaling events required for fertilization. *Dev Cell* 9: 249–259, 2005.
19. **Hinton BT, Turner TT.** Is the epididymis a kidney analogue? *Physiology* 3: 28–31, 1988.
20. **Krogh A.** *Osmotic Regulation in Fresh Water Fishes by Active Absorption of Chloride Ions*. Copenhagen: University of Copenhagen, 1937.

21. **Kumai Y, Kwong RW, Perry SF.** The role of cAMP-mediated intracellular signaling in regulating Na^+ uptake in zebrafish larvae. *Am J Physiol Regul Integr Comp Physiol* 306: R51–R60, 2014.
22. **Kuna RS, Girada SB, Asalla S, Vallentyne J, Maddika S, Patterson JT, Smiley DL, DiMarchi RD, Mitra P.** Glucagon-like peptide-1 receptor-mediated endosomal cAMP generation promotes glucose-stimulated insulin secretion in pancreatic β-cells. *Am J Physiol Endocrinol Metab* 305: E161–E170, 2013.
23. **Ludwig MG, Vanek M, Guerini D, Gasser JA, Jones CE, Junker U, Hofstetter H, Wolf RM, Seuwen K.** Proton-sensing G-protein-coupled receptors. *Nature* 425: 93–98, 2003.
24. **Parks SK, Tresguerres M, Goss GG.** Interactions between Na^+ channels and Na^+-HCO_3^- cotransporters in the freshwater fish gill MR cell: a model for transepithelial Na^+ uptake. *Am J Physiol Cell Physiol* 292: C935–C944, 2007.
25. **Pastor-Soler N, Beaulieu V, Litvin TN, Da Silva N, Chen Y, Brown D, Buck J, Levin LR, Breton S.** Bicarbonate-regulated adenylyl cyclase (sAC) is a sensor that regulates pH-dependent V-ATPase recycling. *J Biol Chem* 278: 49523–49529, 2003.
26. **Paunescu TG, Da Silva N, Russo LM, McKee M, Lu HAJ, Breton S, Brown D.** Association of soluble adenylyl cyclase with the V-ATPase in renal epithelial cells. *Am J Physiol Renal Physiol* 294: F130–F138, 2008.
27. **Paunescu TG, Ljubojevic M, Russo LM, Winter C, McLaughlin MM, Wagner CA, Breton S, Brown D.** cAMP stimulates apical V-ATPase accumulation, microvillar elongation, and proton extrusion in kidney collecting duct A-intercalated cells. *Am J Physiol Renal Physiol* 298: F643–F654, 2010.
28. **Piermarini PM, Verlander JW, Royaux IE, Evans DH.** Pendrin immunoreactivity in the gill epithelium of a euryhaline elasmobranch. *Am J Physiol Regul Integr Comp Physiol* 283: R983–R992, 2002.
29. **Ramos LS, Zippin JH, Kamenetsky M, Buck J, Levin LR.** Glucose and GLP-1 stimulate cAMP production via distinct adenylyl cyclases in INS-1E insulinoma cells. *J Gen Physiol* 132: 329–338, 2008.
30. **Roa JN, Munévar CL, Tresguerres M.** Feeding induces translocation of vacuolar proton ATPase and pendrin to the membrane of leopard shark (*Triakis semifasciata*) mitochondrion-rich gill cells. *Comp Biochem Physiol A Mol Integr Physiol* 174: 29–37, 2014.
31. **Royaux IE, Wall SM, Karniski LP, Everett LA, Suzuki K, Knepper MA, Green ED.** Pendrin, encoded by the Pendred syndrome gene, resides in the apical region of renal intercalated cells and mediates bicarbonate secretion. *Proc Natl Acad Sci USA* 98: 4221–4226, 2001.
32. **Sabolić I, Brown D, Gluck SL, Alper SL.** Regulation of AE1 anion exchanger and H^+-ATPase in rat cortex by acute metabolic acidosis and alkalosis. *Kidney Int* 51: 125–137, 1997.
33. **Sahara Y, Horie S, Fukami H, Goto-Matsumoto N, Nakanishi-Matsui M.** Functional roles of V-ATPase in the salivary gland. *J Oral Biosci* 57: 102–109, 2015.
34. **Seamon KB, Daly JW.** Forskolin: a unique diterpene activator of cyclic AMP-generating systems. *J Cyclic Nucleotide Res* 7: 201–224, 1981.
35. **Smith HW.** The absorption and excretion of water and salts by the elasmobranch fishes. *Am J Physiol* 98: 296, 1931.
36. **Strazzabosco M, Fiorotto R, Melero S, Glaser S, Francis H, Spirli C, Alpini G.** Differentially expressed adenylyl cyclase isoforms mediate secretory functions in cholangiocyte subpopulation. *Hepatology* 50: 244–252, 2009.
37. **Sun X, Yang LV, Tiegs BC, Arend LJ, McGraw DW, Penn RB, Petrovic S.** Deletion of the pH sensor GPR4 decreases renal acid excretion. *J Am Soc Nephrol* 21: 1745–1755, 2010.
38. **Tresguerres M, Buck J, Levin LR.** Physiological carbon dioxide, bicarbonate, and pH sensing. *Pflügers Arch* 460: 953–964, 2010.
39. **Tresguerres M, Katoh F, Fenton H, Jasinska E, Goss GG.** Regulation of branchial V-H^+-ATPase, Na^+/K^+-ATPase and NHE2 in response to acid and base infusions in the Pacific spiny dogfish (*Squalus acanthias*). *J Exp Biol* 208: 345–354, 2005.
40. **Tresguerres M, Katz S, Rouse GW.** How to get into bones: proton pump and carbonic anhydrase in *Osedax* boneworms. *Proc Biol Sci* 280: 20130625, 2013.
41. **Tresguerres M, Levin LR, Buck J, Grosell M.** Modulation of NaCl absorption by [HCO_3^-] in the marine teleost intestine is mediated by soluble adenylyl cyclase. *Am J Physiol Regul Integr Comp Physiol* 299: R62–R71, 2010.
42. **Tresguerres M, Levin LR, Buck J.** Intracellular cAMP signaling by soluble adenylyl cyclase. *Kidney Int* 79: 1277–1288, 2011.
43. **Tresguerres M, Parks SK, Katoh F, Goss GG.** Microtubule-dependent relocation of branchial V-H^+-ATPase to the basolateral membrane in the Pacific spiny dogfish (*Squalus acanthias*): a role in base secretion. *J Exp Biol* 209: 599–609, 2006.
44. **Tresguerres M, Parks SK, Salazar E, Levin LR, Goss GG, Buck J.** Bicarbonate-sensing soluble adenylyl cyclase is an essential sensor for acid/base homeostasis. *Proc Natl Acad Sci USA* 107: 442–447, 2010.
45. **Tresguerres M, Parks SK, Wood CM, Goss GG.** V-H^+-ATPase translocation during blood alkalosis in dogfish gills: interaction with carbonic anhydrase and involvement in the postfeeding alkaline tide. *Am J Physiol Regul Integr Comp Physiol* 292: R2012–R2019, 2007.
46. **Villanger O, Veel T, Raeder MG.** Secretin causes H^+/HCO_3^- secretion from pig pancreatic ductules by vacuolar-type H^+-adenosine triphosphatase. *Gastroenterology* 108: 850–859, 1995.
47. **Wagner CA, Finberg KE, Breton S, Marshansky V, Brown D, Geibel JP.** Renal vacuolar-ATPase. *Physiol Rev* 84: 1263–1314, 2004.
48. **Wood CM, Bucking C, Fitzpatrick J, Nadella S.** The alkaline tide goes out and the nitrogen stays in after feeding in the dogfish shark, *Squalus acanthias*. *Respir Physiol Neurobiol* 159: 163–170, 2007.
49. **Wood CM, Kajimura M, Mommsen TP, Walsh PJ.** Alkaline tide and nitrogen conservation after feeding in an elasmobranch (*Squalus acanthias*). *J Exp Biol* 208: 2693–2705, 2005.
50. **Wood CM, Schultz AG, Munger RS, Walsh PJ.** Using omeprazole to link the components of the postprandial alkaline tide in the spiny dogfish, *Squalus acanthias*. *J Exp Biol* 212: 684–692, 2009.

Chapter III, in full, is a reprint of the material as it appears in the following citation: Roa JN, Tresguerres M. 2016. Soluble adenylyl cyclase is an acid-base sensor in epithelial base-secreting cells. American Journal of Physiology, Cell Physiology 311: C340–C349. doi: 10.1152/ajpcell.00089.2016. The dissertation author was the primary investigator and author of this paper.

CHAPTER IV

Bicarbonate-sensing soluble adenylyl cyclase is present in the cell cytoplasm and nucleus of multiple shark tissues

Physiological Reports

Open Access

Physiological Reports ISSN 2051-817X

ORIGINAL RESEARCH

Bicarbonate-sensing soluble adenylyl cyclase is present in the cell cytoplasm and nucleus of multiple shark tissues

Jinae N. Roa & Martin Tresguerres

Marine Biology Research Division, Scripps Institution of Oceanography, University of California San Diego, La Jolla, California, USA

Keywords
adcy10, cAMP, cyclic AMP, microdomain, pH sensing, phosphorylation, regulation of gene expression, signal transduction.

Correspondence
Martin Tresguerres, 9500 Gilman Drive, Mail Code 0202, La Jolla, CA 92093.
Tel: 858 534 5895
Fax: 858 534 7313
E-mail: mtresguerres@ucsd.edu

Funding Information
JNR is supported by the William Townsend Porter Predoctoral Fellowship from the American Physiological Society. This research was supported by NIH Training Grant in Marine Biotechnology (GM067550) to JNR and NSF grant IOS 1354181 to MT.

Received: 29 November 2016; Accepted: 30 November 2016

doi: 10.14814/phy2.13090

Physiol Rep, 5 (2), 2017, e13090, doi:10.14814/phy2.13090

Abstract

The enzyme soluble adenylyl cyclase (sAC) is directly stimulated by bicarbonate (HCO_3^-) to produce the signaling molecule cyclic adenosine monophosphate (cAMP). Because sAC and sAC-related enzymes are found throughout phyla from cyanobacteria to mammals and they regulate cell physiology in response to internal and external changes in pH, CO_2, and HCO_3^-, sAC is deemed an evolutionarily conserved acid-base sensor. Previously, sAC has been reported in dogfish shark and round ray gill cells, where they sense and counteract blood alkalosis by regulating the activity of V-type H^+- ATPase. Here, we report the presence of sAC protein in gill, rectal gland, cornea, intestine, white muscle, and heart of leopard shark *Triakis semifasciata*. Co-expression of sAC with transmembrane adenylyl cyclases supports the presence of cAMP signaling microdomains. Furthermore, immunohistochemistry on tissue sections, and western blots and cAMP-activity assays on nucleus-enriched fractions demonstrate the presence of sAC protein in and around nuclei. These results suggest that sAC modulates multiple physiological processes in shark cells, including nuclear functions.

Introduction

The acid-base status of physiological fluids is largely dictated by pH, CO_2, and bicarbonate (HCO_3^-) levels, and acid-base status is one of the most tightly regulated physiological processes because even small deviations from the acid-base set point can affect the structure and function of enzymes and other cellular components. In animals, the acid-base status of extracellular fluids is regulated by specialized organs such as gills, lungs, and kidneys, which provide a stable acid-base environment to the rest of the cells in the body.

An essential requirement for acid-base regulation is the ability to sense acid-base conditions in the first place. One evolutionarily conserved acid-base sensing mechanism relies on the enzyme soluble adenylyl cyclase (sAC, adcy10), which is directly regulated by HCO_3^- to produce the ubiquitous messenger molecule cyclic adenosine monophosphate (cAMP) (Buck et al. 1999; Chen et al. 2000). In vivo, the HCO_3^- that stimulates sAC can originate from the carbonic anhydrase-catalyzed hydration of CO_2 from external or metabolic origin, from intracellular CO_2/HCO_3^- elevations resulting from changes in external pH, or from HCO_3^- entry through ion transporting proteins (reviewed in Tresguerres et al. 2014, 2011; Tresguerres 2014). In recent years, sAC has been established as a sensor and regulator of blood acid-base status in the mammalian kidney (Paunescu et al. 2008, 2010; Gong et al. 2010) and in gills of dogfish shark (Tresguerres et al.

2010c) and round rays (Roa and Tresguerres 2016), as well as in neuronal chemo-sensitive cells known to regulate lung ventilation (Imber et al. 2014; Nunes et al. 2014). In addition to sAC, the organs mentioned above posses other putative acid-base sensors (reviewed in Tresguerres et al. 2010a), some of which also produce cAMP. For example, some cells in the mammalian kidney express H^+-sensing G-protein coupled receptors (GPCRs) linked to transmembrane adenylyl cyclases (tmACs) (Ludwig et al. 2003; Sun et al. 2010, 2015), and round ray gill acid- and base-secreting cells contain both sAC and tmACs (Roa and Tresguerres 2016). The existence of multiple sources of cAMP raises questions about how downstream signaling is regulated and coordinated. Simply put, how can a single messenger molecule regulate multiple, often antagonistic, processes in a same cell? In response to these questions, the "cAMP signaling microdomain" model has been proposed, whereby cAMP-producing enzymes are tethered to the cell membrane, to cytoskeletal components, and inside the nucleus and mitochondria, together with phosphodiesterase enzymes that degrade cAMP thus preventing cAMP diffusion and cross-communication between cAMP-producing focal points (reviewed in Cooper 2003; Lefkimmiatis and Zaccolo 2014; Tresguerres et al. 2011). Although this model is supported by studies in several mammalian cells such as HT22, AtT20, and 3T3-L1 from brain, pituitary, and embryonic tissues, respectively (Inda et al. 2016), evidence in other animals is mostly lacking. Thus, the first aim of this study was to explore whether acid- and base-secreting gill cells from the leopard shark (*Triakis semifasciata*) have the two sources of cAMP (sAC and tmACs), and therefore if the cAMP microdomain model is widespread in vertebrate animals.

In addition to acid-base regulatory epithelia, variations in pH, CO_2, and HCO_3^- levels are known to affect virtually every physiological process. While many of these effects may be due to the direct action of H^+ or HCO_3^- on specific effector proteins (Sadowski et al. 1976; Aronson et al. 1982; Srivastava et al. 2007), many other effects have been recently been found to be mediated by sAC-derived cAMP regulation. For example, in response to extracellular alkalosis, sAC has been shown to simulate ion and water transport across fish intestinal epithelia (Tresguerres et al. 2010b; Carvalho et al. 2012), and mammalian renal collecting duct (Hallows et al. 2009) and pancreas (Strazzabosco et al. 2009), heart beat rate in hagfish recovering from anoxia (Wilson et al. 2016), sperm flagellar movement and capacitation (Esposito et al. 2004; Hess et al. 2005), and metabolic coupling between neurons and astrocytes in rat (Choi et al. 2012), among others Tresguerres et al. 2014 Tresguerres et al. 2010a. Because sharks experience a pronounced blood alkalosis in the postfeeding period, also known as the "alkaline tide" (Wood et al. 2005, 2007a, 2010), HCO_3^--stimulated sAC is a good candidate to mediate multiple physiological adjustments. Thus, the second objective of this study was to examine the presence of sAC in shark organs that accomplish physiological functions known to be modulated by acid-base conditions, and for which there is evidence for the involvement of sAC in similar organs from mammals and fish. With this in mind, we examined the rectal gland, cornea, muscle, heart, and intestine.

Finally, sAC has been reported in the nucleus of some mammalian cells, where it is proposed to form a cAMP signaling microdomain that regulates gene expression by cAMP/PKA-dependent phosphorylation of transcription factors (Zippin et al. 2003, 2004). Metabolic alkalosis and the postfeeding alkaline tide are known to upregulate the abundance of various proteins in gill (Tresguerres et al. 2006) and rectal gland (Dowd et al. 2008), as well as the activity of metabolic and iono-regulatory enzymes in rectal gland (Walsh et al. 2006; Wood et al. 2008). Thus, the third and final aim of this study was to determine whether sAC is present in the nucleus of shark gill and rectal gland cells, as a first step to identifying the molecular mechanisms that may modulate gene transcription in response to alkalosis.

Methods

Experimental animals

All experiments were approved by the SIO-UCSD animal care committee under protocol number #S10320 in compliance with the IACUC guidelines for the care and use of experimental animals. Leopard sharks were caught from La Jolla Shores, CA, housed in tanks with flowing seawater, and were fed chopped squid or mackerel three times a week.

Tissue sampling

Specimens were killed by an overdose of tricaine methanesulfonate (0.5 $g{\cdot}L^{-1}$) and samples from the various organs were taken for the different experimental procedures. For immunohistochemistry, samples were fixed in 0.2 mol/L cacodylate buffer, 3.2% paraformaldehyde, 0.3% glutaraldehyde for 6 h, transferred to 50% ethanol for 6 h, and stored in 70% ethanol until further processing as described in Tresguerres et al. (2005). For western blot analysis, gill samples were flash frozen in liquid nitrogen and stored at −80°C. For nuclei isolation, gill and rectal gland samples were placed ice-cold shark saline (280 mmol/L NaCl, 6 mmol/L KCl, 5 mmol/L $NaHCO_3$,

3 mmol/L $MgCl_2$, 0.5 mmol/L $NaSO_4$, 1 mmol/L Na_2HPO_4, 350 mmol/L urea, 70 mmol/L trimethylamine N-oxide, 5 mmol/L glucose, 1:100 protease inhibitor cocktail [1 mmol/L dithiothreitol, 1 mmol/L phenylmethylsulfonyl fluoride, 10 mmol/L benzamidine hydrochloride hydrate; SigmaAldrich], pH 7.7) and processed immediately.

Nuclei isolation

Nuclei were isolated from the gills and rectal gland of leopard sharks using methods adapted from research on nuclear sAC in mammals (Zippin et al. 2004).A quantity of 100 mg of fresh tissues were homogenized (30 sec, 4°C) by hand using a glass pestle tissue grinder with 1 mL of shark saline and differential centrifugation used to separate nuclear, membrane, and cytoplasmic fractions. Initially, homogenates were centrifuged for 2 min at 1000*g*. Cytoplasmic and membrane fractions remained in the supernatant and were removed, while the nucleus-containing pellet was resuspended in a mix of fresh shark saline, a sucrose solution (1 mol/L), and Optiprep density gradient medium (1:1:2) (SigmaAldrich, St. Louis, MO) and then centrifuged for 20 min at 10,000*g* to obtain a nuclear-enriched pellet.

Antibodies and reagents

Two custom-made polyclonal rabbit antibodies were used: one specifically recognizes an epitope in the second catalytic domain of dogfish sAC (dfsAC) (INNEFRNYQGRINKC) (Tresguerres et al. 2010c) and the other specifically recognizes a conserved region in the VHA B-subunit (AREEVPGRRGFPGY) (Roa et al. 2014). Both antibodies were custom made and produced GenScript (Piscataway, NJ). Na^+/K^+-ATPase (NKA) was immunolocalized using a monoclonal mouse antibody raised against the chicken α-subunit (Lebovitz et al. 1989), purchased from the Developmental Studies Hybridoma Bank (Iowa City, IA). Horseradish peroxidase (HRP)-conjugated goat anti-mouse and goat anti-rabbit antibodies (BioRad, Hercules, CA) were used for immunoblot detection. Fluorescent goat anti-mouse Alexa Fluor 568 and goat anti-rabbit Alexa Fluor 488 and Alexa Fluor 555 secondary antibodies (Invitrogen, Grand Island, NY) were used for immunolocalization. BODIPY-FL Forskolin dye (ThermoFisher Scientific, Waltham, MA) was used to determine tmAC localization; the BODIPY-FL Forskolin conjugate utilizes forskolin, a compound that selectively binds to tmACs (Seamon and Daly 1981; Buck et al. 1999), to localize tmACs and has recently been used in mammalian cell cultures (Calebiro et al. 2009; Kuna et al. 2013), zebrafish (Kumai et al. 2014), and round rays (Roa and Tresguerres 2016). KH7 was a kind gift of Dr. Lonny Levin and Dr. Jochen Buck (Weill Cornell Medical College). Forskolin was purchased from Enzo Life Sciences (Farmingdale, NY), and DDA (2′, 5′-dideoxyadenosine) from CalBiotech (Spring Valley, CA).

Western blotting

Tissue samples were processed for western blots in a manner similar to Roa et al. (2014) and Roa and Tresguerres (2016). In brief, 20 μg of proteins were separated on 7.5% polyacrylamide mini gel (60 V 15 min, 200 V 45 min) and transferred to a polyvinylidene difluoride (PVDF) membrane (Bio-Rad). After transfer, PVDF membranes were incubated in blocking buffer (tris-buffered saline, 1% tween, 5% skim milk) at room temperature (RT) for 1 h and incubated in the primary antibody at 4°C overnight (anti-dfsAC = 3 μg/mL; anti-NKA = 1.5 μg/mL). PVDF membranes were washed 3× (10 min each) in tris-buffered saline + 1% tween (TBS-T), incubated in the appropriate anti-rabbit or anti-mouse secondary antibodies (1:10,000) at RT for 1 h, and washed 3× (10 min each) in TBS-T. Bands were made visible through addition of ECL Prime Western Blotting Detection Reagent (GE Healthcare, Waukesha, WI) and imaged and analyzed in a BioRad Universal III Hood using ImageQuant software (BioRad). PVDF membranes incubated in blocking buffer with anti-dfsAC antibodies and 300-fold excess blocking peptide served as control and did not show any bands.

Immunostaining of tissue sections and isolated nuclei

Tissue samples fixed and stored in 70% ethanol as described above were processed into 7 μm histological sections following Roa et al. (2014) and Roa and Tresguerres (2016). After blocking (1 h, PBS, 2% normal goat serum, 0.02% keyhole limpet hemocyanin, pH 7.7), sections were incubated in the anti-dfsAC primary antibodies at 4°C overnight (12 μg/mL). Slides were washed 3× in PBS, incubated in goat anti-rabbit Alexa Fluor 488 secondary antibodies (1:500) at RT for 1 h, incubated with the nuclear stain Hoechst 33342 (Invitrogen) (5 μg/mL) for 5 min, washed 3× in PBS, and permanently mounted in Fluorogel with tris buffer (Electron Microscopy Sciences, Hatfield, PA). Immunofluorescence was detected using an epifluorescence microscope (Zeiss AxioObserver Z1) connected to a metal halide lamp and appropriate filters. Digital images were adjusted, for brightness and contrast, using Zeiss Axiovision software and Adobe Photoshop. Antigen retrieval was required for anti-dfsAC, which involved incubating slides in heated (95°C) citrate

unmasking buffer (10 mmol/L citric acid, 0.05% Tween20, pH 6.0) for 30 min following rehydration. For anti-dfsAC, control sections incubated in blocking buffer with anti-dfsAC antibodies and 300-fold excess blocking peptide showed no visible sAC immunoreactivity. For localization of sAC in all gill cells at longer exposure times and for localization of sAC to the cell nucleus of histological sections, images were captured using structured illumination (Zeiss Apotome2).

Following isolation, nuclei were resuspended in 100 μL of saline, allowed to settle on poly-L-lysine-coated coverslips for 1 h, fixed for 20 min (3.2% paraformaldehyde, and 0.3% glutaraldehyde in shark saline, RT), incubated in blocking buffer for 1 h (RT), incubated in anti-dfsAC antibodies at 4°C overnight (12 μg/mL), and processed for immunocytochemistry as described above.

Co-expression of sAC with NKA, VHA, tmACs

For immunolocalization of sAC to NKA-rich cells, sections were processed as described above then incubated in a mixture of anti-dfsAC (rabbit) and anti-NKA (mouse) antibodies overnight (4°C), followed by a mixture of goat anti-rabbit Alexa Fluor 488 and goat anti-mouse Alexa Fluor 568 secondary antibodies as described in Roa et al. (2014). For immunolocalization of sAC to VHA-rich cells, sections were first incubated in anti-dfsAC antibodies alone overnight (4°C). This was followed by incubation in goat anti-rabbit Alexa Fluor 488 secondary antibodies (1 h, RT), blocking buffer (1 h, RT), anti-VHA antibodies (4 h, RT), goat anti-rabbit Alexa Fluor 555 secondary antibodies (1 h, RT), and processed as described above. Similarly, to show co-expression of sAC and tmACs, sections were incubated alone in anti-dfsAC antibodies overnight (4°C), followed by goat anti-rabbit Alexa Fluor 555 secondary antibodies (1°h, RT) and BODIPY-FL Forskolin dye (30 min, RT) as described in Roa and Tresguerres (2016) (anti-dfsAC = 12 μg/mL; anti-VHA = 6 μg/mL; anti-NKA = 6 μg/mL; BODIPY-FL Forskolin = 10 μmol/L).

cAMP assays

Tissue homogenates and isolated nuclei were incubated for 30 min at RT on an orbital shaker (300 rpm) in 100 mmol/L Tris (pH 7.5), 5 mmol/L ATP, 10 mmol/L $MgCl_2$, 0.1 mmol/L $MnCl_2$, 0.5 mmol/L IBMX, 1 mmol/L dithiothreitol (DTT), 20 mmol/L creatine phosphate (CP), and 100 U·mL^{-1} creatine phosphokinase (CPK). For inhibition of sAC activity, samples were incubated in 50 μmol/l KH7, a concentration known to inhibit elasmobranch sAC but not tmAC (Tresguerres et al. 2010c; Roa and Tresguerres 2016). For inhibition of tmAC activity, tissue homogenates were incubated in 10 μmol/L forskolin and combinations 50 μmol/L KH7 and 100 μmol/L DDA, a concentration known to inhibit elasmobranch tmACs but not sAC (Roa and Tresguerres 2016). cAMP concentrations were determined using DetectX Direct Cyclic AMP Enzyme Immunoassay (Arbor Assays, Ann Arbor, MI).

Statistical analysis

All quantitative data from experimental groups were analyzed for significant differences using a one-way repeated measures ANOVA and Tukey's Multiple Comparison Test ($P < 0.001$). All analysis completed using GraphPad Prism software (GraphPad, La Jolla, CA).

Results

sAC is present in acid-base regulatory gill cells

Anti-dfsAC antibodies recognized the predicted ~110 kDa band for shark sAC in western blots from leopard shark gill extracts, but not in control blots (Fig. 1A). Gill extracts incubated in 40 mmol/L HCO_3^- produced significantly more cAMP than gill extracts incubated in control conditions (65 ± 7 pmol μL^{-1} vs. 43 ± 3 pmol μL^{-1}, Fig. 1B); HCO_3^--stimulated cAMP production was inhibited by the sAC-specific small molecule inhibitor KH7 (Fig. 1B), which is a hallmark of sAC activity. In histological sections, sAC immunofluorescence was present throughout the cytoplasm of acid-base regulatory cells along the interlamellar gill region (Fig. 1C) but was absent in control sections (Fig. 1D). Increasing the exposure time revealed sAC is also present in all other cell types (Fig. 1E), although at much lower abundance. However, this sAC immunostaining was also specific as no signal was present in time-matched control sections, also imaged at longer exposure times (Fig. 1F). Additionally, double immunolabeling demonstrated sAC is highly abundant in both shark acid-base regulatory cell types, as strong sAC immunoreactivity was co-expressed with either NKA or VHA in acid-secreting NKA-rich cells (Fig. 2A–C) and base-secreting VHA-rich cells (Fig. 2D–F).

sAC and tmACs in leopard shark gills

Similar to reports from round ray (Roa and Tresguerres 2016), tmACs were present and co-expressed with sAC in leopard shark gill acid-base regulatory cells, indicating the presence of two separate sources of cAMP in these cells (Fig. 3A–C). Gill extracts incubated in the tmAC agonist

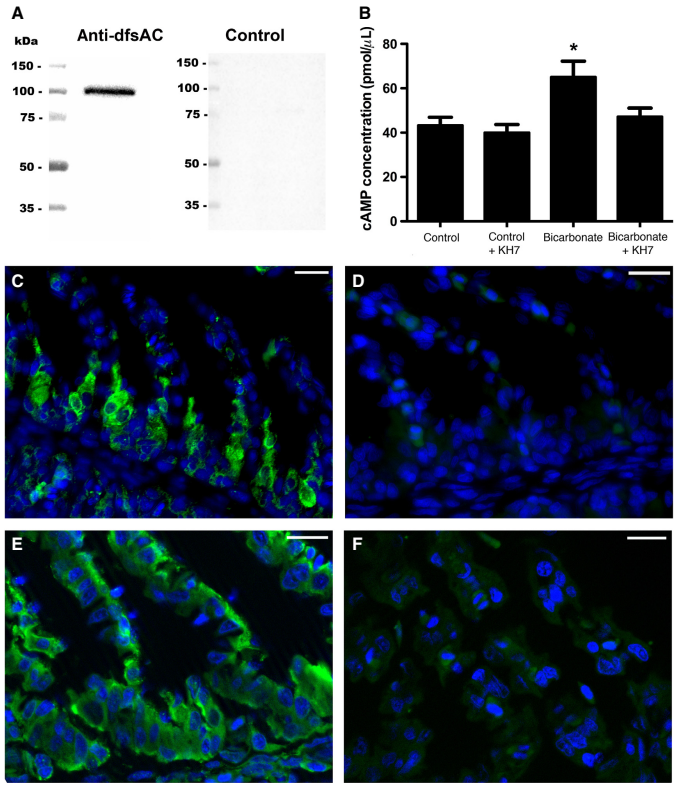

Figure 1. sAC in leopard shark gills. (A) anti-dogfish sAC (dfsAC) antibodies specifically recognized the 110-kDa shark sAC in western blots from 20 μg of gill crude homogenate, but not in peptide preabsorption control blots. (B) 40 mmol/L HCO_3^- (+DMSO) stimulated cAMP production in gill crude homogenates, which was blocked by the sAC-specific inhibitor KH7 ($n = 5$, $P < 0.001$). (C–D) sAC immunoreactivity was highly abundant in acid-base regulatory cells from leopard shark gills (C, green), but not in peptide preabsorption control sections (D). (E–F) At longer exposure times, sAC immunoreactivity was present in all leopard shark gill cells (E, green), but not in peptide preabsorption control sections (F). Nuclei stained in blue. Scale bars = 20 μm. cAMP, cyclic adenosine monophosphate; sAC, soluble adenylyl cyclase.

forskolin produced significantly more cAMP than gill extracts incubated in control conditions (971 $\pm$ 206 pmol μL^{-1} vs. 348 $\pm$ 90 pmol μL^{-1}, Fig. 3D). Forskolin-stimulated cAMP production was inhibited by the tmAC-specific inhibitor DDA but not inhibited by the sAC-specific inhibitor KH7.

sAC is present throughout leopard shark tissues

Anti-dfsAC antibodies recognized the predicted ~110 kDa band for shark sAC in western blots from leopard shark rectal gland, cornea, intestine, white muscle, and heart (Fig. 4A). The smaller molecular weight bands showed in Figure 4A likely correspond to sAC splice variants or isoforms as described for mammalian sAC (Geng et al. 2005; Farrell et al. 2008); however, these bands are much fainter compared to the 110 KDa band and only appear at relatively long exposure time.

In histological sections, sAC immunofluorescence was present throughout the cytoplasm of cells in the rectal gland, eye, and intestine. In the rectal gland, sAC immunofluorescence was strongest in the tubule cells, which secrete Na^+ and Cl^- ions into the gland lumen (Fig. 4B). In the cornea, sAC immunofluorescence was strongest in epithelial cells and stroma keratocytes, and it was also present in endothelial cells (Fig. 4C), and in the intestine sAC was highly abundant in all epithelial cells (Fig. 4D). In addition, some cells showed sAC immunostaining in the nucleus, which was further explored in gill

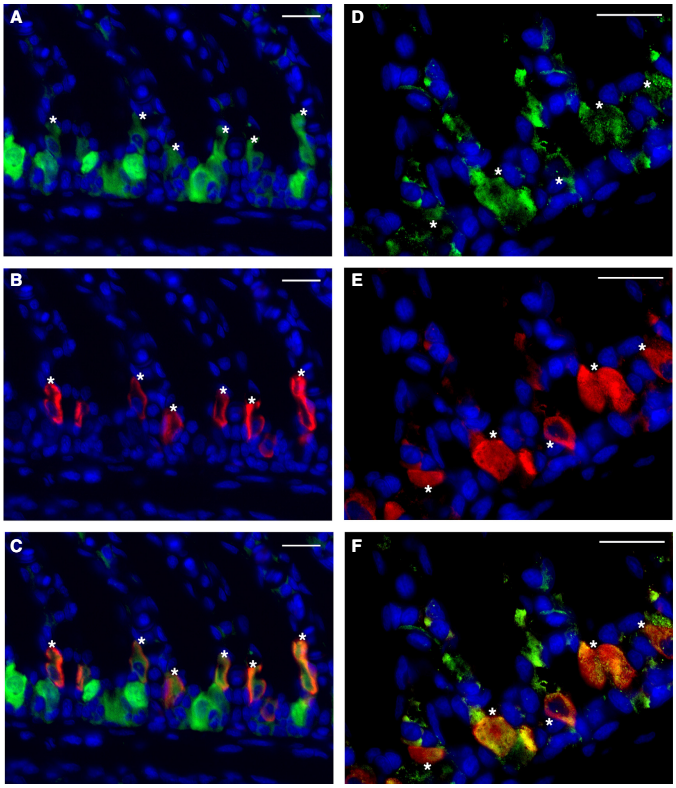

Figure 2. sAC in Na^+/K^+-ATPase (NKA)-rich and vacuolar-type H^+-ATPase (VHA)-rich gill cells. (A–C) sAC immunoreactivity (A, green) and NKA immunoreactivity (B, red) are co-expressed together in cells along the interlamellar gill region (C). Cells marked with asterisks (*) co-express sAC and NKA. (D–F): sAC immunoreactivity (D, green) and VHA immunoreactivity (E, red) colocalize together in the cytoplasm of cells along the interlamellar gill region (F). Cells marked with asterisks (*) co-express sAC and VHA. Nuclei stained in blue. Scale bars = 20 μm. NKA, Na_+/K_+-ATPase; VHA, vacuolar-type H^+-ATPase; sAC, soluble adenylyl cyclase.

and rectal gland tissues as described below. sAC immunofluorescence was absent in control sections incubated in anti-dfsAC antibodies and 300-fold excess sAC peptide.

sAC is present and active in leopard shark cell nuclei

Differential centrifugation separated crude homogenate, cytoplasm, membrane, and nuclear fractions from gill extracts. Anti-dfsAC antibodies recognized the ~110 kDa band for shark sAC in western blots from gill crude homogenate, cytoplasm, and nuclear fractions, but no band was detected in the membrane fraction, consistent with the lack of transmembrane domains in the sAC protein, and also suggesting sAC in shark gill cells is not strongly associated with membrane proteins (Fig. 5A). Unfortunately, commercial antibodies against the mammalian nuclear marker proteins CREB and histone did not work in shark tissues. Thus, validation of the cell fractionation protocol was performed by western blots that detected Na^+/K^+-ATPase in the membrane fraction only (Fig. 5B), and by visual inspection that confirmed enrichment of Hoechst-stained nuclei in the nuclear fraction (Fig. 5C).

The presence of sAC in gill cell nuclei was additionally confirmed by cAMP activity assays on isolated nuclei, and by immunostaining of gill sections and isolated nuclei. Isolated gill nuclei incubated in 40 mmol/L HCO_3^- produced significantly more cAMP than nuclei incubated in

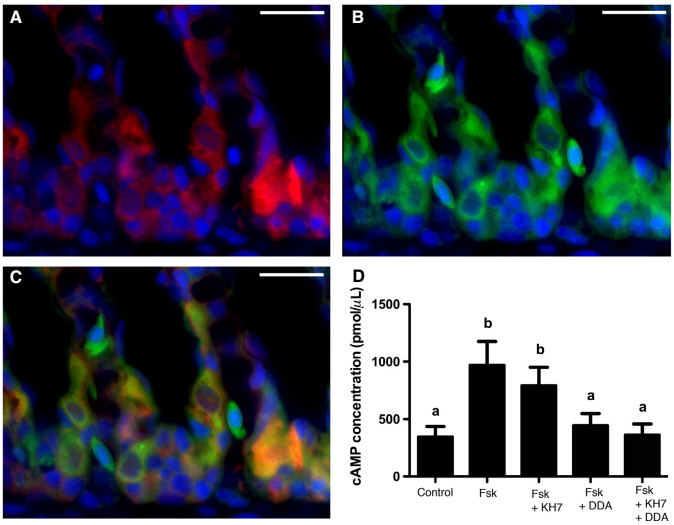

Figure 3. sAC and transmembrane adenylyl cyclases (tmACs) in leopard shark gills. (A–C) sAC immunoreactivity (A, red) and BODIPY-FL forskolin-labeled tmACs (B, green) are found together in cells along the interlamellar gill region (C). (D) Forskolin stimulated cAMP production in gill crude homogenates, which was blocked by the tmAC-specific inhibitor 2′, 5′-dideoxyadenosine (DDA) but not by the sAC-specific inhibitor KH7 ($n = 4$, $P < 0.001$). Nuclei stained in blue. Scale bars = 20 μm. cAMP, cyclic adenosine monophosphate; sAC, soluble adenylyl cyclase.

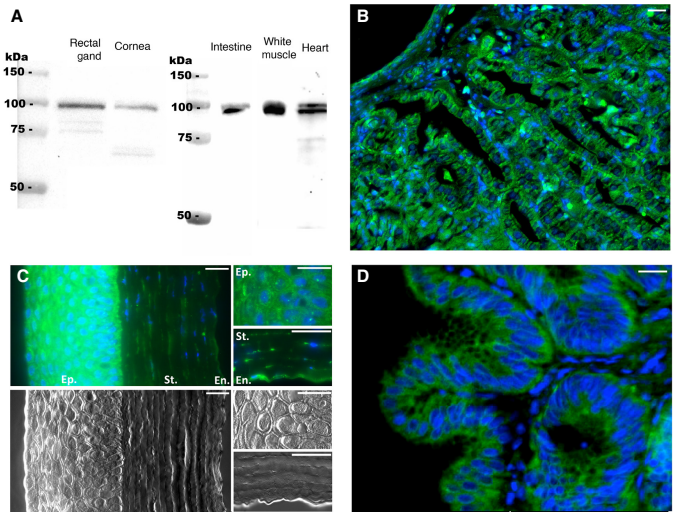

Figure 4. sAC in leopard shark tissues. (A) anti-dogfish sAC (dfsAC) antibodies specifically recognized the 110-kDa shark sAC in western blots using crude homogenates of rectal gland, cornea, intestine, white muscle, and heart (20 μg total protein in each lane). (B–D) sAC immunoreactivity (green) was highly abundant in leopard shark (B) rectal gland, (C) cornea – sAC immunoreactivity on top 3 panels, corresponding DIC images on lower 3 panels – with sAC immunoreactivity strongest in the epithelium (Ep.) and stroma (St.) but also present in endothelial cells (En.), and (D) intestine. Nuclei stained in blue. Scale bars = 20 μm. sAC, soluble adenylyl cyclase.

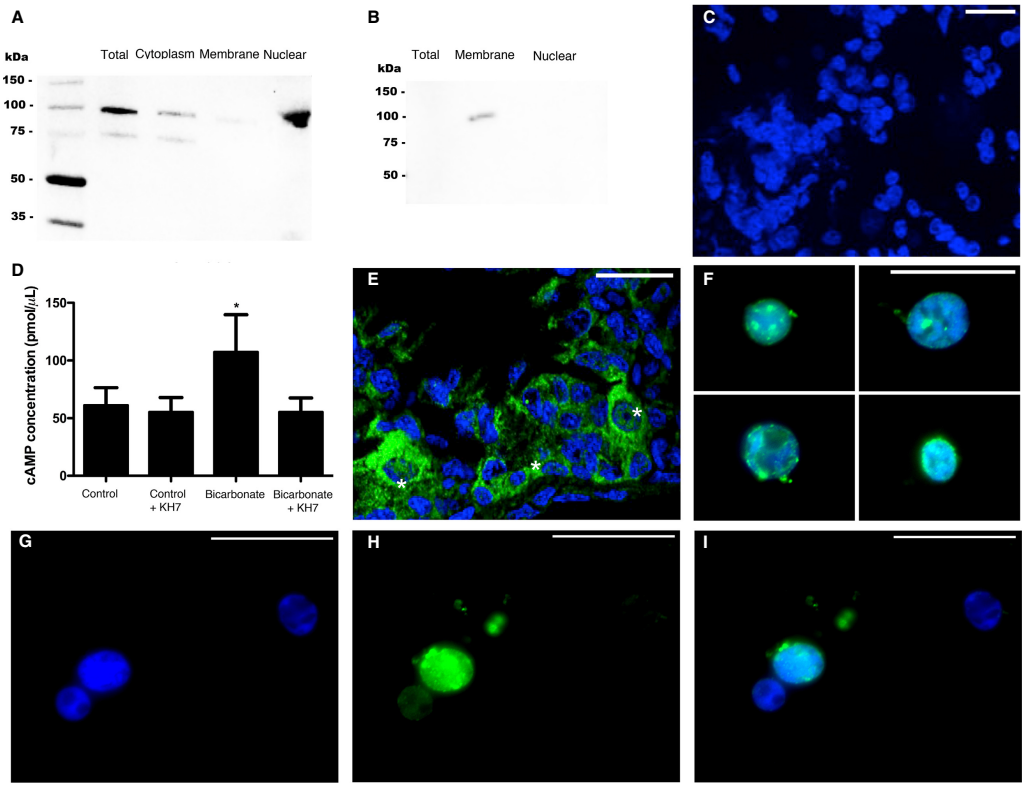

Figure 5. sAC in nuclei of leopard shark gill cells. (A) anti-dogfish sAC (dfsAC) antibodies specifically recognized the 110-kDa shark sAC in western blots from 20 μg of gill total crude homogenate, cytoplasmic, and nuclear cell fractions; but not in the membrane fraction. (B) anti-Na^+/K^+-ATPase (NKA) antibodies specifically recognized the 100-kDa NKA band in the membrane fraction, but not in total crude homogenate or in the nuclear fraction. (C) Representative image of Hoechst-stained isolated nuclei (blue) gathered using nuclear enrichment protocol. (D) 40 mmol/L HCO_3^- (+DMSO) stimulated cAMP production in nuclei isolated from gill cells, which was blocked by the sAC-specific inhibitor KH7 ($n = 5$, $P < 0.001$). (E–F) sAC immunoreactivity (green) was highly abundant in some nuclei in gill histological sections (E, *) – imaged using epifluorescence structured illumination – and in nuclei isolated from gill cells (F). Nuclei also stained in blue. (G–I) Representative images of isolated nuclei (G, blue) and sAC immunoreactivity (H, green), showing sAC is present in some, but not all, nuclei isolated from leopard shark gill cells (I). Scale bars = 20 μm. cAMP, cyclic adenosine monophosphate; sAC, soluble adenylyl cyclase.

control conditions (107 ± 32 pmol μL^{-1} vs. 61 ± 15 pmol μL^{-1}, Fig. 5D), and this HCO_3^--stimulated activity was inhibited by the sAC-specific small molecule inhibitor KH7 (Fig. 5D). sAC immunofluorescence was detected in and around nuclei from gill histological sections (Fig. 5E), as well as in isolated nuclei (Fig. 5F). However, similar to nuclei in histological sections (Figs. 3C and 5E) not all isolated gill nuclei display sAC immunofluorescence (Fig. 5G–I). Similar to gill, rectal gland cell nuclei display HCO_3^--stimulated, KH7-sensitive cAMP producing activity, and sAC immunofluorescence was detected in and around some, but not all, nuclei from rectal gland histological sections (Fig. 6).

Discussion

In this study, we investigated the cellular and subcellular localization of the evolutionarily conserved acid-base sensor sAC in various leopard shark tissues. We found sAC highly abundant throughout the cytoplasm of gill NKA- and VHA-rich cells, which respectively are acid- and base-secreting cells responsible for blood acid-base

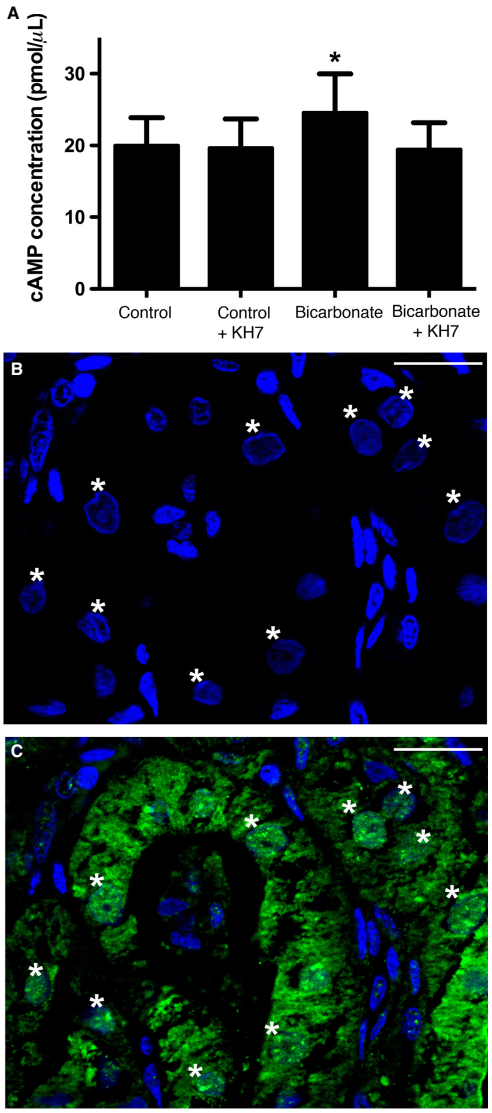

Figure 6. sAC in nuclei of leopard shark rectal gland cells. (A) 40 mmol/L HCO_3^- (+DMSO) stimulated cAMP production in nuclei isolated from rectal gland cells, which was blocked by the sAC-specific inhibitor KH7 ($n = 5$, $P < 0.001$). (B–C) nuclei (B, C, blue) and sAC (C, green) colocalize in rectal gland cells. Images acquired using epifluorescence structured illumination and sAC-positive nuclei marked with asterisks (*). Scale bars = 20 μm. cAMP, cyclic adenosine monophosphate; sAC, soluble adenylyl cyclase.

regulation. Additionally, sAC was co-expressed with tmACs in these cells, an indication that leopard sharks have two sources of cAMP in gill acid-base regulatory cells. sAC was also present in other tissues such as rectal gland, eye, intestine, white muscle, and heart, where it likely regulates tissue-specific responses to acid-base conditions. Finally, sAC was found associated with the cell nucleus of certain cells, where we propose it may regulate gene expression.

The presence of sAC in gill VHA-rich base-secreting cells has been previously reported in dogfish shark (Tresguerres et al. 2010c) and round ray (Roa and Tresguerres 2016). Extensive research on those two species has elucidated a mechanism for sensing and counteracting of blood alkalosis, whereby sAC in base-secreting cells senses blood alkalosis and triggers the translocation of VHA from cytoplasmic vesicles to the basolateral membrane. From that location, VHA moves H^+ into the blood and energizes excretion of HCO_3^- into seawater via the apical anion exchanger pendrin (Tresguerres et al. 2005,2007,2010b; Roa et al. 2014; Roa and Tresguerres 2016) reviewed in Tresguerres 2016). Thus, our evidence would suggest that the sAC-dependent mechanism to sense and counteract blood alkalosis applies to gills from all marine elasmobranchs.

In addition to base-secreting VHA-rich cells, sAC was highly abundant in NKA-rich acid-secreting cells. We propose that sAC in these cells acts to downregulate acid secretion during blood alkalosis, but experimental evidence would be required to support this model. Another interesting topic for future research is the interaction between sAC and tmACs, as these two cAMP-producing enzymes were co-expressed in leopard shark gill epithelial cells. In agreement with the cAMP microdomain model that predicts multiple cAMP sources with different downstream effects (reviewed in Cooper 2003; Tresguerres et al. 2011), sAC and tmACs have been reported to exert opposing effects on the VHA translocation in round ray base-secreting cells (Roa and Tresguerres 2016), as well as having differential effects on fish intestinal ion and water transport (Tresguerres et al. 2010b; Carvalho et al. 2012) and hagfish heart beat rate (Wilson et al. 2016). The co-expression of sAC and tmAC in both acid- and base-secreting cells found in this study suggests a more extensive and complex regulation of acid-base transport by cAMP in the shark gill epithelium.

In this study, sAC was found more highly abundant in acid-base regulatory cells of leopard shark, but sAC was more evenly expressed in all gill epithelial cells of round ray in a previous study (Roa and Tresguerres 2016). However, increasing the exposure time during

immunofluorescence detection revealed sAC is also present in all other gill epithelial cells of leopard shark, only at lower abundance. sAC localization in acid- and base-secreting cells was not studied in detail in dogfish, although strong presence in some pillar cells was noted (Tresguerres et al. 2010c). In any case, sAC is likely to play additional physiological roles in non-acid-base regulatory gill cells.

Elasmobranch fishes regularly experience pronounced blood acid-base disturbances as a result of their normal activities and ecophysiology. For example, they might experience metabolic acidosis as a result of exhaustive exercise (Richards et al. 2003), metabolic alkalosis in the post-feeding period (Wood et al. 2005, 2007a, 2010), and elevations in plasma HCO_3^- as a result of environmental oxygen, CO_2, and temperature levels (reviewed in Heisler 1988). Our finding that sAC protein is expressed in multiple shark tissues in addition to the gills, namely rectal gland, eye, intestine, white muscle, and heart, suggests sAC plays multiple general and organ-specific roles in these tissues. Furthermore, sAC has also been reported in dogfish shark red blood cells and testis (Tresguerres et al. 2014).

Based on published effects of HCO_3^- and cAMP, and reports from mammalian sAC, we hypothesize sAC may have multiple physiological functions in the shark tissues examined. In the rectal gland, sAC may regulate NaCl secretion, as this function is dependent on the blood acid-base status (Wood et al. 2007b), and it is well established to be regulated by cAMP as originally reported by (Stoff et al. (1977) and confirmed multiple times since. Additionally, alkalosis induces important transcriptional and enzymatic changes in rectal gland (Walsh et al. 2006; Deck et al. 2013), which may be mediated by sAC located in the nucleus as discussed below.

In the cornea, sAC is likely activated by high HCO_3^- in the aqueous humor (Maren et al. 1975) where it can facilitate fluid and ion balance necessary for proper vision. The cornea of elasmobranchs is an interesting tissue because it does not swell when placed in diluted saline solutions or even distilled water (Smelser 1962; Candia et al. 1976), unlike the mammalian cornea where swelling occurs and can lead to an opaque cornea, blurred vision, and even blindness. However, similar to sharks (this study), sAC is expressed throughout the mammalian cornea (Lee et al. 2014), where it regulates chloride permeability (Sun et al. 2004) and mediates protective HCO_3^--dependent effects on cell health (Li et al. 2011). Future research could explore whether sAC in shark cornea modulates ion and fluid transport as well as cell survival and protection, and whether these potential mechanisms are relevant for human cornea health.

The potential roles of sAC in muscle are varied, as myocytes generate large amounts of CO_2 and H^+ (Hochachka and Somero 2002). Furthermore, sAC has been recently shown to modulate heart beat rate in hagfish in response to HCO_3^- (Wilson et al. 2016). The presence of sAC in shark heart raises the question of whether the mechanism reported for hagfish also applies to elasmobranchs and other fishes.

Finally, sAC was abundantly expressed in shark intestinal epithelial cells, which resembles the intestine of marine teleost fish (Tresguerres et al. 2010b). However, while sAC in the marine bony fish intestine modulates NaCl and water absorption for hypo-osmoregulation (Tresguerres et al. 2010b; Carvalho et al. 2012), marine sharks are osmoconfomers or slight hyper-regulators and therefore sAC in the shark intestine must have some other function (s). Two testable hypotheses include the potential sAC-dependent regulation of intestinal nutrient and ammonia absorption, both of which are upregulated during the postfeeding alkaline tide (Wood and Bucking 2011). However, it is important to stress the potential sAC-dependent functions in shark rectal gland, cornea, muscle, heart and intestine mentioned above are speculative and their confirmation awaits experimental evidence.

Due to low availability of custom-made anti-shark sAC antibodies, we only screened for the presence of sAC protein in tissues that (Aronson et al. 1982) had not been previously examined in elasmobranchs, and (Baudouin-Legros et al. 2008) we are planning to conduct follow-up studies on. However, similar to humans (Uhlén et al. 2015), www.proteinatlas.org), sAC is likely to be ubiquitously expressed throughout elasmobranch tissues. This opens exciting research opportunities to elucidate sAC universal and cell-specific physiological roles.

In addition to the expected cytosolic localization, sAC was present in or around the nucleus of cells of the shark tissues examined, especially in gill, cornea, and rectal gland. We further investigated this potential subcellular localization of sAC by western blotting, enzyme activity assays, and immunolabeling in isolated nuclei from gill cells. Western blotting confirmed the presence of the predicted 110 KDa band corresponding to elasmobranch sAC (37, 54, this study). And enzyme activity assays confirmed HCO_3^--stimulated and KH7-sensitive cAMP production, a hallmark of sAC activity (Hess et al. 2005). However, it is important to note that although KH7 significantly reduced sAC activity in gill and rectal gland nuclei, we did observe KH7 insensitive cAMP in our preparations, which could be explained by contamination with sAC or tmACs from whole cells or other cellular components, as well as from tmACs presence around the nucleus. To rule these possibilities out, we first verified that the presumed nuclear-enriched fraction did not contain NKA, which would have been an indication of contamination with cell plasma membrane (Li and Donowitz

2014). Secondly, visual inspection of samples incubated with the DNA stain Hoechst 33342 confirmed the presumed nuclear-enriched fraction was indeed enriched in nuclei and devoid of whole cells. Finally, immunolabeling of isolated cell nuclei confirmed the presence of sAC in and around nuclei. Unfortunately, the tools (i.e., tmAC-specific antibodies) necessary to explore tmAC localization in or around the nucleus have yet to be developed for shark tmACs, and this remains an active area of investigation. Altogether, the evidence demonstrates sAC is present in the nuclei of shark gill cells and based on a subset of experiments, sAC is also present in other shark tissues, including rectal gland, cornea, and intestine. Interestingly, sAC was not present in all nuclei, suggesting sAC might move to the cell nucleus in response to acid-base stress (e.g., alkalosis) in order to regulate nuclear functions.

Nuclear sAC localization has previously only been described in cultured mammalian cell lines (Zippin et al. 2003, 2004; Schmitz et al. 2014), in cancer cells (Desman et al. 2014; Zippin et al. 2010), and in liver cells (Zippin et al. 2004). To the best of our knowledge, sAC in the nucleus of liver cells is the only other report (aside from this study) of nuclear sAC in a nonpathological, native organ, and similar to our results in sharks, only a fraction of cells had nuclear sAC immunostaining (Zippin et al. 2004). In the nucleus of mammalian cells, the only proposed role of sAC is to regulate the expression of certain genes *via* phosphorylation of the transcription factor CREB (Zippin et al. 2004; Baudouin-Legros et al. 2008; Li et al. 2011; Schmitz et al. 2014). Exploring this model in shark cells awaits the development of antibodies that specifically recognize shark CREB in its unphosphorylated and phosphorylated states.

Perspectives and Significance

Although sAC was already known to be present in elasmobranch gills and to sense and regulate blood acid-base status (Tresguerres et al. 2010c; Roa and Tresguerres 2016), its presence in organs not specialized in systemic acid-base regulation indicate multiple other physiological functions. The presence of sAC in the nucleus of shark cells opens new avenues of research on regulation of gene expression in response to acid-base disturbances. Furthermore, since sAC is an evolutionarily conserved acid-base sensor (Buck et al. 1999; Chen et al. 2000), nuclear sAC might serve a similar role in many other organisms. Elasmobranch fishes regularly experience large variations in pH, CO_2, and HCO_3^- levels as part of their normal physiology, and elasmobranch sAC is fairly well characterized at the biochemical, pharmacological, and cellular level. Thus, elasmobranch fishes are an excellent model to study acid-base sensing by sAC and its multiple downstream physiological effects. Another important finding of our study is that shark cells, like mammalian cells, have at least two different sources of cAMP and therefore must also possess cAMP signaling microdomains. This novel information for future research on cAMP signaling, as well for revisiting studies on cAMP that were published before the existence of sAC (and microdomains) was known.

Acknowledgments

Mr. Phil Zerofski (SIO) provided exceptional assistance with experimental animal capture and husbandry and general aquarium matters. Ms. Radha Karra and Ms. Mikayla Ortega helped with animal husbandry. The authors are also grateful to Prof. Gary Conrad (Kansas State University) for ideas on cornea biology.

Conflict of Interest

All the authors declared no competing interests.

References

Aronson, P. S., J. Nee, and M. A. Suhm. 1982. Modifier role of internal H^+ in activating the Na^+–H^+ exchanger in renal microvillus membrane vesicles. Nature 299:161–163.

Baudouin-Legros, M., N. Hamdaoui, F. Borot, J. Fritsch, M. Ollero, G. Planelles, et al. 2008. Control of basal CFTR gene expression by bicarbonate-sensitive adenylyl cyclase in human pulmonary cells. Cell. Physiol. Biochem. 21:75–86.

Buck, J., M. L. Sinclair, L. Schapal, M. J. Cann, and L. R. Levin. 1999. Cytosolic adenylyl cyclase defines a unique signaling molecule in mammals. Proc. Natl Acad. Sci. USA 96:79–84.

Calebiro, D., V. O. Nikolaev, M. C. Gagliani, T. de Filippis, C. Dees, C. Tacchetti, et al. 2009. Persistent cAMP-Signals Triggered by Internalized G-Protein–Coupled Receptors. PLoS Biol. 7:e1000172.

Candia, A., C. Adrian, M. Hogben, and P. I. Cook. 1976. Electrical parameters of the isolated cornea of the dogfish. Squalus acanthias. Invest Ophthalmol 15:1002–1005.

Carvalho, E. S. M., S. F. Gregório, D. M. Power, A. V. M. Canário, and J. Fuentes. 2012. Water absorption and bicarbonate secretion in the intestine of the sea bream are regulated by transmembrane and soluble adenylyl cyclase stimulation. J Comp Physiol B, Biochem Syst Environ Physiol 182:1069–1080.

Chen, Y., M. J. Cann, T. N. Litvin, V. Iourgenko, M. L. Sinclair, L. R. Levin, et al. 2000. Soluble adenylyl cyclase as an evolutionarily conserved bicarbonate sensor. Science 289:625–628.

Choi, H. B., G. R. J. Gordon, N. Zhou, C. Tai, R. L. Rungta, J. Martinez, et al. 2012. Metabolic communication between

astrocytes and neurons via bicarbonate-responsive soluble adenylyl cyclase. Neuron 75:1094–1104.

Cooper, D. M. F. 2003. Regulation and organization of adenylyl cyclases and cAMP. Biochem J 375:517–529.

Deck, C. A., S. J. McKay, T. J. Fiedler, C. M. R. LeMoine, M. Kajimura, C. M. Nawata, et al. 2013. Transcriptome responses in the rectal gland of fed and fasted spiny dogfish shark (*Squalus acanthias*) determined by suppression subtractive hybridization. Comp. Biochem. Physiol. Part D Genomics Proteomics 8:334–343.

Desman, G., C. Waintraub, and J. H. Zippin. 2014. Investigation of cAMP microdomains as a path to novel cancer diagnostics. Biochim. Biophys. Acta 1842:2636–2645.

Dowd, W. W., C. M. Wood, M. Kajimura, P. J. Walsh, and D. Kültz. 2008. Natural feeding influences protein expression in the dogfish shark rectal gland: a proteomic analysis. Comp. Biochem. Physiol. Part D Genomics Proteomics 3:118–127.

Esposito, G., B. S. Jaiswal, F. Xie, M. A. M. Krajnc-Franken, T. J. A. A. Robben, A. M. Strik, et al. 2004. Mice deficient for soluble adenylyl cyclase are infertile because of a severe sperm-motility defect. Proc. Natl Acad. Sci. USA 101:2993–2998.

Farrell, J., L. Ramos, M. , M. Kamenetsky, L. R. Levin, and J. Buck. 2008. Somatic 'soluble' adenylyl cyclase isoforms are unaffected in Sacy tm1Lex/Sacy tm1Lex "knockout" mice. PLoS ONE 3:e3251.

Geng, W., Z. Wang, J. Zhang, B. Y. Reed, C. Y. C. Pak, and O. W. Moe. 2005. Cloning and characterization of the human soluble adenylyl cyclase. Am. J. Physiol. Cell Physiol. 288: C1305–C1316.

Gong, F., R. Alzamora, C. Smolak, H. Li, S. Naveed, D. Neumann, et al. 2010. Vacuolar H^+-ATPase apical accumulation in kidney intercalated cells is regulated by PKA and AMP-activated protein kinase. Am. J. Physiol. Renal. Physiol. 298:F1162–F1169.

Hallows, K. R., H. Wang, R. S. Edinger, M. B. Butterworth, N. M. Oyster, H. Li, et al. 2009. Regulation of epithelial Na^+ transport by soluble adenylyl cyclase in kidney collecting duct cells. J. Biol. Chem. 284:5774–5783.

Heisler, N. 1988. Acid-Base Regulation. Pp. 215–252. in Physiology of elasmobranch fishes. Springer Berlin Heidelberg,.Berlin, Heidelberg.

Hess, K. C., B. H. Jones, B. Marquez, Y. Chen, T. S. Ord, M. Kamenetsky, et al. 2005. The "soluble" adenylyl cyclase in sperm mediates multiple signaling events required for fertilization. Dev. Cell 9:249–259.

Hochachka, P. W., and G. N. Somero. 2002. Biochemical Adaptation. Oxford University Press, Oxford.

Imber, A. N., J. M. Santin, C. D. Graham, and R. W. Putnam. 2014. A HCO3–dependent mechanism involving soluble adenylyl cyclase for the activation of Ca^{2+} currents in locus coeruleus neurons. Biochim. Biophys. Acta 1842:2569–2578.

Inda, C., P. A. Santos Claro Dos, J. J. Bonfiglio, S. A. Senin, G. Maccarrone, C. W. Turck, et al. 2016. Different cAMP sources are critically involved in G protein-coupled receptor CRHR1 signaling. J. Cell Biol. 214:181–195.

Kumai, Y., R. W. M. Kwong, and S. F. Perry. 2014. The role of cAMP-mediated intracellular signaling in regulating Na^+ uptake in zebrafish larvae. Am. J. Physiol. Regul. Integr. Comp. Physiol. 306:R51–R60.

Kuna, R. S., S. B. Girada, S. Asalla, J. Vallentyne, S. Maddika, J. T. Patterson, et al. 2013. Glucagon-like peptide-1 receptor-mediated endosomal cAMP generation promotes glucose-stimulated insulin secretion in pancreatic β-cells. Am. J. Physiol. Endocrinol. Metab. 305:E161–E170.

Lebovitz, R. M., K. Takeyasu, and D. M. Fambrough. 1989. Molecular characterization and expression of the (Na^+ + K^+)-ATPase alpha-subunit in *Drosophila melanogaster*. EMBO J. 8:193–202.

Lee, Y. S., L. Y. Marmorstein, and A. D. Marmorstein. 2014. Soluble adenylyl cyclase in the eye. Biochim. Biophys. Acta 1842:2579–83.

Lefkimmiatis, K., and M. Zaccolo. 2014. cAMP signaling in subcellular compartments. Pharmacol. Ther. 143:295–304.

Li, X., and M. Donowitz. 2014. Fractionation of subcellular membrane vesicles of epithelial and non-epithelial cells by OptiPrep™ density gradient ultracentrifugation. Methods Mol. Biol. 1174:85–99.

Li, S., K. T. Allen, and J. A. Bonanno. 2011. Soluble adenylyl cyclase mediates bicarbonate-dependent corneal endothelial cell protection. Am. J. Physiol. Cell Physiol. 300:C368–C374.

Ludwig, M.-G., M. Vanek, D. Guerini, J. A. Gasser, C. E. Jones, U. Junker, et al. 2003. Proton-sensing G-protein-coupled receptors. Nature 425:93–98.

Maren, T. H., P. Wistrand, E. R. Swenson, and A. B. Talalay. 1975. The rates of ion movement from plasma to aqueous humor in the dogfish. Squalus acanthias. Invest Ophthalmol 14:662–673.

Nunes, A. R., E. Monteiro, and E. Gauda. 2014. Soluble adenylyl cyclase in the locus coeruleus. Respir. Physiol. Neurobiol. 201:34–37.

Paunescu, T. G., N. Da Silva, L. M. Russo, M. McKee, H. A. J. Lu, S. Breton, et al. 2008. Association of soluble adenylyl cyclase with the V-ATPase in renal epithelial cells. Am. J. Physiol. Renal. Physiol. 294:F130–F138.

Paunescu, T. G., M. Ljubojevic, L. M. Russo, C. Winter, M. M. McLaughlin, C. A. Wagner, et al. 2010. cAMP stimulates apical V-ATPase accumulation, microvillar elongation, and proton extrusion in kidney collecting duct A-intercalated cells. Am. J. Physiol. Renal. Physiol. 298: F643–F654.

Richards, J. G., G. J. F. Heigenhauser, and C. M. Wood. 2003. Exercise and recovery metabolism in the Pacific spiny dogfish (*Squalus acanthias*). J Comp Physiol B, Biochem Syst Environ Physiol 173:463–474.

Roa, J. N., and M. Tresguerres. 2016. Soluble adenylyl cyclase is an acid/base sensor in epithelial base-secreting cells. Am. J. Physiol. Cell Physiol. 311:C340–C349.

Roa, J. N., C. L. Munévar, and M. Tresguerres. 2014. Feeding induces translocation of vacuolar proton ATPase and pendrin to the membrane of leopard shark (*Triakis semifasciata*) mitochondrion-rich gill cells. Comp Biochem Physiol Part A Mol Integr Physiol 174:29–37.

Sadowski, J. A., C. T. Esmon, and J. W. Suttie. 1976. Vitamin K-dependent carboxylase. Requirements of the rat liver microsomal enzyme system. J Biological Chem. 251: 2770–2776.

Schmitz, B., J. Nedele, K. Guske, M. Maase, M. Lenders, M. Schelleckes, et al. 2014. Soluble adenylyl cyclase in vascular endothelium: gene expression control of epithelial sodium channel-α, Na^+/K^+-ATPase-α/β, and mineralocorticoid receptor. Hypertension 63:753–761.

Seamon, K. B., and J. W. Daly. 1981. Forskolin: a unique diterpene activator of cyclic AMP-generating systems. J Cyclic Nucleotide Res 7:201–224.

Smelser, G. K. 1962. Corneal hydration. Comparative physiology of fish and mammals. Invest Ophthalmol 1:11–32.

Srivastava, J., D. L. Barber, and M. P. Jacobson. 2007. Intracellular pH sensors: design principles and functional significance. Physiology (Bethesda) 22:30–39.

Stoff, J. S., P. Silva, M. Field, J. Forrest, A. Stevens, and F. H. Epstein. 1977. Cyclic AMP regulation of active chloride transport in the rectal gland of marine elasmobranchs. J. Exp. Zool. 199:443–448.

Strazzabosco, M., R. Fiorotto, S. Melero, S. Glaser, H. Francis, C. Spirli, et al. 2009. Differentially expressed adenylyl cyclase isoforms mediate secretory functions in cholangiocyte subpopulation. Hepatology 50:244–252.

Sun, X. C., M. Cui, and J. A. Bonanno. 2004. [HCO_3^-]-regulated expression and activity of soluble adenylyl cyclase in corneal endothelial and Calu-3 cells. BMC Physiol. 4:8.

Sun, X., L. V. Yang, B. C. Tiegs, L. J. Arend, D. W. McGraw, R. B. Penn, et al. 2010. Deletion of the pH sensor GPR4 decreases renal acid excretion. J. Am. Soc. Nephrol. 21:1745–1755.

Sun, X., L. Stephens, T. D. DuBose, and S. Petrovic. 2015. Adaptation by the collecting duct to an exogenous acid load is blunted by deletion of the proton-sensing receptor GPR4. Am. J. Physiol. Renal. Physiol. 309:F120–F136.

Tresguerres, M. 2014. sAC from aquatic organisms as a model to study the evolution of acid/base sensing. Biochim. Biophys. Acta 1842:2629–35.

Tresguerres, M. 2016. Novel and potential physiological roles of vacuolar-type H^+-ATPase in marine organisms. J. Exp. Biol. 219:2088–2097.

Tresguerres, M., F. Katoh, H. Fenton, E. Jasinska, and G. G. Goss. 2005. Regulation of branchial V-H^+-ATPase, Na^+/K^+-ATPase and NHE2 in response to acid and base infusions in the Pacific spiny dogfish (*Squalus acanthias*). J. Exp. Biol. 208:345–354.

Tresguerres, M., S. K. Parks, F. Katoh, and G. G. Goss. 2006. Microtubule-dependent relocation of branchial V-H^+-ATPase to the basolateral membrane in the Pacific spiny dogfish (*Squalus acanthias*): a role in base secretion. J. Exp. Biol. 209:599–609.

Tresguerres, M., S. K. Parks, C. M. Wood, and G. G. Goss. 2007. V-H^+-ATPase translocation during blood alkalosis in dogfish gills: interaction with carbonic anhydrase and involvement in the postfeeding alkaline tide. Am. J. Physiol. Regul. Integr. Comp. Physiol. 292:R2012–R2019.

Tresguerres, M., J. Buck, and L. R. Levin. 2010a. Physiological carbon dioxide, bicarbonate, and pH sensing. Pflügers Archiv Eur J Physiol 460:953–964.

Tresguerres, M., L. R. Levin, J. Buck, and M. Grosell. 2010b. Modulation of NaCl absorption by [HCO_3^-] in the marine teleost intestine is mediated by soluble adenylyl cyclase. Am. J. Physiol. Regul. Integr. Comp. Physiol. 299:R62–R71.

Tresguerres, M., S. K. Parks, E. Salazar, L. R. Levin, G. G. Goss, and J. Buck. 2010c. Bicarbonate-sensing soluble adenylyl cyclase is an essential sensor for acid/base homeostasis. Proc. Natl Acad. Sci. USA 107:442–447.

Tresguerres, M., L. R. Levin, and J. Buck. 2011. Intracellular cAMP signaling by soluble adenylyl cyclase. Kidney Int. 79:1277–1288.

Tresguerres, M., K. L. Barott, M. E. Barron, and J. N. Roa. 2014. Established and potential physiological roles of bicarbonate-sensing soluble adenylyl cyclase (sAC) in aquatic animals. J. Exp. Biol. 217:663–672.

Uhlén, M., L. Fagerberg, B. M. Hallström, C. Lindskog, P. Oksvold, A. Mardinoglu, et al., 2015. Proteomics. Tissue-based map of the human proteome. Science 347:1260419.

Walsh, P. J., M. Kajimura, T. P. Mommsen, and C. M. Wood. 2006. Metabolic organization and effects of feeding on enzyme activities of the dogfish shark (*Squalus acanthias*) rectal gland. J. Exp. Biol. 209:2929–2938.

Wilson, C. M., J. N. Roa, G. K. Cox, M. Tresguerres, and A. P. Farrell. 2016. Introducing a novel mechanism to control heart rate in the ancestral pacific hagfish. J. Exp. Biol. 219:3227–3236.

Wood, C. M., C. Bucking 2011. Fish physiology: the multifunctional gut of fish. 1st ed. Academic Press, Cambridge.

Wood, C. M., M. Kajimura, T. P. Mommsen, and P. J. Walsh. 2005. Alkaline tide and nitrogen conservation after feeding in an elasmobranch (*Squalus acanthias*). J. Exp. Biol. 208:2693–2705.

Wood, C. M., M. Kajimura, C. Bucking, and P. J. Walsh. 2007a. Osmoregulation, ionoregulation and acid-base regulation by the gastrointestinal tract after feeding in the elasmobranch (*Squalus acanthias*). J. Exp. Biol. 210:1335–1349.

Wood, C. M., R. S. Munger, J. Thompson, and T. J. Shuttleworth. 2007b. Control of rectal gland secretion by blood acid-base status in the intact dogfish shark (*Squalus acanthias*). Respir. Physiol. Neurobiol. 156:220–228.

Wood, C. M., M. Kajimura, T. P. Mommsen, and P. J. Walsh. 2008. Is the alkaline tide a signal to activate

metabolic or ionoregulatory enzymes in the dogfish shark (*Squalus acanthias*)? Physiol. Biochem. Zool. 81:278–287.

Wood, C. M., P. J. Walsh, M. Kajimura, G. B. McClelland, and S. F. Chew. 2010. The influence of feeding and fasting on plasma metabolites in the dogfish shark (*Squalus acanthias*). Comp Biochem Physiol Part A Mol Integr Physiol 155:435–444.

Zippin, J. H., Y. Q. Chen, P. Nahirney, M. Kamenetsky, M. S. Wuttke, D. A. Fischman, et al. 2003. Compartmentalization of bicarbonate-sensitive adenylyl cyclase in distinct signaling microdomains. FASEB J 17:82–84.

Zippin, J. H., J. Farrell, D. Huron, M. Kamenetsky, K. C. Hess, D. A. Fischman, et al. 2004. Bicarbonate-responsive, "soluble" adenylyl cyclase defines a nuclear cAMP microdomain. J. Cell Biol. 164:527–534.

Zippin, J. H., P. A. Chadwick, L. R. Levin, J. Buck, and C. M. Magro. 2010. Soluble adenylyl cyclase defines a nuclear cAMP microdomain in keratinocyte hyperproliferative skin diseases. J Invest Dermatol 130:1279–1287.

Chapter IV, in full, is a reprint of the material as it appears in the following citation: Roa JN, Tresguerres M. 2017. Bicarbonate-sensing soluble adenylyl cyclase is present in the cell cytoplasm and nucleus of multiple shark tissues. Physiological Reports 5: e13090. doi: 10.14814/phy2.13090. The dissertation author was the primary investigator and author of this paper.

CHAPTER V

Introducing a novel mechanism to control heart rate in the ancestral Pacific hagfish

© 2016. Published by The Company of Biologists Ltd | Journal of Experimental Biology (2016) 219, 3227-3236 doi:10.1242/jeb.138198

RESEARCH ARTICLE

Introducing a novel mechanism to control heart rate in the ancestral Pacific hagfish

Christopher M. Wilson[1,*,‡], Jinae N. Roa[2,*], Georgina K. Cox[1], Martin Tresguerres[2] and Anthony P. Farrell[1,3]

ABSTRACT

Although neural modulation of heart rate is well established among chordate animals, the Pacific hagfish (*Eptatretus stoutii*) lacks any cardiac innervation, yet it can increase its heart rate from the steady, depressed heart rate seen in prolonged anoxia to almost double its normal normoxic heart rate, an almost fourfold overall change during the 1-h recovery from anoxia. The present study sought mechanistic explanations for these regulatory changes in heart rate. We provide evidence for a bicarbonate-activated, soluble adenylyl cyclase (sAC)-dependent mechanism to control heart rate, a mechanism never previously implicated in chordate cardiac control.

KEY WORDS: Heart rate control, Soluble adenylyl cyclase, Bicarbonate ions, cAMP production, Anoxia tolerance, Cardiac evolution

INTRODUCTION

Hagfishes are extant representatives of the craniate lineage, whose origin dates back 0.5 billion years (Ota and Kuratani, 2007). Beyond their basal position in vertebrate evolution, hagfishes are biologically intriguing because of their anoxia tolerance and their legendary ability to produce copious amounts of slime (Hansen and Sidell, 1983; Stecyk and Farrell, 2006; Cox et al., 2010; Herr et al., 2010). More recently, hagfish have been proposed as champions of CO_2 tolerance (Baker et al., 2015). Although tolerance of environmental extremes suits their habit of burrowing into dead and decaying animals for sustenance (Jørgensen et al., 1998), mechanistic explanations for sustained function under such conditions remain enigmatic. For example, when Pacific hagfish [*Eptatretus stoutii* (Lockington 1878)] are exposed to prolonged (36 h) anoxia, cardiac output is only reduced by approximately 26% because an increased cardiac stroke volume largely compensates for the halving of heart rate (10 to ∼4 beats min^{-1}; Cox et al., 2010; Gillis et al., 2015). Immediately after normoxic conditions are restored, heart rate then increases to 17.5 beats min^{-1}, almost double the normoxic heart rate, and cardiac output increases. Thus, over a 1-h period when the hagfish heart switches from sustained anaerobic metabolism (Hansen and Sidell, 1983; Farrell and Stecyk, 2007; Cox et al., 2011) back to aerobic metabolism, heart rate quadruples (∼4 to 17 beats min^{-1}; Cox et al., 2010). Therefore, it is surprising that the hagfish can regulate its heart rate over such a large range without any cardiac innervation. Consequently, the hagfish offers a fascinating model for the study of aneural mechanisms for controlling heart rate that contrasts with the situation for anoxia-tolerant vertebrates, such as crucian carp and freshwater turtles, which similarly slow heart rate during anoxia but use increased parasympathetic vagal tonus to the heart (Vornanen and Tuomennoro, 1999; Hicks and Farrell, 2000a,b; Stecyk et al., 2004; Stecyk et al., 2007).

Neural control of heart rate in the vertebrate lineage primarily involves sympathetic (stimulatory β-adrenergic) and parasympathetic (inhibitory cholinergic) mechanisms (Nilsson, 1983). The aneural hagfish heart, instead, is known to respond to applied catecholamines and has its own intrinsic store of catecholamines (Greene, 1902; Augustinsson et al., 1956; Jensen, 1961, 1965; Farrell, 2007). Furthermore, given that routine heart rate is dramatically slowed after injection of β-adrenergic antagonists (Fänge and Östlund, 1954; Axelsson et al., 1990; Fukayama et al., 1992), it would seem that routine, normoxic heart rate in hagfish is set by an autocrine adrenergic tonus acting presumably on the primary cardiac pacemaker cells located in the sinoatrial node, which would set the intrinsic cardiac pacemaker rate (Farrell, 2007). To date, the sinoatrial node has not been identified in any hagfish species, but is presumed to be present in *Eptatretus cirrhatus* because a V-wave that is characteristic of cardiac muscle contraction in the sinus venosus preceeds the P-wave associated with atrial contraction (Davie et al., 1987). [Note: a V-wave was not evident in the electrocardiogram of *Myxine glutinosa* (Satchell, 1986).] Combining this knowledge with the observation that stressing hagfish does not trigger the characteristic increase in circulating catecholamines shown by most vertebrates (Perry et al., 1993) has led to the hypothesis that the bradycardia observed in hagfish during anoxia represents a withdrawal of adrenergic tonus. Adrenergic tonus would presumably act by stimulating cAMP production involving transmembrane adenylyl cyclase (tmAC), a mechanism common to all vertebrate hearts (Nilsson, 1983).

Although an increased adrenergic tonus seems an attractive mechanism to explain the post-anoxia tachycardia in hagfish, routine heart rate in normoxic hagfish is notoriously unresponsive to catecholamine stimulation (Fänge and Östlund, 1954; Axelsson et al., 1990; Forser et al., 1992). Therefore, we explored another mechanism to supply cAMP to stimulate heart rate, namely the soluble adenylyl cyclase (sAC). sAC activity was first discovered in mammalian sperm cells (Buck et al., 1999), and sAC activity has subsequently been shown in the kidney, eye, respiratory tract, digestive tract and pancreas, and bone, and has also been shown to be involved in neural and immune functions (reviewed by Tresguerres et al., 2011). Intracellular sAC compartments also include the nucleus, mitochondria, mid-bodies and centrioles (Zippin et al., 2003, 2004; Acin-Perez et al., 2009; Tresguerres

[1]Department of Zoology, University of British Columbia, 6270 University Boulevard, Vancouver, British Columbia, Canada V6T 1Z4. [2]Marine Biology Research Division, Scripps Institution of Oceanography, University of California San Diego, 9500 Gilman Drive, La Jolla, CA 92093, USA. [3]Faculty of Land and Food Systems, University of British Columbia, 2357 Main Mall, Vancouver, British Columbia, Canada V6T 1Z4.
*These authors contributed equally to this work

‡Author for correspondence (cwilson@larrea.cl)

C.M.W., 0000-0002-1471-857X

Received 28 January 2016; Accepted 2 August 2016

RESEARCH ARTICLE Journal of Experimental Biology (2016) 219, 3227-3236 doi:10.1242/jeb.138198

List of symbols and abbreviations

anti-dfsAC	anti-dogfish soluble adenylyl cyclase antibody
BMAC	Bamfield Marine Sciences Centre
cAMP	cyclic adenosine monophosphate
DFO	Department of Fisheries and Oceans Canada
DMSO	dimethyl sulfoxide
EC_{50}	half-maximal effective concentration
HCN	hyperpolarization-activated cyclic nucleotide-gated
I_f	cardiac pacemaker 'funny' current
I_{Kr}	rapid, delayed rectifier potassium current
NBC	Na^+/HCO_3^- cotransporters
NCX	Na^+/Ca^{2+} exchange
PVDF	polyvinylidene difluoride
sAC	soluble adenylyl cyclase
tmAC	transmembrane adenylyl cyclase

et al., 2010a). While mammalian sAC requires both Mg^{2+} and Ca^{2+} as cofactors to produce cAMP from ATP (Litvin et al., 2003), shark sAC seems to require Mg^{2+} and Mn^{2+} (Tresguerres et al., 2010b). Importantly, sAC differs from tmAC by being activated by bicarbonate ions (HCO_3^-) rather than catecholamines (Buck et al., 1999; Chen et al., 2000; Tresguerres et al., 2010b, 2011). Although hagfish sAC has not yet been cloned, sAC genes are present in cartilaginous and bony fishes (Tresguerres et al., 2010b; reviewed in Tresguerres et al., 2014; Tresguerres, 2014), as well as in a variety of invertebrate animals including *Trichoiplax*, sponges, cnidarians, molluscs, echinoderms, insects and cephalochordates (Barott et al., 2013; Tresguerres, 2014; Tresguerres et al., 2010b, 2014). Furthermore, a hallmark of sAC enzymatic activity is HCO_3^--stimulated cAMP production, which is sensitive to the small inhibitor molecule KH7 (Hess et al., 2005; Tresguerres et al., 2010b, 2011). Based on HCO_3^--stimulation and sensitivity to KH7, two independent studies concluded that sAC modulates NaCl absorption across the intestine of marine bony fishes (Tresguerres et al., 2010a; Carvalho et al., 2012). This conclusion was substantiated by detection of a protein band of the predicted ∼110 kDa by heterologous antibodies against shark sAC (Tresguerres et al., 2010a).

Consequently, in addition to proposing that tmAC-mediated cAMP production is suppressed during anoxia and slows heart rate, we tested the hypothesis that sAC-mediated cAMP production plays a role in stimulating heart rate in hagfish, a cardiac control mechanism never previously tested in a chordate heart. To test these hypotheses, heart rate was measured in isolated hearts following sAC and tmAC stimulation, while sAC presence in cardiac tissue was probed using immunofluorescence, western blotting and enzyme activity assays. Immunofluorescence was also used to locate Na^+/HCO_3^- cotransporters (NBC) in the hagfish heart, which could facilitate HCO_3^- movements to modulate sAC activity.

MATERIALS AND METHODS

Animal husbandry

Pacific hagfish (112±1 g; mean±s.e.m.; n=110; male and female; wild caught) were collected using baited traps off the coast of Bamfield Marine Sciences Centre (BMSC), Bamfield, BC, Canada, where they were held until experimentation or transport. *In vivo* anoxia exposure experiments and tissue sampling were carried out at BMSC. Measurements of cAMP, western blotting and immunofluorescence were conducted on tissues shipped to the Scripps Institution of Oceanography, University of California, San Diego, CA, USA. Isolated heart experiments took place at the University of British Columbia, Vancouver, BC, Canada, which required transport to the West Vancouver Laboratory, Department of Fisheries and Oceans Canada (DFO), West Vancouver, BC, Canada, where they were housed in 4000 l tanks supplied with flow-through seawater (10±1°C) and fed frozen squid weekly. Animals were always fasted for a minimum of 1 week prior to an experimental treatment, and all experiments were conducted in accordance with the animal care policies of the University of British Columbia, BMSC and DFO (AUP 12-0001).

Isolated heart experiments

Hagfish were killed by a blow to the head, followed by immediate decapitation. The heart was rapidly excised and immersed in 25 ml chilled (10°C), aerated hagfish saline within a plastic basket containing two electrocardiogram electrodes. The composition of the hagfish saline was (in mmol l^{-1}): 410 NaCl, 10 KCl, 14 $MgSO_4$, 4 urea, 20 glucose, 10 HEPES, 4 $CaCl_2$ (Sigma-Aldrich, St Louis, MO, USA for all chemicals). The pH of the saline was adjusted to 7.9. The electrocardiogram of the excised heart was continuously monitored, stored and analyzed using Biopac and AcqKnowledge software (Goleta, CA, USA). Heart rate (an average over 10 beats) stabilized prior to (<1 h) any testing. Trial runs (data not shown) established that this control normoxic heart rate of the excised heart would remain stable for >24 h under these conditions while the saline was aerated. A different set of hearts was used for each of the following tests.

Nadolol (Tocris Bioscience, Minneapolis, MN, USA), a β-adrenoceptor antagonist, was used to study the inhibition of adrenergic stimulation of tmAC. The bath saline was changed every 30 min to incrementally increase the nadolol concentration from 1.0 pmol l^{-1} to 1 mmol l^{-1}. Then, with maximal adrenergic stimulation, anoxia was induced by bubbling the saline with N_2 for 2 h while recording changes in heart rate. Normoxia was restored by re-aerating the saline and following the change in oxygen saturation with an oxygen probe (Ocean Optics, Dunedin, FL, USA).

The tmAC agonist forskolin (Tocris Bioscience) was used to assess the role of stimulating tmAC in the increase in anoxic heart rate. Hearts that had been first subjected to a 2-h anoxic exposure were stimulated with forskolin, which was added incrementally (1.0 pmol l^{-1} to 100 µmol l^{-1}) every 30 min to the saline bath. Forskolin was dissolved in dimethyl sulfoxide (DMSO; Sigma-Aldrich) for a final DMSO concentration of up to 0.01 µl DMSO ml^{-1} saline in the final preparation. Additions of up to 10 µl DMSO ml^{-1} saline had no effect on heart rate (data not shown).

To assess the role of HCO_3^- stimulation of sAC in the increase of the anoxic heart rate, hearts that had been first subjected to a 2-h anoxic exposure were stimulated with $NaHCO_3$ (Sigma-Aldrich), which was added incrementally (20, 40 and 60 mmol l^{-1}) every 30 min to the saline bath. The pH of the saline was readjusted to 7.9 in the stock salines with NaOH. In separate experiments with anoxic hearts stimulated with 60 mmol l^{-1} HCO_3^-, the sAC antagonist KH7 (Tocris Bioscience) was added at a concentration of 50 µmol l^{-1} (dissolved in DMSO as above).

Anoxic exposure *in vivo*

A simple way to rapidly obtain blood samples for HCO_3^- analysis without the complications of vessel cannulation described by Cox et al. (2011) is from the subcutaneous sinus. Heart samples were also taken at the same time for western blots and for assaying cAMP concentration and production by sAC. Hagfish were held overnight in one of four darkened 2.5 l respirometry chambers that were continuously flushed (0.5 l min^{-1}) with aerated seawater (10±1°C). Under these normoxic conditions, hagfish adopt a curled-up

Journal of Experimental Biology

RESEARCH ARTICLE Journal of Experimental Biology (2016) 219, 3227-3236 doi:10.1242/jeb.138198

posture, but remain immobile and straight when made anoxic, greatly facilitating fish removal from the chamber (Cox et al., 2010; Wilson et al., 2013). The water supply was made anoxic (within <1 h) by supplying the two gas-exchange columns (placed in-series) with N_2. O_2 concentration was monitored every second throughout the experiment using MINI-DO probes (Loligo Systems, Tjele, Denmark). Different batches of four hagfish were sampled after an anoxic exposure of 3, 6, 12 and 24 h. Similarly, following a 24-h anoxic exposure, hagfish were sampled 1 and 6 h after re-aerating the water (achieved in <30 min). By the 6-h sample time, the hagfish had restored their coiled posture. Control animals were held in the same apparatus under normoxic conditions for 42 h before sampling. Each hagfish was killed by a blow to the head and was then decapitated. Blood was rapidly removed from the subcutaneous sinus in the tail and placed on ice. The heart was then rapidly excised and freeze-clamped in liquid N_2. Plasma was separated by centrifugation. All tissue samples were stored at −80°C until analyzed.

Western blots

Hearts (100±17 mg), sampled after either a 24-h anoxic exposure or a 42-h normoxic exposure as described above (n=5 per treatment), were homogenized under liquid N_2 using a pestle and mortar, and then in a glass homogenizer filled with 500 µl homogenization buffer supplemented with a protease inhibitor cocktail (Sigma-Aldrich). Samples were centrifuged (500 ***g*** for 15 min at 4°C) to collect the supernatant and stored at −80°C until analysis. A supernatant sample was mixed with an equal volume of 2× Laemmli sample buffer (Bio-Rad Laboratories, Hercules, CA, USA) with 5% β-mercaptoethanol and heated at 95°C for 5 min. Protein (13 µg; estimated by Bradford assay) was separated by SDS/PAGE and transferred to a polyvinylidene difluoride (PVDF) membrane (Bio-Rad). After transfer, PVDF membranes were incubated in blocking buffer (Tris-buffered saline, 1% Tween, 10% milk, pH 7.4) at room temperature for 30 min and incubated in anti-dogfish sAC (anti-dfsAC) (Tresguerres et al., 2010b) or anti-rat NBC1 [Chemicon International Inc., USA (Schmitt et al., 1999); known to cross-react in fish (Parks et al., 2007)] overnight at 4°C, followed by 1 h incubation with horseradish peroxidase-conjugated goat anti-rabbit antibodies. Membranes were washed three times in TBST (Tris-buffered saline, 1% Tween) for 20 min between antibody treatments. Bands were detected with ECL Prime Western Blotting Detection Reagent (GE Healthcare, Waukesha, WI, USA) and imaged in a Bio-Rad Universal III Hood, with sAC protein abundance quantified using ImageQuant software (Bio-Rad).

Cardiac cAMP concentration

Hearts (mass=89±8 mg; mean±s.e.m.) were pulverized under liquid N_2 using a pestle and mortar, followed by homogenization in a glass Dounce homogenizer filled with homogenization buffer (250 mmol l^{-1} sucrose, 1 mmol l^{-1} EDTA, 30 mmol l^{-1} Tris, pH 7.5) at a ratio of 10:1 weight (mg)/volume (µl), and held on ice for 10 min. Supernatant samples were collected after centrifugation (600 ***g*** for 15 min at 4°C) and stored at −80°C until analysis. cAMP concentration in hearts (control and anoxic exposure for 3, 6, 12 and 24 h; n=5 per treatment) was measured using the Direct Cyclic AMP Enzyme Immunoassay (Arbor Assays).

Cardiac cAMP production by sAC

Heart homogenates were incubated for 45 min at room temperature in an orbital shaker (300 rpm) in 100 mmol l^{-1} Tris (pH 7.5), 5 mmol l^{-1} ATP, 10 mmol l^{-1} $MgCl_2$, 0.1 mmol l^{-1} $MnCl_2$, 0.5 mmol l^{-1} isobutylmethylxanthine, 1 mmol l^{-1} dithiothreitol, 20 mmol l^{-1} creatine phosphate and 100 U ml^{-1} creatine phosphokinase. Homogenates were incubated in concentrations of HCO_3^- and KH7. cAMP production was determined using the DetectX Direct Cyclic AMP Enzyme Immunoassay (Arbor Assays).

Plasma bicarbonate concentration

The HCO_3^- concentration in the plasma sinus blood was estimated by measuring total CO_2 (Cameron, 1971) on plasma samples obtained after 3, 6, 12 and 14 h of anoxia and also after a 0.5 h and a 1 h recovery from a preceding 24 h anoxia exposure.

Cardiac immunohistochemistry

Hearts were fixed in 0.2 mol cacodylate buffer, 3.2% paraformaldehyde and 0.3% glutaraldehyde for 6 h, transferred to 50% ethanol for 6 h, and stored in 70% ethanol. Fixed hearts were serially dehydrated in 95% ethanol (10 min), 100% ethanol (10 min), xylene (3×10 min) and paraffin (55°C) (3×30 min), after which paraffin blocks were left to solidify overnight. Sections of the atrium and ventricle were cut at 7 µm using a rotary microtome; three consecutive sections were placed on slides and left on a slide warmer (37°C) overnight. Paraffin was removed in xylene (10 min×3) and sections were re-hydrated in 100% ethanol (10 min), 95% ethanol (10 min), 70% ethanol (10 min) and phosphate-buffered saline (PBS; Cellgro Corning, Manassas, VA, USA). Non-specific binding was reduced by incubating the sections in blocking buffer (PBS, 2% normal goat serum, 0.02% keyhole limpet hemocyanin, pH 7.8) for 1 h. Sections were then incubated in the primary antibody overnight at 4°C [anti-dfsAC=1:250, anti-rat NBC1=1:100). Slides were washed three times in PBS and sections were incubated in the appropriate secondary antibody (1:500) at room temperature for 1 h, followed by incubation with the nuclear stain Hoechst 33342 (Invitrogen, Grand Island, NY, USA) (1:1000) for 5 min. Slides were then washed three times in PBS and sections were permanently mounted in Fluorogel with Tris buffer (Electron Microscopy Sciences, Hatfield, PA, USA). Immunofluorescence was detected using an epifluorescence microscope (Zeiss AxioObserver Z1) connected to a metal halide lamp and appropriate filters. Digital images were adjusted, for brightness and contrast only, using Zeiss Axiovision software and Adobe Photoshop. Images of atrium and ventricle are representative of hearts from two small hagfish (~100 g). Immunolocalization of sAC in the sinus venosus was performed on the heart of a larger hagfish (~300 g). This was necessary in order to be able to identify the sinus venosus.

Calculations and statistics

Statistical analyses were conducted using SigmaPlot for Windows Version 11.0, Build 11.1.0.102, on a Sager NP7352-Clevo W350ST notebook running Microsoft Windows 7 Ultimate Service Pack 1. Data sets passed normality tests (Shapiro–Wilk) and values are presented as means±s.e.m. Concentration-dependent effects of nadolol (n=8) or forskolin (n=6) on the heart rate of isolated hearts were assessed using a repeated-measures one-way ANOVA followed by a Holm–Sidak test, while the effects of HCO_3^- (n=6) and KH7 (n=6) were assessed using a one-way ANOVA also followed by a Holm–Sidak test. Plasma HCO_3^- concentrations were similarly assessed with a one-way ANOVA followed by a Holm–Sidak test (n=5). Cytosolic cAMP concentrations were also evaluated with a one-way ANOVA followed by a Student–Newman–Keuls test (n=5). sAC abundance was compared between control and 24 h anoxia

RESEARCH ARTICLE Journal of Experimental Biology (2016) 219, 3227-3236 doi:10.1242/jeb.138198

using a one-way ANOVA. Bicarbonate-stimulated cAMP production rates in hagfish heart crude homogenate were assessed using repeated-measures one-way ANOVA and Tukey's multiple comparison test (n=6). Statistical significance was assigned to a P-value <0.05.

RESULTS

Transmembrane adenylyl cyclase

The spontaneous heart rate of normoxic, isolated hagfish hearts at 10°C was 13.4±1.1 beats min^{-1}, i.e. similar to the routine *in vivo* heart rate of 10.4±1.3 beats min^{-1} previously measured for normoxic hagfish at the same temperature (Cox et al., 2010). Application of 1 mmol l^{-1} nadolol, a β-adrenoreceptor antagonist, to the normoxic, isolated hagfish heart significantly decreased (P<0.05) heart rate to 8.6±1.1 beats min^{-1}, 64% of the normoxic heart rate (Fig. 1A). A subsequent 2-h anoxic exposure further reduced heart rate to 5.1±0.5 beats min^{-1}, almost one-third of the normoxic heart rate. The anoxic bradycardia was fully reversible (Fig. 1A). Forskolin, a tmAC agonist, applied to isolated hearts did not significantly change the normoxic heart rate. Instead, 1 and 10 µmol l^{-1} forskolin applied to anoxic isolated hearts restored the depressed heart rate to, but not above, the normoxic heart rate (Fig. 1C). However, 100 µmol l^{-1} forskolin reduced heart rate back to the anoxic rate during anoxia.

Combined, these results are consistent with our suggestion that tonic adrenergic stimulation of the hagfish heart rate via tmAC is present under normoxic conditions and that this tonic stimulation is lost during anoxia. Furthermore, no support is provided for tmAC stimulation increasing heart rate beyond the routine normoxic rate, a result consistent with *in vivo* observations (see Introduction).

The cardiac cytosolic cAMP concentration measured in normoxic hagfish (8.4±0.7 pmol mg^{-1} protein) was significantly (P<0.05) reduced by 33% to 5.6±0.5 pmol mg^{-1} protein after hagfish had been exposed to anoxia for 3 h. Cardiac cAMP concentrations remained stable at this level throughout the 24-h anoxic exposure (Fig. 1B), a result that is consistent with the stable depression of heart rate during anoxia observed both here *in vitro* and previously *in vivo* (Cox et al., 2010).

Soluble adenylyl cyclase

Expression of sAC protein was demonstrated at the expected ~110 kDa band in western blotting analysis of crude homogenate cardiac cell suspensions from hagfish (Fig. 2A). No band was seen when the antibody was pre-incubated with oversaturating concentrations of purified sAC peptide prior to application to the transfer membrane. Moreover, sAC abundance, estimated from western blots, was unchanged following a 24 h anoxic challenge.

cAMP production measured in homogenized hagfish hearts in the presence of HCO_3^- and its inhibition by KH7 provides a causal linkage between sAC and cAMP synthesis. Increasing concentrations of HCO_3^- stimulated cAMP production, producing a maximum twofold increase in cAMP production with 40 mmol l^{-1} HCO_3^- (Fig. 2B). This HCO_3^--mediated cAMP production was completely blocked by 50 µmol l^{-1} KH7 (P<0.05), a small molecule that specifically inhibits sAC activity (Fig. 2C).

Addition of HCO_3^- induced a dose-dependent stimulation of spontaneously beating, anoxic, isolated hearts. Specifically, 20 mmol l^{-1} HCO_3^- significantly (P<0.05) increased the anoxic heart rate from 7.9±1.2 to 16.9±0.9 beats min^{-1}, more than restoring the normoxic heart rate (13.4 beats min^{-1}; Fig. 3A).

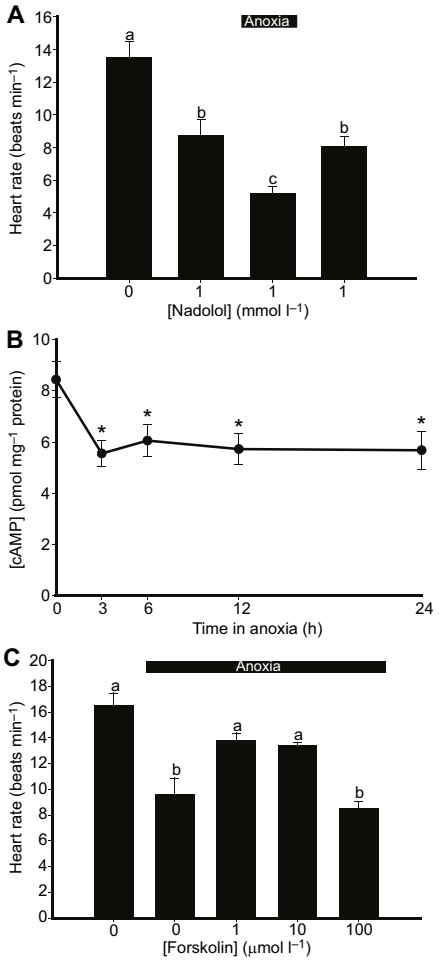

Fig. 1. Effects on hagfish heart rate and cardiac cAMP concentration during anoxia and β-adrenoreceptor blockade or stimulation. (A) Spontaneous heart rate of isolated hearts (n=8) slowed significantly when exposed to the β-adrenoreceptor antagonist nadolol and further when made anoxic (indicated by thick black bar). Removal of anoxia restored heart rate. Different letters indicate statistical differences between treatments (P<0.05, repeated-measures ANOVA). (B) Cardiac cAMP concentration decreased in intact animals (n=5) exposed to prolonged anoxia. Asterisks indicate significant differences from control group (*P<0.05, one-way ANOVA). (C) The tmAC agonist, forskolin, increased the anoxic heart rate of isolated hearts (n=6) (indicated by thick black bar) up to but not beyond routine normoxic heart rate. Different letters indicate statistical differences between treatments (P<0.05, repeated measures one-way ANOVA).

Furthermore, the anoxic heart rate could be further stimulated by 40 and 60 mmol l^{-1} HCO_3^- such that heart rate reached 22.4±2.6 and 23.1±2.6 beats min^{-1}, respectively (Fig. 3A), rates that were 75% higher than the normoxic heart rate (13.4 beats min^{-1}). Thus, maximal stimulation with HCO_3^- nearly tripled the anoxic heart rate (7.9 beats min^{-1}) in this test, and was 4.5 times

RESEARCH ARTICLE Journal of Experimental Biology (2016) 219, 3227-3236 doi:10.1242/jeb.138198

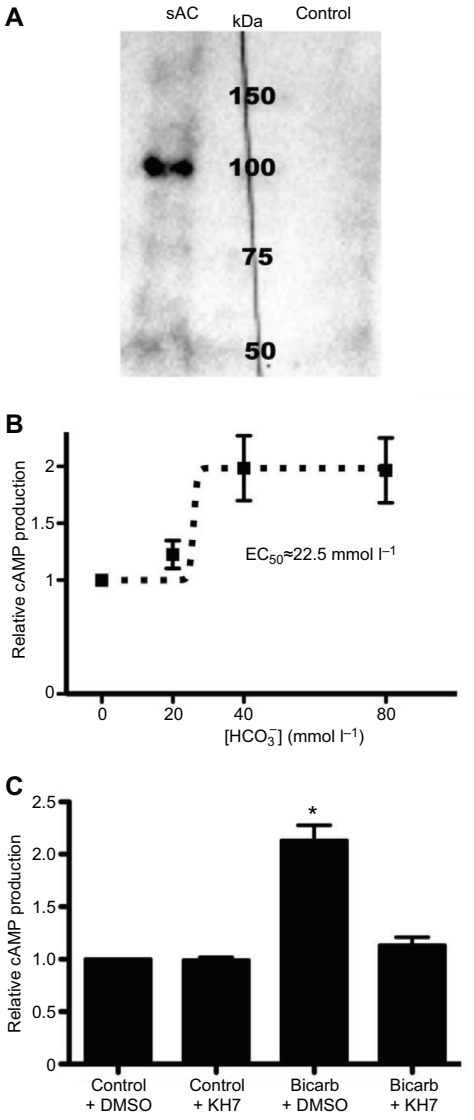

Fig. 2. Soluble adenylyl cyclase (sAC) is present in the hagfish heart. (A) Western blot of hagfish heart crude homogenate using anti-dfsAC antibody in the absence (sAC) or presence (control) of purified sAC peptide; ladder is indicated by kDa. (B) cAMP production in hagfish heart homogenates exposed to increasing HCO_3^- concentrations. Values are normalized to 0 mmol l^{-1} HCO_3^-. At 0 mmol l^{-1} HCO_3^-, cAMP production equaled 18.65 pmol mg^{-1} min^{-1}, increasing twofold at 40 mmol l^{-1} HCO_3^-. n=4. (C) Inhibition of HCO_3^--stimulated cAMP production in hagfish heart homogenates by the sAC inhibitor KH7 (50 µmol l^{-1}). Control=40 mmol l^{-1} NaCl; Bicarb=40 mmol l^{-1} $NaHCO_3$. DMSO is the vehicle for KH7. Asterisk indicates a significant difference between treatments (*P<0.05, repeated-measures one-way ANOVA, Tukey's multiple comparisons test; n=6).

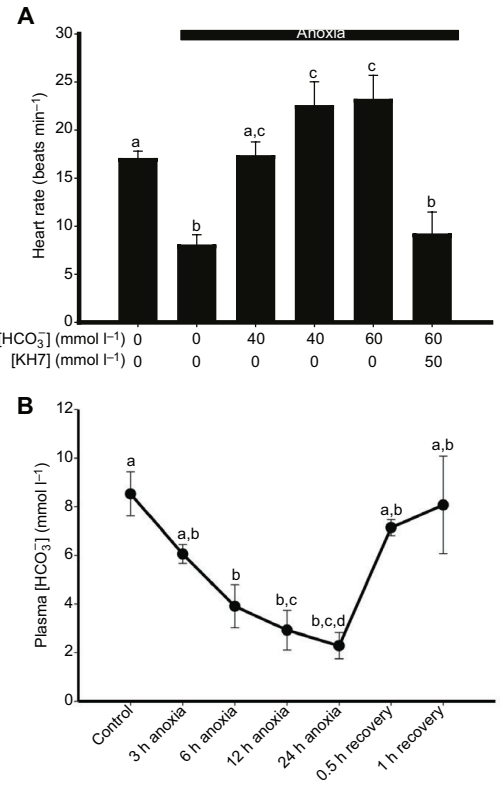

Fig. 3. Role of HCO_3^--stimulated sAC on regulating hagfish heart rate during recovery from anoxia. (A) The anoxic bradycardia of isolated hagfish hearts and the HCO_3^--stimulated tachycardia during anoxia. The sAC antagonist, KH7, completely blocked the HCO_3^--mediated tachycardia. Different letters indicate statistical differences between treatments (P<0.05, one-way ANOVA, n=6). (B) The effects of anoxia and subsequent recovery on plasma HCO_3^- concentration in the subcutaneous sinus of the Pacific hagfish (n=5) and during control normoxia, a 24-h anoxic exposure and normoxic recovery. Different letters indicate significant differences (P<0.05, one-way ANOVA).

higher than the anoxic heart rate after a 2-h anoxic exposure (5.1 beats min^{-1}).

The tachycardia stimulated by 60 mmol l^{-1} HCO_3^- was completely blocked by the sAC-specific antagonist KH7 (50 µmol l^{-1}; Fig. 3A), a finding that directly implicates sAC in the modulation of the hagfish heart rate by HCO_3^-. The normoxic heart rate of the isolated heart was unaffected by the application of either HCO_3^- or KH7.

Significant changes in plasma [HCO_3^-] were noticed in hagfish recovering from anoxia (Fig. 3B). Anoxia significantly decreased (P<0.05) plasma [HCO_3^-] in the subcutaneous sinus from 8.5±0.9 to 2.3±0.5 mmol l^{-1}. The anoxic reduction in plasma [HCO_3^-] was progressive, and reached statistical significance after 6 h. Plasma [HCO_3^-] was restored within 0.5 h of normoxia.

Immunolabelling of hagfish hearts identified sAC distributed throughout atrial and ventricular myocardial cells, with strong

RESEARCH ARTICLE Journal of Experimental Biology (2016) 219, 3227-3236 doi:10.1242/jeb.138198

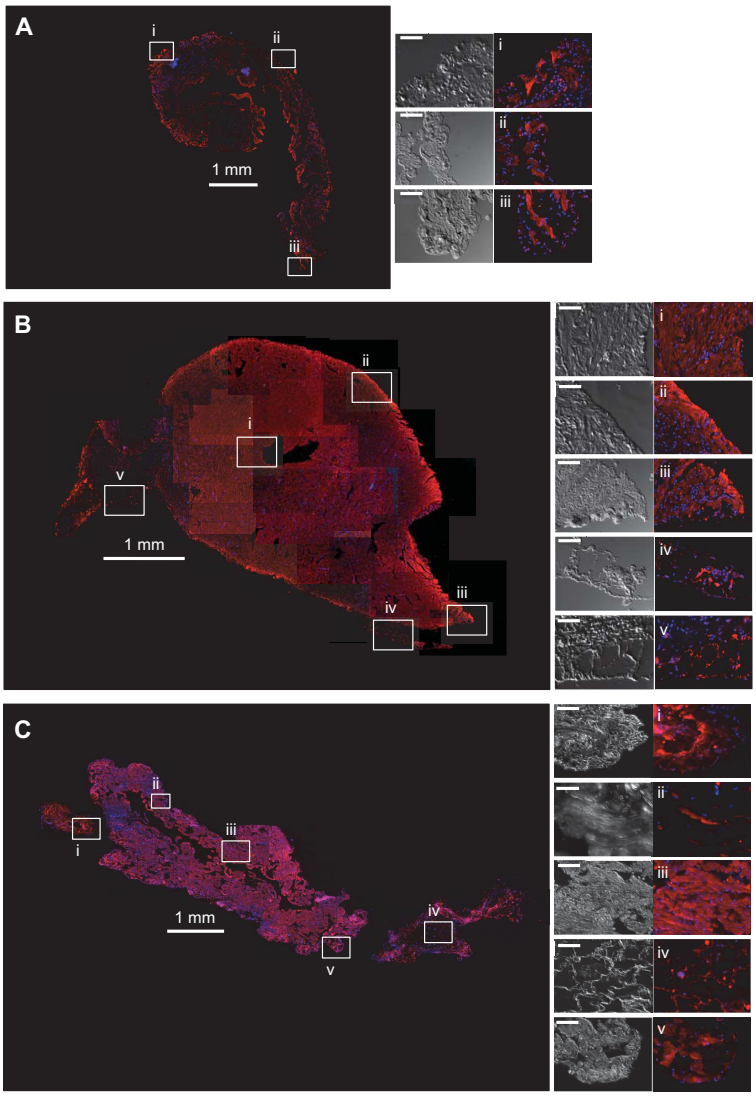

Fig. 4. Immunolocalization of sAC throughout the hagfish heart.
(A) Composite of 18 images showing sAC in the atrium; the boxed areas are shown at higher magnification in i–iii.
(B) Composite of 45 images showing sAC in the ventricle; the boxed areas are shown at higher magnification in i–v.
(C) Composite of 70 images showing sAC in the sinus venosus from a larger hagfish; the boxed areas are shown at higher magnification in i–v. In the higher-magnification images, the left panels are differential interference contrast, and the scale bars represent 50 µm. sAC immunostaining is in red; nuclei are stained in blue.

staining evident in cardiac trabeculae and in the atrium. Fig. 4 shows a composite of sections across an entire heart, with details shown for the atrium (Fig. 4Ai–iii), the ventricle (Fig. 4Bi–v) and the sinus venosus (Fig. 4Ci–v). Although widespread, sAC is not evenly distributed throughout the hagfish heart. Strong sAC immunostaining is seen in atrial areas with a high nuclear density (blue staining, Fig. 4), which could indicate the primary pacemaker region. sAC immunostaining is also most abundantly present in specific regions of cardiomyocytes, presumably A- or I-sarcomeric bands (Fig. 4Cii), but it appears absent in many unidentified cardiac cells (e.g. see Fig. 4Aiii, Biv,v, Ci,ii).

Na^+/HCO_3^- cotransporter immunoreactivity

Hagfish hearts demonstrated a band of the predicted size (~100 kDa) of the mammalian Na^+/HCO_3^- co-transporter (NBC, a member of the SLC4 family) in western blots (Fig. 5A). NBC-like immunoreactivity was observed throughout the atrium and ventricle in cells (Fig. 5B,C).

DISCUSSION

The present study documents the discovery of a novel control pathway to increase heart rate. We are not aware of any previous study on a chordate heart that has implicated HCO_3^- stimulation of

Journal of Experimental Biology

RESEARCH ARTICLE Journal of Experimental Biology (2016) 219, 3227-3236 doi:10.1242/jeb.138198

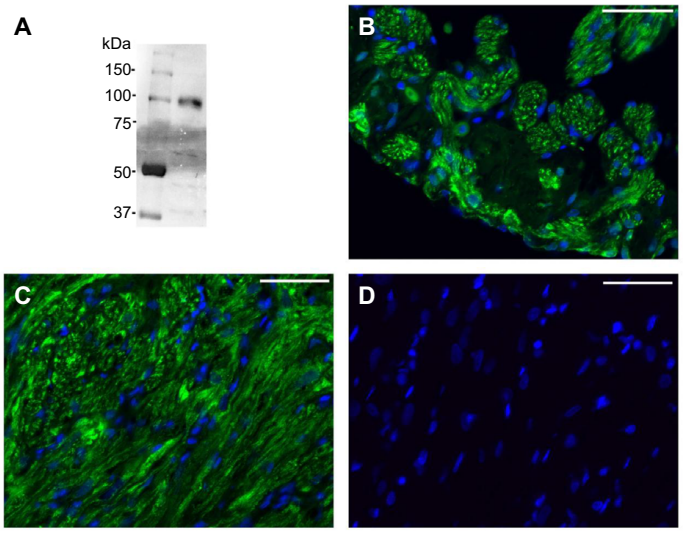

Fig. 5. Immunolocalization of Na^+/HCO_3^- cotransporters (NBC) in the hagfish heart. (A) Western blot of NBC in hagfish heart crude homogenate, with strong staining showing an immunoreactive band at 100 kDa. (B,C) Immunofluorescence of NBC (green) in hagfish atrium and ventricle, respectively, showing co-staining of nuclei (blue). As is the case for sAC, NBC is found throughout the myocardium of both atria and ventricles, with the location of trabeculae shown by the fluorescence of the antibodies. (D) Immunofluorescence control showing solely staining of nuclei in blue. Scale bars in B–D, 20 µm.

intracellular sAC to produce cAMP and stimulate the spontaneous heartbeat. This discovery should spur further research in the functional roles of sAC in vertebrate hearts to determine whether this control mechanism is more widespread in the lineage, or just another remarkable aspect of the biology of hagfishes.

Furthermore, we provide quantitative evidence for and suggest putative mechanisms that could explain the remarkable upregulation of heart rate (from ~4 to 17.5 beats min^{-1}; Cox et al., 2010) when anoxic *in vivo* hagfish emerged from a 36-h anoxic exposure. In this regard, we note excellent quantitative agreement between the heart rates measured in spontaneously beating, isolated hagfish hearts and those measured previously *in vivo* for the normoxic state (13.4 versus 10.1 beats min^{-1}), prolonged anoxia (5.4 versus 4.0 beats min^{-1}) and a maximally stimulated state (23.4 versus 17.5 beats min^{-1}). In addition to supporting the hypothesis that the bradycardia associated with anoxia represents a withdrawal of an autocrine adrenergic tonus mediated by tmAC, a mechanism common to all vertebrate hearts, we provide support for a novel HCO_3^--mediated control of the anoxic heart rate. We further propose that sAC-mediated cAMP production plays a role in the HCO_3^- stimulation of heart rate in hagfish during anoxic recovery because tachycardia was fully blocked by the sAC-specific antagonist KH7. Additional evidence for the presence of sAC in hagfish hearts includes detection of the predicted ~110 kDa protein band in western blots using antibodies against shark sAC, which is the same size as in shark (Tresguerres et al., 2010b) and toadfish (Tresguerres et al., 2010a), immunolabeling throughout the heart, and HCO_3^--stimulated and KH7-sensitive cAMP production by cardiac homogenates, which are hallmarks of sAC enzymatic activity. Consequently, we propose that hagfish have two mechanisms to regulate the heart rate via cAMP production, a sAC pathway working in tandem with a tmAC pathway during recovery from anoxia, and a tmAC pathway during normoxia. These potential distinct physiological functions of sAC- and tmAC-generated cAMP fit the concept of intracellular cAMP microdomains (Schwencke et al., 1999; Rich et al., 2000; Zippin et al., 2004; Tresguerres et al., 2011), which, in fish, has been empirically substantiated by differential effects of sAC and tmAC antagonists and agonists on NaCl and water absorption (Tresguerres et al., 2010a; Carvalho et al., 2012).

This study, taken together with past work, has also greatly increased our understanding of the catecholaminergic control of heart rate in hagfish. Rather than the dual sympathetic and parasympathetic controls found in certain teleosts and tetrapods (Nilsson, 1983), catecholaminergic control appears to act primarily through a paracrine action in hagfish. This is done via modulation of catecholamine release from chromaffin tissue located within the cardiac chambers themselves (Euler and Fänge, 1961; Bloom et al., 1963; Perry et al., 1993; Axelsson et al., 1990; Farrell, 2007). A tonic β-adrenergic stimulation of the hagfish heart is consistent with the bradycardic effects of sotalol *in vivo* (Hansen and Sidell, 1983; Axelsson et al., 1990) and nadolol *in vitro* (present study). Production and recycling of catecholamines involves the rate-limiting conversion of tyrosine to 3,4-dihydroxyphenylalanine, which requires oxygen (Levitt et al., 1965). Plausibly, anoxia could prevent catecholamine re-synthesis and the normal tonic paracrine β-adrenergic stimulation, which would decrease cAMP production, a suggestion consistent with the observed decrease in cardiac cAMP concentration after a 3 h anoxic exposure. Withdrawal of adrenergic stimulatory capacity in anoxia is also seen for the hearts of two other anoxia-tolerant taxa, crucian carp and freshwater turtles (Stecyk et al., 2004, 2007; Stecyk and Farrell, 2006; Hicks and Farrell, 2000b).

Additionally, we propose that tachycardia beyond the normoxic heart rate during the recovery from anoxia relies on the putative autocrine or humoral mechanism HCO_3^- stimulation of sAC identified here. Indeed, 20 mmol l^{-1} HCO_3^- produced a heart rate of 16.9 beats min^{-1} in the isolated anoxic heart, which compares well with the peak heart rate of 17.5 beats min^{-1} measured *in vivo* during normoxic recovery from anoxia in the same species and at the same temperature (Cox et al., 2010). The exact switching point between tmAC and sAC mechanisms is an interesting issue that was not addressed here. Our hypothesis is that tmAC is reactivated as soon as O_2 is available for catecholamine production (as above).

RESEARCH ARTICLE Journal of Experimental Biology (2016) 219, 3227-3236 doi:10.1242/jeb.138198

This stimulation, together with that from sAC, causes heart rate to increase beyond routine levels, and eventually the sAC mechanism decays under normoxia. Resolving this switch would involve mixtures of adrenergic and HCO_3^- stimulation at different levels of oxygenation.

The vertebrate heartbeat is initiated in sinoatrial pacemaker cells, but very little is known of pacemaker cell activity in hagfish. Icardo et al. (2016) were unable to observe specialized nodal tissue in the sinus wall or at the sinoatrial junction. Yet, electrocardiogram recordings in *E. cirrhatus* (Davie et al., 1987) showed a depolarization specific to only the central region of the sinus venosus, something not seen, however, in *M. glutinosa* (Arlock, 1975; Satchell, 1991). Therefore, we must still presume that pacemaker cells exist in hagfish hearts, and initiate the heartbeat as they do in all vertebrate hearts. Our investigation revealed areas of high nuclear density in the atrium (Fig. 2), which may represent primary pacemaker tissue, but confirmation will require electrophysiological mapping of action potentials. Therefore, until further work is performed specifically on pacemaker tissue in hagfishes, we can only presume that catecholamines and HCO_3^- act on pacemaker cells to increase heart rate. This task will be all the more difficult because the different HCN channels identified in *E. stoutii* hearts compared with mammals (Wilson et al., 2013) may make the available immunofluorescent markers for pacemaker cells less specific. Alternatively or additionally, sAC may mediate the observed increase in heartbeat rate by mechanisms at sites different from the pacemaker cells. For example, the presence of sAC in cardiomyocytes suggests a role in regulating their contractibility and therefore cardiac function more generally.

The atrium and ventricle of *E. stoutii* are rich in hyperpolarization-activated cyclic nucleotide-gated (HCN) ion channels (Wilson et al., 2013), which have been implicated in the control of pacemaker activity of the vertebrate heart (Qu et al., 2008). Application of an HCN channel blocker (zatebradine) completely stopped all spontaneous atrial contractions and almost all spontaneous ventricular contractions of isolated *E. stoutii* hearts (Wilson and Farrell, 2013), something not observed in vertebrate hearts, where the effect is just a slowing, and not a cessation, of the spontaneous heartbeat (Baruscotti et al., 2010; Monfredi et al., 2013). Thus, the most parsimonious explanation is that zatebradine blocked pacemaker HCN channels, especially because the ventricular cells have their own, slower spontaneous heartbeat (Wilson et al., 2013) and HCN channels are central to the control of intrinsic beating of atrial and ventricular chamber of *E. stoutii*. The difference in the efficacy of HCN channel blockers between *E. stoutii* and other vertebrates is perhaps because both HCN and Ca^{2+} cycling have been implicated in contributing to mammalian pacemaker rhythm (Monfredi et al., 2013). The major side effect, and concern, with using HCN blockers in humans is QRT prolongation and atrial fibrillation. However, zatebradine and ivabradine, which were initially considered to be specific blockers of HCN channels, can also inhibit the cardiac rapid, delayed rectifier potassium current (I_{Kr}) (Lees-Miller et al., 2015; Melgari et al., 2015). I_{Kr} is a major repolarizing current of fish hearts and so cardiac repolarization would be prolonged if zatebradine blocked I_{Kr} (Lees-Miller et al., 2015; Melgari et al., 2015), an action that would tend to decrease heart rate. Thus, the effect of zatebradine on hagfish heart rate could be due to either I_{Kr} or the cardiac pacemaker 'funny' current (I_f), or both. However, Wilson and Farrell (2013) did not observe atrial fibrillation in *E. stoutii* after zetabradine, but rather a cessation of all spontaneous atrial activity, an action that would require a complete blockage of I_{Kr}. Another important difference between hagfish and vertebrate hearts is the effect of ryanodine, which had no effect on normoxic heart rate in *E. stoutii*. In contrast, ryanodine and Ca^{2+} cycling have been shown to have a greater effect in lamprey (Vornanen and Haverninen, 2013) and the more active *Myxine glutinosa* (Bloom, 1962; Helle and Storesund, 1975). It would be of interest to compare the effects of zatebradine and sAC on these animals with those on other vertebrate species and *E. stoutii*.

Therefore, until additional electrophysiological studies are performed with hagfish, an approach that has up to now proven too challenging in our laboratory, we propose the following parsimonious mechanism as a working hypothesis for the control of cardiac pacemaker activity in *E. stoutii.* Removing adrenergic tonus decreases intracellular cAMP, which could primarily decrease I_f via HCN channels and, potentially, secondarily Na^+ influx through the sodium/calcium exchange channel (NCX) activated by Ca^{2+} cycling through the sarcoplasmic reticulum, as seen in mammalian hearts (Monfredi et al., 2013). Reducing these ion currents would decrease the diastolic depolarization rate of pacemaker cells, slowing heart rate. During anoxia, we suggest that gating of HCN channels by cAMP becomes minimal, and is restored with normoxia. Indeed, tmAC may be nearly fully activated in normoxia given that forskolin, which stimulates cAMP and bypasses tmAC, failed to increase heart rate in either normoxia or beyond routine rates in anoxia. Importantly, forskolin does not fit into the pseudosymmetrical site at the sAC pseudodimer interface, which in tmACs results in stimulation of cAMP, and as a result sAC is insensitive to forskolin (Chen et al., 2000; Kleinboelting et al., 2014). The explanation for the inhibition of heart rate by the highest pharmacological dose of forskolin is unknown, but it resembles biphasic effects of forskolin reported in other systems (Szabo et al., 1990; Tian, et al., 2009). Tachycardia without tmAC involvement would also explain mechanistically why all previous studies with normoxic hagfish have seen, at best, modest increases in heart rate with injections of β-adrenergic agonists (Euler and Fänge, 1961; Chapman et al., 1963; Axelsson et al., 1990; Johnsson and Axelsson, 1996).

The proposed role of sAC as a mechanism to gate HCN channels and control heart rate in hagfish may not be the only role of sAC in vertebrate hearts. Indeed, if HCN gating was its only role, sAC might not be omnipresent throughout the atrial and ventricular cardiomyocytes, as we discovered for hagfish using sAC protein expression. Furthermore, sAC has been found in mammalian cardiac myocytes and implicated in the apoptosis signalling pathway (Kumar et al., 2009; Appukuttan et al., 2012; Chen et al., 2012). Also, the roles of cAMP as a second messenger are many, especially via cAMP-dependent protein kinase A. Therefore, as this is the first time that sAC has been implicated in the control of heart rate, new roles for sAC in vertebrate hearts become a possibility. For example, hypercapnia produced tachycardia in embryonic zebrafish, a response blocked by atenolol, a β-adrenergic antagonist, and by a carbonic anhydrase inhibitor (Miller et al., 2014). Thus, it would be interesting to investigate whether KH7 might block this tachycardia, which would implicate a sAC-mediated control of heart rate in this case. As another example, the common eel, *Anguilla anguilla*, tolerates extreme hypercapnia and plasma HCO_3^- reaches 70 mmol l^{-1}, while arterial blood oxygen saturation is halved (McKenzie, 2003). How eels regulate heart rate during hypoxic hypercapnia is unknown.

Our findings regarding both tmAC and sAC have allowed us to propose a more complete model for the control of heart rate in the ancestral hagfish during anoxia. What remains very much unclear, and requiring much more study, is how cellular HCO_3^- concentrations are regulated in the hagfish heart, and whether

HCO_3^- stimulation is directed to sinoatrial pacemaker tissues. During anoxia, it is easy to envision both plasma (as observed here) and intracellular HCO_3^- concentrations being driven down by the absence of CO_2 production from aerobic metabolism and by the metabolic acidosis developing through glycolytic ATP production (Cox et al., 2011). Normoxic recovery from anoxia rapidly elevates O_2 consumption (Cox et al., 2011) and CO_2 production, which then increases HCO_3^- levels throughout the body, including blood plasma and inside cardiomyocytes. While our activity assays with hagfish heart crude homogenates suggest an apparent EC_{50} (half-maximal effective concentration) for HCO_3^- of approximately 20 mmol l^{-1}, obtaining the exact value would require cloning of hagfish sAC followed by enzymatic characterization on purified recombinant protein. As a reference, the EC_{50} for HCO_3^- varies considerably between sAC from vertebrates, ranging from ~5 mmol l^{-1} in sharks (Tresguerres et al., 2010b) to ~20 mmol l^{-1} in mammals (Chen et al., 2000; Litvin et al., 2003; Tresguerres, 2014). Of course, *in vivo* and unlike the continuously anoxic situation used here *in vitro*, there is an increase in oxygen as well as HCO_3^- during recovery, and so it would be interesting to examine the interactive effects of oxygen, catecholamines and HCO_3^- on heart rate. Minimally, we have demonstrated that heart rate can increase with HCO_3^- without the presence of oxygen.

In proposing that sAC acts as a metabolic sensor of changes in the concentration of CO_2/HCO_3^-, the heart can adjust its beating frequency reasonably rapidly without cardiac innervation. sAC could be stimulated by HCO_3^- entry into cardiomyocytes from the plasma through NBC-like transporters (which likely occurred when HCO_3^- was added to the extracellular saline), as well as by CO_2 and HCO_3^- generated within cardiomyocytes. Unfortunately, the limited information on *in vivo* tissue and plasma HCO_3^- concentrations in hagfish limits further speculation. Hagfish plasma HCO_3^- concentrations can reach a remarkable 70 mmol l^{-1} during sustained hypercapnia (Baker et al., 2015), a level well beyond that needed to obtain maximal cardiac sAC stimulation. However, hagfish are notoriously difficult to anaesthetize to reliably sample blood and tissues, and they routinely tie knots in indwelling catheters used to provide stress-free blood samples. Although sampling blood from the subcutaneous sinus of hagfish is rapid, easy and without excessive stress, we caution that subcutaneous sinus blood may not accurately reflect the rapidity or full extent of the changes in venous blood HCO_3^- concentration during the first hour of anoxic recovery because subcutaneous sinus blood takes 8–18 h to equilibrate with the venous circulation (Forster et al., 1989). Thus, intracellular and extracellular measurements of HCO_3^- within the heart are still needed to fully validate the *in vivo* regulation of heart rate by sAC activity, and to determine whether HCO_3^- is derived extracellularly or by a burst of intracellular, aerobic CO_2 production when the heart increases its work rate post-anoxia (Cox et al., 2010), or both.

In summary, the main finding of the present study is the discovery of a novel mechanism to control heart rate and a more detailed analysis of catecholamine control of heart rate. This allowed us to propose a more complete picture of the control mechanisms for heart rate in the ancestral hagfish. While putative upstream mechanisms are proposed, much work is still needed to establish the exact pathways. The implications of our discovery of sAC-mediated control of heart rate could open up a new field of cardiovascular research.

Acknowledgements

Gratitude is given to support staff at Bamfield Marine Sciences Centre and Department of Fisheries and Oceans Centre for Aquaculture and Environmental Research West Vancouver Laboratories for assistance with animal collection and care. The aid of Adam Goulding during experimental set-up at the University of British Columbia is vastly appreciated. We are grateful to Phil Zerofski (Scripps Institution of Oceanography) for his assistance with aquarium matters.

Competing interests

The authors declare no competing or financial interests.

Author contributions

C.M.W. was involved in study conception and design, carried out all experiments with live animals and isolated hearts, contributed to the sAC biochemical experiments and produced the first draft of the manuscript. J.N.R. performed most of the sAC and NBC biochemical and microscopy experiments. G.K.C. conducted the plasma bicarbonate measurements. M.T. designed the biochemical and microscopy portion of the study and contributed to the microscopy experiments. A.P.F. was involved in study conception and design. All authors analyzed the data, critically assessed and revised the manuscript, and gave final approval for publication.

Funding

J.N.R. is supported by a Porter Fellowship from the American Physiological Society. M.T. is supported by the National Science Foundation [grant IOS 1354181] and an Alfred P. Sloan Foundation Research Fellowship [BR2013-103]. A.P.F. is supported by a Discovery Grant from the Natural Sciences and Engineering Research Council of Canada, and the Canada Research Chairs.

References

Acin-Perez, R., Salazar, E., Kamenetsky, M., Buck, J., Levin, L. R. and Manfredi, G. (2009). Cyclic AMP produced inside mitochondria regulates oxidative phosphorylation. *Cell Metab.* **9**, 265-276.

Appukuttan, A., Kasseckert, S. A., Micoogullari, M., Flacke, J.-P., Kumar, S., Woste, A., Abdallah, Y., Pott, L., Reusch, H. P. and Ladilov, Y. (2012). Type 10 adenylyl cyclase mediates mitochondrial Bax translocation and apoptosis of adult rat cardiomyocytes under simulated ischaemia/reperfusion. *Cardiovasc. Res.* **93**, 340-349.

Augustinsson, K.-B., Fänge, R., Johnels, A. and Östlund, E. (1956). Histological, physiological and biochemical studies on the heart of two cyclostomes, hagfish (*Myxine*) and lamprey (*Lampetra*). *J. Physiol.* **131**, 257-276.

Axelsson, M., Farrell, A. P. and Nilsson, S. (1990). Effects of hypoxia and drugs on the cardiovascular dynamics of the atlantic hagfish *Myxine glutinosa*. *J. Exp. Biol.* **151**, 297-316.

Baker, D. W., Sardella, B., Rummer, J. L., Sackville, M. and Brauner, C. J. (2015). Hagfish: Champions of CO_2 tolerance question the origins of vertebrate gill function. *Sci. Rep.* **5**, 11182.

Barott, K. L., Helman, Y., Haramaty, L., Barron, M. E., Hess, K. C., Buck, J., Levin, L. R. and Tresguerres, M. (2013). High adenylyl cyclase activity and in vivo cAMP fluctuations in corals suggest central physiological role. *Sci. Rep.* **3**, 1379.

Baruscotti, M., Barbuti, A. and Bucchi, A. (2010). The cardiac pacemaker current. *J. Mol. Cell. Cardiol.* **48**, 55-64.

Bloom, G. D. (1962). The fine structure of cyclostome cardiac muscle cells. *Z. Zellforsch. Mikrosk. Anat.* **57**, 213-239.

Bloom, G., Östlund, E. and Fänge, R. (1963). Functional aspects of cyclostome hearts in relation to recent structural findings. In *The Biology of Myxine* (ed. A. Brodal and R. Fänge), pp. 317-339. Oslo: Universitetsforlaget.

Buck, J., Sinclair, M. L., Schapal, L., Cann, M. J. and Levin, L. R. (1999). Cytosolic adenylyl cyclase defines a unique signaling molecule in mammals. *Proc. Natl. Acad. Sci. USA* **96**, 79-84.

Cameron, J. N. (1971). Rapid method for determination of total carbon dioxide in small blood samples. *J. Appl. Physiol.* **31**, 632-634.

Carvalho, E. S. M., Gregório, S. F., Power, D. M., Canário, A. V. M. and Fuentes, J. (2012). Water absorption and bicarbonate secretion in the intestine of the sea bream are regulated by transmembrane and soluble adenylyl cyclase stimulation. *J. Comp. Physiol. B Biochem. Syst. Environ. Physiol.* **182**, 1069-1080.

Chapman, C. B., Jensen, D. and Wildenthal, K. (1963). On circulatory control mechanisms in the Pacific hagfish. *Circ. Res.* **12**, 427-440.

Chen, Y., Cann, M. J., Litvin, T. N., Lourgenko, V., Sinclair, M. L., Levin, L. R. and Buck, J. (2000). Soluble adenylyl cyclase as an evolutionarily conserved bicarbonate sensor. *Science* **289**, 625-628.

Chen, J., Levin, L. R. and Buck, J. (2012). Role of soluble adenylyl cyclase in the heart. *Am. J. Physiol. Circ. Physiol.* **302**, H538-H543.

Cox, G. K., Sandblom, E. and Farrell, A. P. (2010). Cardiac responses to anoxia in the Pacific hagfish, *Eptatretus stoutii*. *J. Exp. Biol.* **213**, 3692-3698.

Cox, G. K., Sandblom, E., Richards, J. G. and Farrell, A. P. (2011). Anoxic survival of the Pacific hagfish (*Eptatretus stoutii*). *J. Comp. Physiol. B* **181**, 361-371.

Davie, P. S., Forster, M. E., Davison, B. and Satchell, G. H. (1987). Cardiac function in the New Zealand hagfish (*Eptatretus cirrhatus*). *Physiol. Zool.* **60**, 233-240.

Euler, U. S. v. and Fänge, R. (1961). Catecholamines in nerves and organs of *Myxine glutinosa*, *Squalus acanthias*, and *Gadus callarias*. *Gen. Comp. Endocrinol.* **1**, 191-194.

Fänge, R. and Östlund, E. (1954). The effects of adrenaline, noradrenaline, tyramine and other drugs on the isolated heart from marine vertebrates and a cephalopod (*Eledone cirrosa*). *Acta Zool.* **35**, 289-305.
Farrell, A. P. (2007). Cardiovascular systems in primitive fishes. *Fish Physiol.* **26**, 53-120.
Farrell, A. P. and Stecyk, J. A. W. (2007). The heart as a working model to explore themes and strategies for anoxic survival in ectothermic vertebrates. *Comp. Biochem. Physiol. A Mol. Integr. Physiol.* **147**, 300-312.
Forster, M. E., Davison, W., Satchell, G. H. and Taylor, H. H. (1989). The subcutaneous sinus of the hagfish, Eptatretus cirrhatus and its relation to the central circulating blood volume. *Comp. Biochem. Physiol. A Physiol.* **93**, 607-612.
Forster, M. E., Davison, W., Axelsson, M. and Farrell, A. P. (1992). Cardiovascular responses to hypoxia in the hagfish, *Eptatretus cirrhatus*. *Respir. Physiol.* **88**, 373-386.
Fukayama, S., Tashjian, A. H., Jr. and Bringhurst, F. R. (1992). Forskolin-induced homologous desensitization via an adenosine 3′, 5′-monophosphate-dependent mechanism in human osteoblast-like SaOS-2 cells. *Endocrinology* **131**, 1770-1776.
Gillis, T. E., Regan, M. D., Cox, G. E., Harter, T. S., Brauner, C. J., Richards, J. G. and Farrell, A. P. (2015). Characterizing the metabolic capacity of the anoxic hagfish heart. *J. Exp. Biol.* **218**, 3754-3761.
Greene, C. W. (1902). Contributions to the physiology of the California hagfish, *Polistotrema stouti*—II. The absence of regulative nerves for the systemic heart. *Am. J. Physiol.* **6**, 318-324.
Hansen, C. A. and Sidell, B. D. (1983). Atlantic hagfish cardiac muscle: metabolic basis of tolerance to anoxia. *Am. J. Physiol. Regul. Integr. Comp. Physiol.* **244**, R356-R362.
Helle, K. B. and Storesund, A. (1975). Ultrastructural evidence for a direct connection between the myocardial granules and the sarcoplasmic reticulum in the cardiac ventricle of *Myxine glutinosa* (L.). *Cell Tissue Res.* **163**, 353-363.
Herr, J. E., Winegard, T. M., O'Donnell, M. J., Yancey, P. H. and Fudge, D. S. (2010). Stabilization and swelling of hagfish slime mucin vesicles. *J. Exp. Biol.* **213**, 1092-1099.
Hess, K. C., Jones, B. H., Marquez, B., Chen, Y., Ord, T. S., Kamenetsky, M., Miyamoto, C., Zippin, J. H., Kopf, G. S., Suarez, S. S. et al. (2005). The "soluble" adenylyl cyclase in sperm mediates multiple signaling events required for fertilization. *Dev. Cell* **9**, 249-259.
Hicks, J. M. and Farrell, A. P. (2000a). The cardiovascular responses of the red-eared slider (*Trachemys scripta*) acclimated to either 22 or 5°C. I. Effects of anoxic exposure on *in vivo* cardiac performance. *J. Exp. Biol.* **203**, 3765-3774.
Hicks, J. M. and Farrell, A. P. (2000b). The cardiovascular responses of the red-eared slider (*Trachemys scripta*) acclimated to either 22 or 5°C. II. Effects of anoxia on adrenergic and cholinergic control. *J. Exp. Biol.* **203**, 3775-3784.
Icardo, J. M., Colvee, E., Scjorno, S., Lauriano, E. R., Fudge, D. S., Glover, C. N. and Zaccone, G. (2016). Morphological analysis of the hagfish heart. II. The venous pole and the pericardium. *J. Morphol.* **277**, 8853-8865.
Jensen, D. (1961). Cardioregulation in an aneural heart. *Comp. Biochem. Physiol.* **2**, 181-201.
Jensen, D. (1965). The aneural heart of the hagfish. *Ann. N. Y. Acad. Sci.* **127**, 443-458.
Johnsson, M. and Axelsson, M. (1996). Control of the systemic heart and the portal heart of *Myxine glutinosa*. *J. Exp. Biol.* **199**, 1429-1434.
Jørgensen, J. M., Lomholt, J. P., Weber, R. E. and Malte, H. (1998). *The Biology of Hagfishes*. Dordrecht: Springer Netherlands.
Kleinboelting, S., Diaz, A., Moniot, S., van den Huevel, J., Weyand, M., Levin, L. R., Buck, J. and Steegborn, C. (2014). Crystal structures of human soluble adenylyl cyclase reveal mechanisms of catalysis and of its activation through bicarbonate. *Proc. Natl. Acad. Sci. USA* **111**, 3727-3732.
Kumar, S., Kostin, S., Flacke, J.-P., Reusch, H. P. and Ladilov, Y. (2009). Soluble adenylyl cyclase controls mitochondria-dependent apoptosis in coronary endothelial cells. *J. Biol. Chem.* **284**, 14760-14768.
Lees-Miller, J. P., Guo, J., Wang, Y., Perissinotti, L. L., Noskov, S. Y. and Duff, H. J. (2015). Ivabradine prolongs phase 3 of cardiac repolarization and blocks the $hERG_1$ ($KCNH_2$) current over a concentration-range overlapping with that required to block HCN_4. *J. Mol. Cell. Cardiol.* **85**, 71-78.
Levitt, M., Spector, S., Sjoerdsma, A. and Udenfriend, S. (1965). Elucidation of the rate-limiting step in norepinephrine biosynthesis in the perfused guinea-pig heart. *J. Pharmacol. Exp. Ther.* **148**, 1-8.
Litvin, T. N., Kamenetsky, M., Zarifyan, A., Buck, J. and Levin, L. R. (2003). Kinetic properties of "soluble" adenylyl cyclase: synergism between calcium and bicarbonate. *J. Biol. Chem.* **278**, 15922-15926.
McKenzie, D. J. (2003). Tolerance of chronic hypercapnia by the European eel *Anguilla anguilla*. *J. Exp. Biol.* **206**, 1717-1726.
Melgari, D., Brack, K. E., Zhang, C., Zhang, Y., El Harchi, A., Mitcheson, J. S., Dempsey, C. E., Ng, G. E. and Hancox, J. C. (2015). hERG potassium channel blockade by the HCN channel inhibitor bradycardic agent ivabradine. *J. Am Heart. Assoc.* **4**, e001813.
Miller, S., Pollack, J., Bradshaw, J., Kumai, Y. and Perry, S. F. (2014). Cardiac responses to hypercapnia in larval zebrafish (*Danio rerio*): the links between CO_2 chemoreception, catecholamines and carbonic anhydrase. *J. Exp. Biol.* **217**, 3569-3578.
Monfredi, O., Maltsev, V. A. and Lakatta, E. G. (2013). Modern concepts concerning the origin of the heartbeat. *Physiology* **28**, 74-92.
Nilsson, S. (1983). *Autonomic Nerve Function in the Vertebrates*. Berlin: Springer-Verlag.
Ota, K. G. and Kuratani, S. (2007). Cyclostome embryology and early evolutionary history of vertebrates. *Integr. Comp. Biol.* **47**, 329-337.
Parks, S. K., Tresguerres, M. and Goss, G. G. (2007). Interactions between Na^+ channels and Na^+-HCO_3^- cotransporters in the freshwater fish gill MR cell: a model for transepithelial Na^+ uptake. *Am. J. Physiol. Cell Physiol.* **292**, C935-C944.
Perry, S. F., Fritsche, R. and Thomas, S. (1993). Storage and release of catecholamines from the chromaffin tissue of the Atlantic hagfish *Myxine glutinosa*. *J. Exp. Biol.* **183**, 165-184.
Qu, Y., Whitaker, G. M., Hove-Madsen, L., Tibbits, G. F. and Accili, E. A. (2008). Hyperpolarization-activated cyclic nucleotide-modulated 'HCN' channels confer regular and faster rhythmicity to beating mouse embryonic stem cells. *J. Physiol.* **586**, 701-716.
Rich, T. C., Fagan, K. A., Nakata, H., Schaak, J., Cooper, D. M. F. and Karpen, J. W. (2000). Cyclic nucleotide–gated channels colocalize with adenylyl cyclase in regions of restricted cAMP diffusion. *J. Gen. Physiol.* **116**, 147-162.
Satchell, G. H. (1986). Cardiac function in the hagfish, *Myxine* (Myxinoidea: Cyclostomata). *Acta Zoologica* (Stockholm) **67**, 115-122.
Satchell, G. H. (1991). *Physiology and Form of Fish Circulation*. Cambridge: Cambridge University Press.
Schmitt, B. M., Biemesderfer, D., Romero, M. F., Boulpaep, E. L. and Boron, W. F. (1999). Immunolocalization of the electrogenic Na^+-HCO_3^- cotransporter in mammalian and amphibian kidney. *Am. J. Physiol. Ren. Physiol.* **276**, F27-F38.
Schwencke, C., Yamamoto, M., Okumura, S., Toya, Y., Kim, S.-J. and Ishikawa, Y. (1999). Compartmentation of cyclic adenosine 3′,5-′ monophosphate signaling in caveolae. *Mol. Endocrinol.* **13**, 1061-1070.
Stecyk, J. A. W. and Farrell, A. P. (2006). Regulation of the cardiorespiratory system of common carp (*Cyprinus carpio*) during severe hypoxia at three seasonal acclimation temperatures. *Physiol. Biochem. Zool.* **79**, 614-627.
Stecyk, J. A. W., Stensløkken, K.-O., Farrell, A. P. and Nilsson, G. E. (2004). Maintained cardiac pumping in anoxic crucian carp. *Science* **306**, 77.
Stecyk, J. A. W., Paajanen, V., Farrell, A. P. and Vornanen, M. (2007). Effect of temperature and prolonged anoxia exposure on electrophysiological properties of the turtle (*Trachemys scripta*) heart. *Am. J. Physiol. Integr. Comp. Physiol.* **293**, R421-R437.
Szabo, M., Staib, N. E., Collins, B. J. and Cuttler, L. (1990). Biphasic action of forskolin on growth hormone and prolactin secretion by rat anterior pituitary cells *in vitro*. *Endocrinology* **127**, 1811-1817.
Tian, Q., Zhang, J. X., Zhang, Y., Wu, F., Tang, Q., Wang, C., Shi, Z. Y., Zhang, J. H., Liu, S., Wang, Y. et al. (2009). Biphasic effects of forskolin on tau phosphorylation and spatial memory in rats. *J. Alzheimers Dis.* **17**, 631-642.
Tresguerres, M. (2014). sAC from aquatic organisms as a model to study the evolution of acid/base sensing. *Biochem. Biophys. Acta* **1842**, 2629-2635.
Tresguerres, M., Levin, L. R., Buck, J. and Grosell, M. (2010a). Modulation of NaCl absorption by [HCO_3^-] in the marine teleost intestine is mediated by soluble adenylyl cyclase. *Am. J. Physiol. Regul. Integr. Comp. Physiol.* **299**, R62-R71.
Tresguerres, M., Parks, S. K., Salazar, E., Levin, L. R., Goss, G. G. and Buck, J. (2010b). Bicarbonate-sensing soluble adenylyl cyclase is an essential sensor for acid/base homeostasis. *Proc. Natl. Acad. Sci. USA* **107**, 442-447.
Tresguerres, M., Levin, L. R. and Buck, J. (2011). Intracellular cAMP signaling by soluble adenylyl cyclase. *Kidney Int.* **79**, 1277-1288.
Tresguerres, M., Barott, K. L., Barron, M. E. and Roa, J. N. (2014). Established and potential physiological roles of bicarbonate-sensing soluble adenylyl cyclase (sAC) in aquatic animals. *J. Exp. Biol.* **217**, 663-672.
Vornanen, M. and Haverinen, J. (2013). A significant role of sarcoplasmic reticulum in cardiac contraction of a basal vertebrate, the river lamprey (*Lampetra fluviatilis*). *Acta Physiol.* **207**, 269-279.
Vornanen, M. and Tuomennoro, J. (1999). Effects of acute anoxia on heart function in crucian carp: importance of cholinergic and purinergic control. *Am. J. Physiol. Integr. Comp. Physiol.* **277**, R465-R475.
Wilson, C. M. and Farrell, A. P. (2013). Pharmacological characterization of the heartbeat in an extant vertebrate ancestor, the Pacific hagfish, *Eptatretus stoutii*. *Comp. Biochem. Physiol. A. Mol. Integr. Physiol.* **164**, 258-263.
Wilson, C. M., Stecyk, J. A. W., Couturier, C. S., Nilsson, G. E. and Farrell, A. P. (2013). Phylogeny and effects of anoxia on hyperpolarization-activated cyclic nucleotide-gated channel gene expression in the heart of a primitive chordate, the Pacific hagfish (*Eptatretus stoutii*). *J. Exp. Biol.* **216**, 4462-4472.
Zippin, J. H., Chen, Y., Nahirney, P., Kamenetsky, M., Wuttke, M. S., Fischman, D. A., Levin, L. R. and Buck, J. (2003). Compartmentalization of bicarbonate-sensitive adenylyl cyclase in distinct signaling microdomains. *FASEB J.* **17**, 82-84.
Zippin, J. H., Farrell, J., Huron, D., Kamenetsky, M., Hess, K. C., Fischman, D. A., Levin, L. R. and Buck, J. (2004). Bicarbonate-responsive "soluble" adenylyl cyclase defines a nuclear cAMP microdomain. *J. Cell Biol.* **164**, 527-534.

Chapter V, in full, is a reprint of the material as it appears in the following citation: Wilson CM, Roa JN, Cox GK, Tresguerres M, Farrell AP. 2016. Introducing a novel mechanism to control heart rate in the ancestral pacific hagfish. Journal of Experimental Biology 219: 3227–3236. doi: 10.1242/jeb.138198. The dissertation author was the co-primary investigator and co-author of this paper.

CHAPTER VI

General discussion

Synopsis. The primary goal of this dissertation was to characterize mechanisms for acid-base sensing and regulation in marine animals at the molecular, cellular, and whole-animal level. Chapter II focused on gill acid- and base-secreting cells; the results show both acid-secreting NKA-rich and base-secreting VHA-rich gill cells are mitochondrion-rich (MR) cells, and that all MR cells are either NKA- or VHA-rich cells. Chapter II also studied the translocation of ion-transporting proteins in VHA-rich cells during post-feeding blood alkalosis. In these cells, VHA and pendrin translocated to the basolateral and apical membranes, respectively. VHA translocation to the basolateral membrane had already been described in dogfish shark gills (Tresguerres et al., 2006; Tresguerres et al., 2010; Tresguerres et al., 2007), but my dissertation provided the first evidence of pendrin translocation to the apical membrane. Altogether, these results suggest that protein translocation to/away from the cell membrane is a widespread regulatory cellular mechanism for acid-base regulation. Chapter III focused on acid-base sensing and regulation by sAC in isolated VHA-rich gill cells. I showed KH7-sensitive translocation of VHA to the cell membrane of isolated cells exposed to extracellular alkalosis, an indication that sAC present in the VHA-rich cells themselves, and not whole-animal signals, plays an essential role in blood acid-base sensing in VHA-rich cells. Chapter IV focused on sAC as an acid-base sensor in the cell cytoplasm and nucleus of multiple shark tissues. I found sAC was abundantly expressed in the cytoplasm and nuclei of gill acid-

and base-secreting cells, as well as rectal gland, cornea, intestine, white muscle, and heart tissues. Furthermore, sAC was present and active in isolated nuclei. Finally, Chapter V focused on acid-base sensing by sAC in hagfish hearts; the results show sAC is essential for regulating heart beat rate in hearts recovering from anoxia.

Acid-base regulation is facilitated through protein translocation. Translocation of ion-transporting proteins is an important mechanism used by base-secreting VHA-rich gill cells to regulate blood acid-base status. The results from Chapter II confirmed that the previously observed VHA translocation in dogfish shark gills also occurs in leopard shark gills. Under normal conditions VHA is present throughout the cytoplasm (presumably in vesicles), but during blood alkalosis VHA translocates to the basolateral membrane where it actively pumps H^+ into the blood to help compensate blood alkalosis and energize apical HCO_3^- secretion (reviewed in Tresguerres et al., 2014). VHA translocation occurs during experimentally induced blood alkalosis as well as during the natural post-feeding 'alkaline tide' (Tresguerres et al., 2006; Tresguerres et al., 2007; Tresguerres et al., 2010; Tresguerres et al., 2005). However, the fraction of cells with basolateral membrane VHA expression depends on the source and duration of acid-base stress, with the highest fraction observed following 24 hour and then 6 hour intravenous base-infusion (24h = 85%; 6h = 56%) (Tresguerres et al., 2006) and the lowest

fraction observed 24 hours after feeding (10%) (Chapter II). During milder periods of alkalosis blood pH is likely fully compensated for by fewer base-secreting cells or by less VHA in the basolateral membrane, resulting in more cells with 'intermediate' VHA expression where VHA is cycling between inactive cytoplasmic vesicles and the basolateral membrane (24h = 11%; 6h = 30%) (Tresguerres et al., 2006).

The results from Chapter II also show for the first time pendrin translocates from the cytoplasm to the apical membrane of base-secreting cells where it is likely responsible for secreting excess HCO_3^- into the seawater. In mammalian kidney collecting duct cells, pendrin is expressed in base-secreting B-ICs. In elasmobranchs, pendrin was first identified in VHA-rich gill cells from Atlantic stingray (*Dasyatis sabina*) (Piermarini et al., 2002) and bull sharks (*Carcharhinus leucas*) (Reilly et al., 2011), but these studies focused on ionregulation instead of acid-base regulation. Although those studies reported differences in the number of VHA- and pendrin-expressing cells in gills from freshwater and seawater acclimated animals, they did not observe translocation of pendrin to the apical membrane. Potential explanations include the ionregulatory focus of those studies, or perhaps the peroxidase-based immunohistochemical method used for protein localization did not allow for more detailed sub-cellular localization analyses. Although peroxidase-based methods are well suited to determine if a specific protein is present/absent from a population of cells, they use time-sensitive

accumulation of a solid substrate that can oversaturate and obscure specific intracellular protein localization. Instead, in my dissertation I used a fluorescence-based method to determine protein localization. This allowed me to easily optimize fluorescence exposure times (which is equivalent to substrate accumulation time) and provide detailed intracellular localization of proteins using structured illumination. It would be interesting to use these techniques to explore localization of other acid-base regulatory proteins and determine if more translocate to/away from the cell membrane during acid-base stress. In fact, previous reports from dogfish shark gills show apical/subapical NHE3 expression in acid-secreting gill cells (Choe et al., 2007) as well as cytoplasmic and/or apical membrane NHE2 expression in acid- and base-secreting cells (Claiborne et al., 2008). Further analysis would be necessary to determine if these proteins translocate to/away from the cell membrane during different types of acid-base stress.

Blood acid-base status is locally sensed and regulated by epithelial gill cells. VHA translocation to the basolateral membrane of base-secreting cells is essential for blood acid-base regulation (Tresguerres et al., 2010); however, prior to this dissertation, it was unclear if this process was controlled at the whole-animal or cellular level. To address this question, I generated primary cultures of isolated gill cells and exposed them to extracellular alkalosis *in vitro*. I found that, similar to whole animal experiments,

VHA translocated to the cell membrane of base-secreting cells, and, therefore, must be controlled at the cellular level. At the same time, I used these isolated cells to explore the role of sAC, tmACs, and the cAMP signal transduction pathway in VHA translocation. I found that VHA translocation was blocked by KH7 but not DDA, an indication that sAC (not tmACs) is essential for VHA translocation to the cell membrane of base-secreting cells. Interestingly, VHA moved away from the cell membrane and accumulated at the center of cells exposed to the tmAC-activator forskolin, which is perhaps an indication of an opposing and/or complimentary acid-base regulatory mechanism triggered through tmAC activation. Interestingly, VHA translocation was not induced in cells incubated with the cell-permeable cAMP analogue sp-cAMP. It is possible sp-cAMP simultaneously mimicked cAMP from both sAC and tmACs, with the end result of sAC and tmAC signals cancelling each other out. However, this hypothesis needs further exploration with additional research using cell-permeable cAMP analogues in the presence/absence of sAC/tmAC inhibitors.

sAC is an acid-base sensor in sharks, rays, and hagfish. As discussed in previous sections, at the beginning of my dissertation there was already evidence that sAC was an essential acid-base sensor in base-secreting cells. In addition, my results presented in Chapter IV showed sAC is also abundant in acid-secreting cells as well. The presence of sAC in acid-

and base-secreting cells begs the question: how can a single acid-base sensor facilitate acid-base regulation in two distinct cell populations whose regulatory functions correct opposite forms of acid-base stress? Although it is still unclear what role sAC plays in acid-secreting cells, I believe the likely answer involves another pH-sensing acid-base sensor such as the pH_e-sensor GPR4 found in mammals. The combination of HCO_3^--responsive sAC and a pH-responsive GPR4/tmAC complex would allow acid-secreting cells to distinguish between blood alkalosis and blood acidosis in order to facilitate proper acid-base regulation. In short, two sensors would allow acid-secreting cells to be active during blood acidosis and inactive during blood alkalosis, and *vice versa* for base-secreting cells. This hypothesis is somewhat supported by data presented in Appendix I where glycogen utilization in acid-secreting cells is high in normal acid-stressed sharks and low in post-fed base-stressed sharks, and *vice versa* for base-secreting cells. Additionally, this hypothesis is supported by data from Chapters III and IV showing coexpression of sAC and tmACs in the same population of cells in shark and ray gills; however, more research is necessary to determine what GPCRs and tmACs are present in shark and ray gills and if those that are present are capable of acid-base sensing.

Chapter IV also showed sAC is widely expressed in multiple shark tissues, including the rectal gland, cornea, intestine, white muscle, and heart. This is a first step to understanding the role of sAC outside the context of its

role in blood acid-base regulation; however, more research is required to understand the functional relevance of sAC in these tissues and how sAC activity regulates tissue-specific physiological processes. With that in mind, Chapter V looked at the relationship between sAC activity and tissue function of hagfish hearts; and the data showed sAC in hagfish is an essential acid-base sensor that regulates heart beat frequency during recovery from anoxia. Hagfish hearts are an excellent model to study local control of heart physiology because, unlike mammals, they lack cardiac innervation, but, similar to mammals, use cAMP signal transduction to regulate heart function (reviewed in Farrell, 2007). And because hagfish are the closest vertebrate relative, it is possible sAC-dependent regulation of heart beat rate also applies to vertebrates. Ongoing research in the Tresguerres and Farrell laboratories are exploring if sAC regulation of heart function is a trait retained by higher vertebrates; or if this is an evolutionarily adapted trait exclusive for hagfish that may be related to their survivability in anoxic conditions. Nevertheless, the data from hagfish heart show sAC is clearly an essential acid-base sensor in tissues other than those responsible for blood acid-base regulation.

Chapter IV also showed sAC is present and active in the nucleus of shark cells. This is the first time nuclear sAC has been identified in a non-mammalian species, and it supports the hypothesis that sAC-dependent regulation of gene expression may be also present in sharks and rays. However, nuclear sAC was present in only a subset of cells, which raises the

question: does cytoplasmic sAC translocate to the nucleus or is nuclear sAC intermittently produced in response to local changes in intracellular acid-base homeostasis? Similar to my results on sharks, nuclear sAC was present in only ~10% of cells in mammalian liver hepatocytes (Zippin et al., 2004), but they also did not explore the mechanism(s) that determine sAC nuclear localization. Interestingly, Zippin and colleagues (2004) also reported sAC- and PKA-dependent CREB phosphorylation, suggesting a self-contained nuclear sAC-PKA-CREB microdomain that presumably regulates gene expression. In contrast, tmAC-stimulation resulted in delayed increases in CREB phosphorylation (Zippin et al., 2004). Perhaps these differences in CREB phosphorylation rate are indicative of the rapid and acute changes in intracellular acid-base homeostasis responsible for sAC activation, the slower whole-animal hormonal changes traditionally responsible for tmAC activation, and the requirements cells have to modify expression of genes involved in those processes in a similar timeframe. Whatever the case, more research is necessary to understand nuclear sAC in sharks and rays and what processes are potentially influenced by sAC-regulated changes in gene expression.

Future Directions. There are several logical steps one could pursue to expand on the knowledge presented in my dissertation. The first is a deeper exploration into the interplay between sAC, cAMP, and PKA during protein translocation, glycogen utilization, and acid-base regulation in base-secreting

cells. To date, there have been few studies in traditional mammalian kidney models that focus on base-secreting cells; and the majority of these are either descriptive or highlight ion reabsorption (reviewed in Roy et al., 2015). And, to my knowledge, there has only been one study about cAMP-dependent acid-base regulation in mammalian kidney base-secreting cells (Paunescu et al., 2010), and none from base-secreting cells from any other organism. Paunescu et al. (2010) showed that, while cAMP analogues induced apical VHA translocation in acid-secreting cells, it had no effect on VHA localization in base-secreting cells (Paunescu et al., 2010). This seems counterintuitive because both acid- and base-secreting cells express sAC proteins (Paunescu et al., 2008); however, it is similar to my results in isolated ray gill base-secreting cells. The picture is more clear in mammalian acid-secreting cells in the epididymis and kidney: sAC triggers the translocation of VHA to the apical membrane *via* the cAMP signal transduction pathway and PKA phosphorylation of VHA subunit A at Ser-175 (Alzamora et al., 2010; Gong et al., 2010; Pastor-Soler et al., 2003). It is unclear if base-secreting cells use a similar cAMP-sAC-PKA pathway but if cAMP produces different results in acid- and base-secreting cells (as observed by Paunescu and colleagues), both cell types should be studied for a complete understanding of how acid-base regulation is achieved. My results demonstrate that, similar to epididymal clear cells serving as a model system for kidney acid-secreting cells, VHA-rich gill cells can serve as a model system for kidney base-secreting cells.

The first step involved in using isolated base-secreting gill cells to explore sAC-cAMP-PKA mediated acid-base regulation is optimization of molecular tools routinely used in mammalian model systems. These tools include, but are not limited to, PKA inhibitors like H89 (Acin-Perez et al., 2009) or myristoylated protein kinase A inhibitor (Alzamora et al., 2010), PKA activators like N^6-monobutyryl-cAMP (Alzamora et al., 2010), as well as anti-PKA and anti-PKA-substrate antibodies (Zippin et al., 2004). Once these tools have been optimized I would use an experimental design similar to that described in Chapter III, measuring VHA translocation in isolated cells exposed to (1) control saline, (2) control saline + PKA activator, (3) 40 mM HCO_3^-, (4) 40 mM HCO_3^- + KH7, (5) 40 mM HCO_3^- + KH7 + PKA activator, and (6) 40 mM HCO_3^- + PKA inhibitor. If my hypothesis of sAC-PKA facilitated acid-base regulation is correct, the results should show VHA translocation in conditions 2, 3, and 5 and no VHA translocation in conditions 1 and 4. A set of follow-up experiments should then utilize the PKA antibodies to determine PKA distribution and PKA-dependent phosphorylation during acid-base stress in both isolated cells and whole gills; isolated cells directly exposed to acid base stress (Chapter III) and gill histological sections from animals after feeding (Chapter II) or following acid-base infusions (Tresguerres et al., 2005). Additionally, those experiments could be conducted with isolated nuclei (Chapter IV) and expanded upon with CREB and phospho-CREB antibodies (Zippin et al., 2004) in order to further explore the nuclear sAC-cAMP

microdomain in sharks and rays. However, antibodies specific against anti-shark CREB and shark phosphorylated CREB would have to be developed, as I have tested commercially available reagents that do not seem to work in shark samples.

Isolated shark and ray gill cells are easy to culture and maintain; however, drawbacks of using them as a model system are the lack of genomic information as well as the relative lack of molecular tools compared to mammalian model systems. Thus, another important next step for pushing this research further would be production of leopard shark and/or Pacific round ray deep transcriptomes or genomes. Furthermore, it would be ideal to create a transcriptome using MR acid- and base-secreting cells as source of mRNA. This could be achieved by fluorescence-activated cell sorting (FACS) on isolated gill cells labeled with MitoTracker Red. MR acid- and base-secreting gill cells could be sorted by selecting cells between 10-20 μm with the highest fluorescence intensity. During the optimization phase cell sorting should be verified using anti-NKA and anti-VHA antibodies: most, if not all, cells should have strong NKA/VHA immunoreactivity and MitoTracker fluorescence intensity because these traits are indicative of acid-base regulatory cells and MR cells, respectively. Once verified, these cells could be used to construct a baseline transcriptome that, at minimum, should include sAC, NKA, and VHA. As a follow-up, these sorted MR cells could be exposed to acidosis/alkalosis in the presence of KH7 or DMSO, and used to determine what transcriptional

changes occur as a result of acid-base stress, potentially highlighting other proteins and enzymatic pathways involved in acid-base regulation.

If successful, a comprehensive baseline transcriptome would also be beneficial in determining which GPCR/tmAC complexes are present in gill MR cells. To do this I would first look for GPCRs that share similarities with the mammalian pH_e-sensing GPR4. Once identified, I would then find and optimize commercial antibodies that recognize mammalian GPCRs or I would develop novel antibodies tailored to sharks or rays, using similar techniques used to develop anti-sAC antibodies for dogfish shark sAC (Tresguerres et al., 2010). These optimized antibodies could then be used to determine GPCR/tmAC localization in gill histological sections as well as relative protein abundances through Western blot analysis. I would also confirm this localization in isolated cells. It would be interesting to see if distribution of any pH_e-sensing GPCRs mirrors that of sAC and is expressed in both acid- and base-secreting cells, or if distribution would be limited to one cell type. Depending on the specific cell type(s) it is expressed in, a pH_e-sensor could activate acid-secreting cells or inactivate base-secreting cells during blood acidosis, or both. To test this I would repeat some of the isolated cell experiments, but instead expose the cells to extracellular acidosis in the presence tmAC-selective inhibitor DDA. If tmACs are required for acid-secretion by NKA-rich cells, pH_i regulation (discussed below) should be normal in control cells and absent in tmAC-inhibited cells. If tmACs are

required to inactivate VHA-rich cells, VHA should translocate to the cell membrane in tmAC-inhibited cells and remain cytoplasmic in control cells.

Finally, another benefit of an optimized cell sorting protocol and an enriched population of gill MR cells is these cells could be loaded with the pH_i-sensitive dye SNARF-1. To do this I suggest switching from sorting cells with MitoTracker Red, which I used throughout my dissertation, to MitoTracker Green, which operates outside of the orange-red fluorescence of SNARF-1 and therefore would not interfere with pH_i measurements. Briefly, SNARF-1 fluorescence is excited at 540 nm and emission captured at 585 and 640 nm. The data gathered at 585 nm serves as the internal loading/bleaching control and data gathered at 640 nm is proportional to H^+ concentration; pH_i is determined using a calibration curve based on emission at 640/585 nm. These SNARF-1 loaded cells could be used to determine real-time changes in pH_i associated with extracellular acidosis or alkalosis, and the role of sAC, tmACs, and PKA during this process could be determined using one or more of the specific inhibitors discussed in previous sections of this dissertation.

Final Thoughts. My dissertation established that sAC-dependent acid-base sensing and regulation is conserved in sharks, rays, and hagfish. Similar to the mammalian kidney, sAC in elasmobranch gills plays an essential role in regulating blood acid-base homeostasis. In a nutshell, sAC in specialized acid-base regulatory cells senses changes in acid-base status; this results in cAMP

production, translocation of ion-transporting proteins to the cell membrane, and a draw down of glycogen stores. Additional research is required to understand the role of sAC in other tissues and potential interactions between sAC and other acid-base sensors.

References

Acin-Perez, R., Salazar, E., Kamenetsky, M., Buck, J., Levin, L. R. and Manfredi, G. (2009). Cyclic AMP produced inside mitochondria regulates oxidative phosphorylation. *Cell Metab.* **9**, 265–276.

Alzamora, R., Thali, R. F., Gong, F., Smolak, C., Li, H., Baty, C. J., Bertrand, C. A., Auchli, Y., Brunisholz, R. A., Neumann, D., Hallows, K. R. and Pastor-Soler, N. M. (2010). PKA regulates vacuolar H^+-ATPase localization and activity via direct phosphorylation of the A subunit in kidney cells. *J. Biol. Chem.* **285**, 24676–24685.

Choe, K. P., Edwards, S. L., Claiborne, J. B. and Evans, D. H. (2007). The putative mechanism of Na^+ absorption in euryhaline elasmobranchs exists in the gills of a stenohaline marine elasmobranch, *Squalus acanthias*. *Comp. Biochem. Physiol., Part A Mol. Integr. Physiol.* **146**, 155–162.

Claiborne, J. B., Choe, K. P., Morrison-Shetlar, A. I., Weakley, J. C., Havird, J., Freiji, A., Evans, D. H. and Edwards, S. L. (2008). Molecular detection and immunological localization of gill Na^+/H^+ exchanger in the dogfish (*Squalus acanthias*). *Am. J. Physiol. Regul. Integr. Comp. Physiol.* **294**, R1092–R1102.

Farrell, A. P. (2007). Cardiovascular systems in primitive fishes. *Fish Physiol.* **26**, 53-120.

Gong, F., Alzamora, R., Smolak, C., Li, H., Naveed, S., Neumann, D., Hallows, K. R. and Pastor-Soler, N. M. (2010). Vacuolar H^+-ATPase apical accumulation in kidney intercalated cells is regulated by PKA and AMP-activated protein kinase. *Am. J. Physiol. Renal Physiol.* **298**, F1162–9.

Pastor-Soler, N., Beaulieu, V., Litvin, T. N., Da Silva, N., Chen, Y., Brown, D., Buck, J., Levin, L. R. and Breton, S. (2003). Bicarbonate-regulated adenylyl cyclase (sAC) is a sensor that regulates pH-dependent V-ATPase recycling. *J. Biol. Chem.* **278**, 49523–49529.

Paunescu, T. G., Da Silva, N., Russo, L. M., McKee, M., Lu, H. A. J., Breton, S. and Brown, D. (2008). Association of soluble adenylyl cyclase with the V-ATPase in renal epithelial cells. *Am. J. Physiol. Renal Physiol.* **294**, F130–8.

Paunescu, T. G., Ljubojevic, M., Russo, L. M., Winter, C., McLaughlin, M.

M., Wagner, C. A., Breton, S. and Brown, D. (2010). cAMP stimulates apical V-ATPase accumulation, microvillar elongation, and proton extrusion in kidney collecting duct A-intercalated cells. *Am. J. Physiol. Renal Physiol.* **298**, F643–54.

Piermarini, P. M., Verlander, J. W., Royaux, I. E. and Evans, D. H. (2002). Pendrin immunoreactivity in the gill epithelium of a euryhaline elasmobranch. *Am. J. Physiol. Regul. Integr. Comp. Physiol.* **283**, R983–92.

Reilly, B. D., Cramp, R. L., Wilson, J. M., Campbell, H. A. and Franklin, C. E. (2011). Branchial osmoregulation in the euryhaline bull shark, *Carcharhinus leucas*: a molecular analysis of ion transporters. *J. Exp. Biol.* **214**, 2883–2895.

Roy, A., Al-Bataineh, M. M. and Pastor-Soler, N. M. (2015). Collecting duct intercalated cell function and regulation. *Clin. J. Am. Soc. Nephrol.* **10**, 305–324.

Tresguerres, M., Barott, K. L., Barron, M. E. and Roa, J. N. (2014). Established and potential physiological roles of bicarbonate-sensing soluble adenylyl cyclase (sAC) in aquatic animals. *J. Exp. Biol.* **217**, 663–672.

Tresguerres, M., Katoh, F., Fenton, H., Jasinska, E. and Goss, G. G. (2005). Regulation of branchial V-H^+-ATPase, Na^+/K^+-ATPase and NHE2 in response to acid and base infusions in the Pacific spiny dogfish (*Squalus acanthias*). *J. Exp. Biol.* **208**, 345–354.

Tresguerres, M., Parks, S. K., Katoh, F. and Goss, G. G. (2006). Microtubule-dependent relocation of branchial V-H^+-ATPase to the basolateral membrane in the Pacific spiny dogfish (*Squalus acanthias*): a role in base secretion. *J. Exp. Biol.* **209**, 599–609.

Tresguerres, M., Parks, S. K., Salazar, E., Levin, L. R., Goss, G. G. and Buck, J. (2010). Bicarbonate-sensing soluble adenylyl cyclase is an essential sensor for acid/base homeostasis. *Proc. Natl. Acad. Sci. USA* **107**, 442–447.

Tresguerres, M., Parks, S. K., Wood, C. M. and Goss, G. G. (2007). V-H^+-ATPase translocation during blood alkalosis in dogfish gills: interaction with carbonic anhydrase and involvement in the postfeeding alkaline tide.

Am. J. Physiol. Regul. Integr. Comp. Physiol. **292**, R2012–R2019.

Zippin, J. H., Farrell, J., Huron, D., Kamenetsky, M., Hess, K. C., Fischman, D. A., Levin, L. R. and Buck, J. (2004). Bicarbonate-responsive "soluble" adenylyl cyclase defines a nuclear cAMP microdomain. *J. Cell Biol.* **164**, 527–534.

APPENDIX I

Glycogen utilization in acid- and base-secreting gill cells

RESULTS :
Anti-glycogen monoclonal antibodies were used to identify glycogen-rich cells in leopard shark gill histological sections. Cells with high glycogen content were present in gill cells along the interlamellar gill region, cells previously characterized as acid-base regulatory cells. Further colocalization with anti-NKA and anti-VHA antibodies confirmed acid-secreting NKA-rich cells and base-secreting VHA-rich cells are enriched for glycogen.

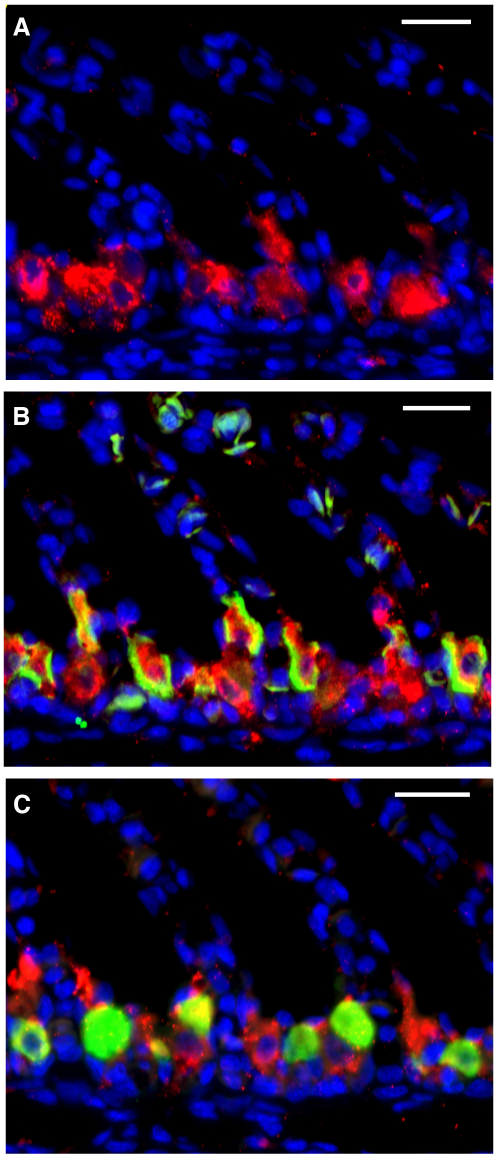

Figure 7.1: Glycogen in acid- and base-secreting gill cells. *A*: Glycogen-rich cells (red) were present along the interlamellar gill region. *B*: Glycogen (red) and NKA (green) coexpression in acid-secreting cells. *C*: Glycogen (red) and VHA (green) coexpression in base-secreting cells. Nuclei stained in blue. Scale bars = 20 µm.

RESULTS :
Gill histological sections were incubated with a combination of polyclonal anti-NKA and anti-VHA antibodies and monoclonal anti-glycogen antibodies in order to determine if all glycogen-rich cells were either acid-secreting NKA-rich cells or base-secreting VHA-rich cells. Most, if not all, glycogen-rich cells expressed either NKA or VHA. In a small subset of glycogen-rich cells NKA/VHA immunoreactivity was reduced and these cells were categorized as potential non-NKA non-VHA glycogen-rich cells, perhaps 'accessory' glycogen-rich cells for nearby acid-base regulatory cells. However, these non-NKA non-VHA glycogen-rich cells could be an artifact of antibodies staining incomplete cells and/or weak NKA/VHA antibody binding in some NKA- and VHA-rich cells. Nonetheless, there were no significant differences in the number of non-NKA non-VHA glycogen-rich cells in starved and fed leopard shark gills, an indication that these 'accessory' cells likely do not play a role in acid-base regulation during post-fed blood alkalosis.

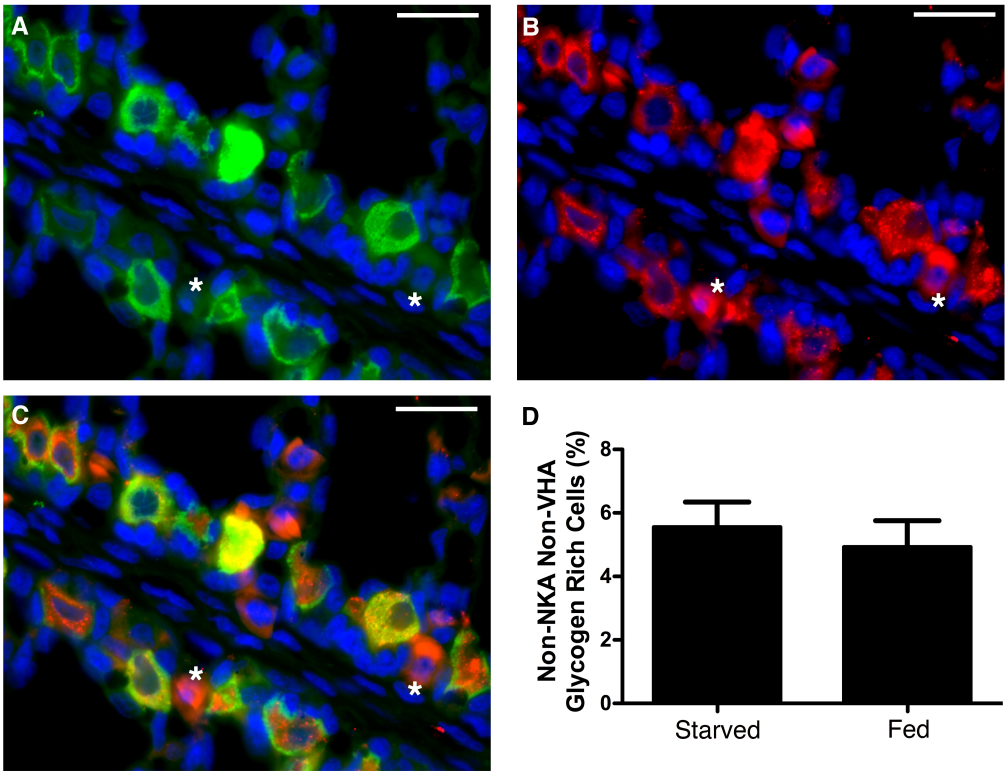

Figure 7.2: Glycogen-rich gill cells from starved and fed sharks. *A*-*C*: NKA- and VHA-rich (*A*, both in green) and glycogen-rich (*B*, red) cells were present together along the interlamellar gill region, with NKA/VHA coexpressed in most glycogen-rich cells (*C*). Asterisks mark potential non-NKA non-VHA glycogen-rich cells with reduced or absent NKA/VHA immunoreactivity. *D:* No significant differences in non-NKA non-VHA glycogen-rich cells from starved (28 of 561 glycogen-rich cells, 5.5%±0.8) and fed (31 of 685 glycogen-rich cells, 4.9%±0.8) leopard sharks. Nuclei stained in blue. Scale bars = 20 μm.

RESULTS :
In starved sharks, VHA is localized to the cell cytoplasm of 99% of VHA-rich cells (Fig. 3A). Feeding induces VHA translocation to the basolateral membrane of 12% of VHA-rich cells (Fig. 3B, asterisk), where it uses energy to move H^+ ions into the blood. We observed higher glycogen content in inactive (cytoplasmic VHA, Cyt VHA) VHA-rich cells and reduced glycogen content in active (membrane VHA, Mem VHA) VHA-rich cells, suggesting glycogen is a source of energy used by active VHA-rich cells. In general, starved sharks had more cytoplasmic VHA cells and fed sharks had more membrane VHA cells; however, both cytoplasmic VHA cells with high glycogen content and membrane VHA cells with reduced glycogen content were present in starved and fed sharks (Fig. 3 C-D).

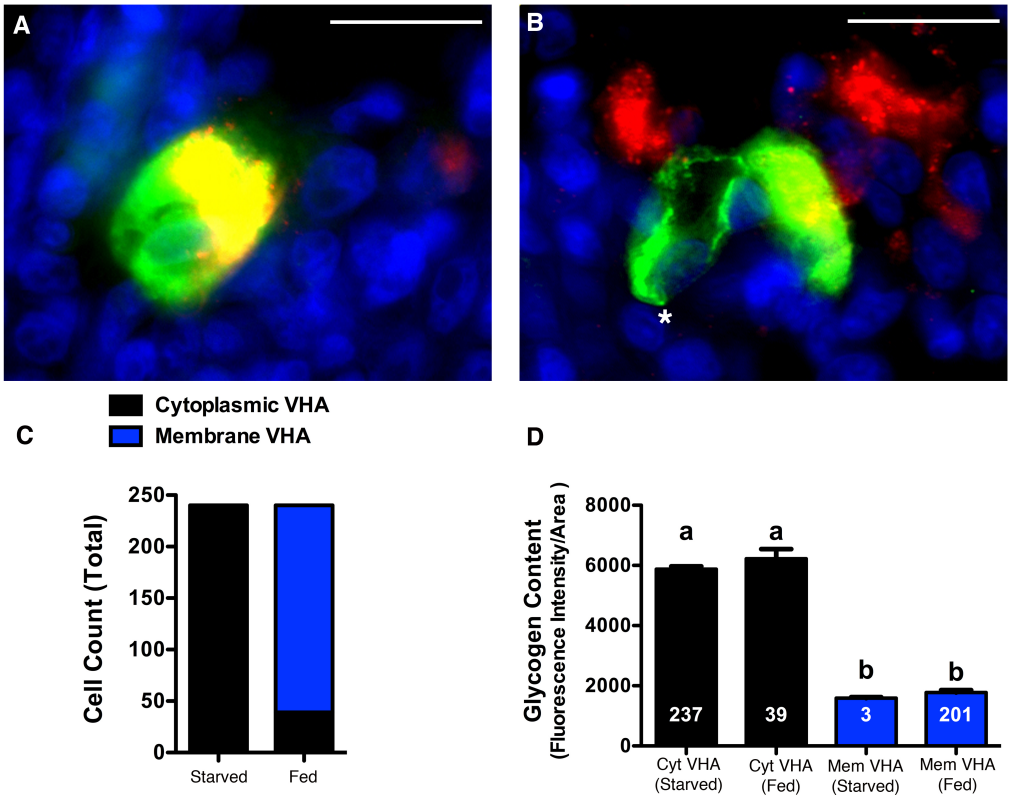

Figure 7.3: Glycogen in VHA-rich cells from starved and fed sharks. *A-B*: Representative images of glycogen (red) and VHA (green) immunoreactivity in starved (*A*) and fed (*B*) leopard shark gills, with reduced glycogen in cells with VHA localized in the basolateral membrane (*B*,*). *C-D*: (*C*) Summary of cells with cytoplasmic VHA from starved (n = 237) and fed (n = 39) leopard shark gills, and cells with membrane VHA in starved (n = 3) and fed (n = 201) leopard shark gills. *(D)* Summary of glycogen content in 60 VHA-rich cells from 4 starved (n = 240 cells) and 4 fed (n = 240 cells) leopard sharks; cells with cytoplasmic VHA had significantly higher glycogen content (C, $P < 0.001$). Nuclei stained in blue. Scale bars = 20 μm.

RESULTS :
Opposite of VHA-rich cells, glycogen content in NKA-rich cells was reduced in starved sharks and higher in fed sharks. While VHA-rich cells are base-secreting cells, NKA-rich cells are acid-secreting cells and both cell populations are likely activated under opposing physiological conditions. And our results support the hypothesis that feeding activates the base-secreting VHA-rich cell population (reducing glycogen content), and inactivates the acid-secreting NKA-rich cell population (maintaining glycogen content). Under normal conditions, NKA-rich cells likely remain active in order to maintain normal blood acid-base status and therefore utilize glycogen as an energy source.

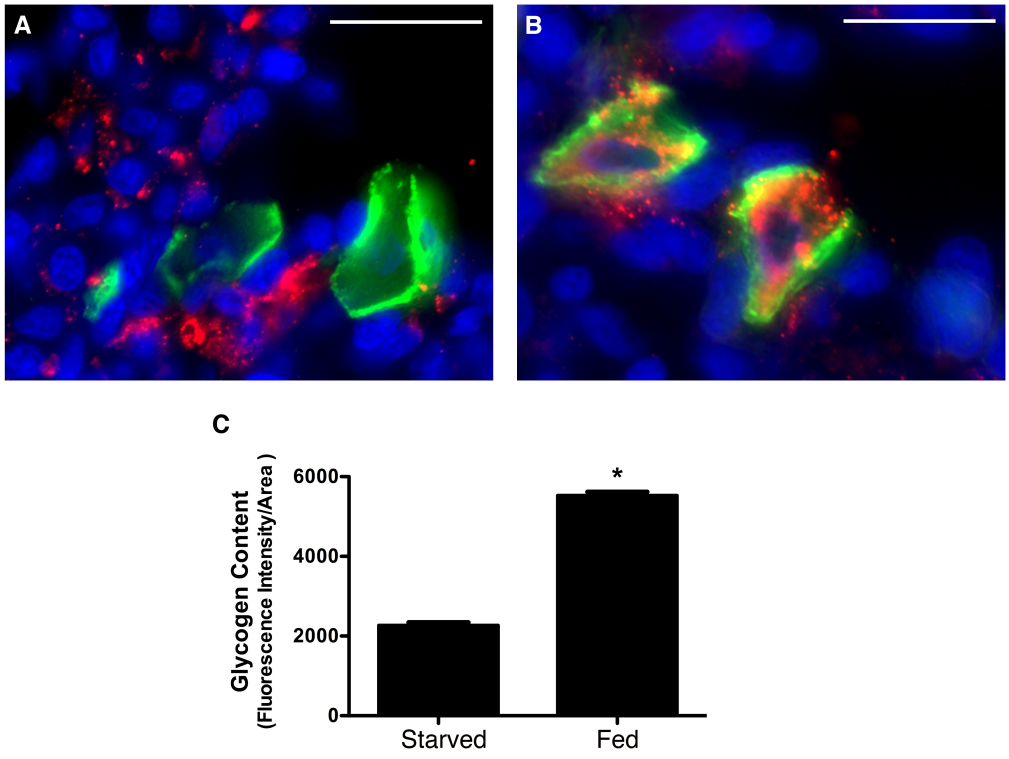

Figure 7.4: Glycogen in NKA-rich cells from starved and fed sharks. *A-B:* Representative images of glycogen (red) and NKA (green) immunoreactivity in starved (*A*) and fed (*B*) leopard shark gills. *C*: Summary of glycogen content in 60 NKA-rich cells from 4 starved (n = 240 cells) and 4 fed (n = 240 cells) leopard shark gills, with significantly higher glycogen content in NKA-rich cells from fed leopard sharks ($P < 0.001$). Nuclei stained in blue. Scale bars = 20 µm.

RESULTS :
Glycogen content remained consistent in isolated acid-secreting cells exposed to control, bicarbonate, and bicarbonate + KH7; intracellular glycogen was low in the cytoplasm and high in/near the membrane (Fig. 5A-C). Glycogen content in base-secreting cells varied between treatments, with high cytoplasmic glycogen in control and KH7 exposed cells and high membrane glycogen in bicarbonate exposed cells (Fig. 5D-F). It is important to note that in each treatment glycogen localization mirrored that of NKA and VHA. NKA is always present in the cell membrane (Fig. 5A-C). VHA is cytoplasmic in control cells (Fig. 5D), translocates to the membrane during high bicarbonate stress (Fig. 5E), and this translocation is blocked by KH7 (Fig. 5F). It is likely that this proximity to glycogen facilitates energy metabolism by NKA and VHA. Also, unlike whole gills (Fig. 3-4), it appears overall glycogen content remained the same in all treatments; perhaps due to the shorter period isolated cells were exposed to stress (30 min) compared to the longer stress exposure for starved (5 days) and post-fed (24 hrs) sharks.

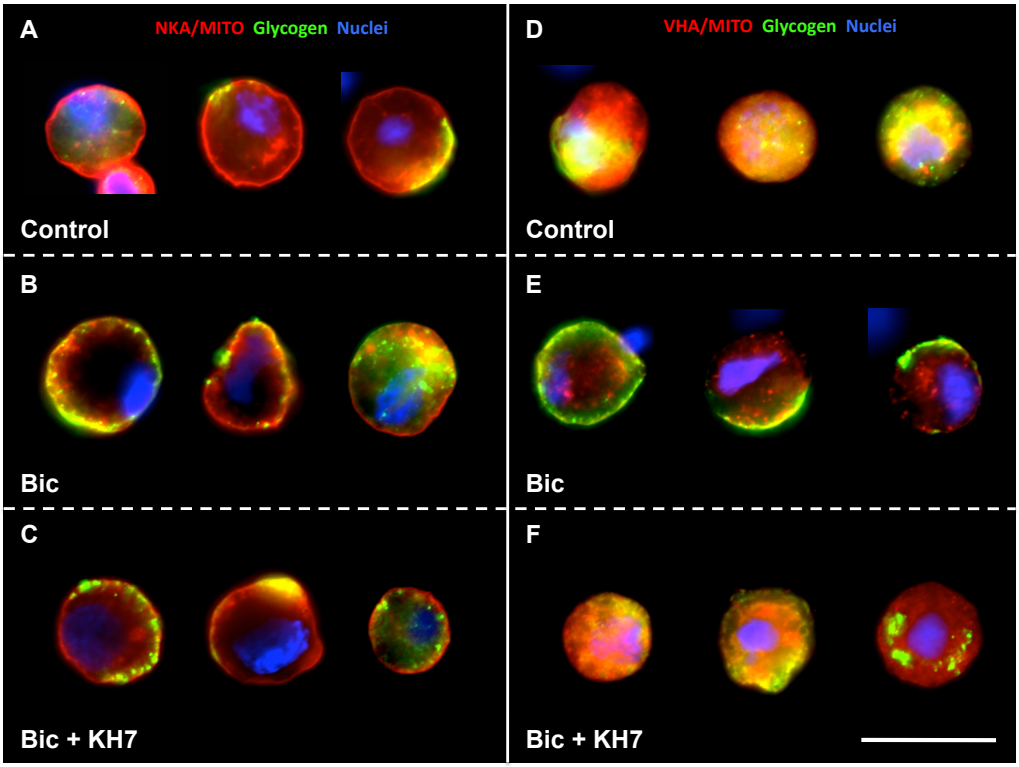

Figure 7.5: Glycogen in isolated gill cells exposed to alkalosis. Cells were exposed to control (5 mM HCO_3^-, pH 7.75), Bic (40 mM HCO_3^-, pH 8.0), and Bic + KH7 (50 µM KH7 + 40 mM HCO_3^-, pH 8.0). *A-C:* Representative images of glycogen (green), NKA (red) and mitochondria (MITO, red) in isolated acid-secreting cells. *D-F*: Representative images of glycogen (green), VHA (red) and mitochondria (MITO, red) in isolated base-secreting cells. In Bic exposed VHA-rich cells (*E*) glycogen (green) and VHA (red) completely colocalize at the cell membrane (seen as green-yellow). Nuclei stained in blue. Scale bar = 20 µm.